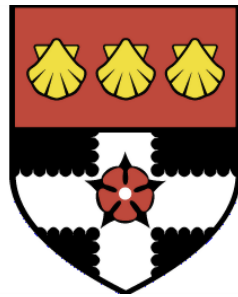


UNIVERSITY OF READING

Department of Meteorology



**Deterministic models of Southern
Hemisphere circulation variability**

Nick Byrne

A thesis submitted for the degree of Doctor of Philosophy

October 2017

Declaration

I confirm that this is my own work and the use of all material from other sources has been properly and fully acknowledged.

Nick Byrne

Abstract

Statistical models of atmospheric variability typically attempt to account for deterministic seasonal variations by constructing a long-term average for each day or month of the year. Year-to-year variability can then be treated as some form of stochastic process about this long-term average. In general, the stochastic processes are assumed to be statistically stationary (invariant under time translation). However, for a non-linear system such as the Earth's atmosphere, multiple seasonal evolutions may be possible for the same external forcing. In the presence of such a multiplicity of solutions, the identification of a seasonal cycle with a long-term average may not be the optimal procedure.

Previous research has suggested that multiple evolutions of the seasonal cycle of the Southern Hemisphere mid-latitude circulation may be possible. The central goal of this thesis is to build on this work and to present evidence for different seasonal evolutions of the Southern Hemisphere mid-latitude circulation. This evidence is initially presented by highlighting a low-frequency peak in an aspect of the Southern Hemisphere mid-latitude circulation that is viewed as a harmonic of the annual cycle (quasi-two year). Statistically stationary models of variability about a long-term average are argued to be unable to account for the presence of this harmonic. Following this, an alternative model of circulation variability is proposed that explicitly references various stages of the seasonal cycle in a deterministic manner. In particular, explicit reference is made to the downward shift and to the final breakdown of the stratospheric polar vortex. A re-interpretation of several previous results in the literature including Southern Annular Mode persistence timescales, Southern Hemisphere mid-latitude climate change and the semi-annual oscillation of the mid-latitude jet is subsequently presented using this alternative perspective.

Acknowledgements

I am extremely grateful to my supervisor, Ted Shepherd, for giving me the opportunity to study at Reading. The depth and breadth of his knowledge has continually challenged me to learn more, and my scientific inquiries have been made all the more rewarding as a result. This thesis would not have been possible without him.

I am extremely grateful to Tim Woollings and Alan Plumb, both of whom provided substantial mentoring and support during my PhD. The content of this thesis developed rapidly following their involvement, and it would not have been possible without them.

Thanks to my committee members, Andrew Charlton-Perez and Tom Frame, for always getting me thinking about my work and keeping me on track.

Thanks to my examiners, Professor David Thompson and Andrew Charlton-Perez, for sharing their insight and their perspective on the relevance of the results of this thesis.

Thanks to all the members of Ted's group for all their help, guidance and companionship during my four years in Reading.

Thanks to all the PhD students and staff in Lyle 3, and to the Met department in general, for providing such a wonderful community environment to work in.

Finally, thank you to my family for always being a constant source of love and support.

Contents

1	Introduction	1
1.1	Mid-latitude circulation variability in re-analyses	2
1.1.1	The troposphere	2
1.1.2	The stratosphere	4
1.2	Factors relevant to mid-latitude circulation variability	5
1.2.1	Baroclinic lifecycles	5
1.2.2	Variations in the stratospheric circulation	7
1.2.3	Stratosphere-troposphere coupling	8
1.2.4	Annular modes of the circulation	10
1.3	Stochastic and deterministic models of circulation variability	12
1.4	Outline and contributions	14
1.4.1	Methods	15
2	Annular modes and apparent eddy feedbacks	16
2.1	Introduction	16
2.2	Data and methods	18
2.3	Results	18
2.3.1	SAM and anomalous eddy momentum flux convergence power spectra	18
2.3.2	Causal attribution and lag regression	21
2.3.3	Seasonality of the lag regression plots	23
2.4	Discussion and conclusion	24
2.A	25
2.B	25
2.C	26

3	The seasonal breakdown of the SH stratospheric polar vortex	29
3.1	Introduction	29
3.2	Data and methods	30
3.3	Composite analysis	32
3.3.1	Climatology	32
3.3.2	Breakdown date composites	34
3.4	Applications	41
3.4.1	Southern Annular Mode persistence timescales	41
3.4.2	Southern Hemisphere high-latitude climate change	43
3.4.3	High-latitude ENSO teleconnection in austral summer	46
3.5	Summary and discussion	48
3.A	51
3.B	51
4	Seasonal persistence of stratospheric circulation anomalies	53
4.1	Introduction	53
4.2	Data and methods	56
4.3	Stratospheric circulation variability	57
4.3.1	Climatology and interannual variability	57
4.3.2	Seasonal persistence of SSPV anomalies	60
4.4	Stratosphere-troposphere coupling	65
4.4.1	Interannual variations	65
4.4.2	Alternative circulation perspective	70
4.5	Summary and discussion	74
4.A	78
5	Conclusion	80
5.1	Summary	80
5.1.1	Evidence for non-stationarity in the mid-latitudes	80
5.1.2	The vortex breakdown event	81
5.1.3	The shift-down of the stratospheric vortex	81
5.2	Discussion	82
5.3	Future work	85
	Bibliography	88

List of Figures

1-1	Zonal indices for SH and NH.	3
1-2	Monthly-mean climatologies of zonal-mean zonal wind.	5
1-3	DJFM climatology for eddy momentum flux convergence and zonal-mean zonal wind.	7
1-4	‘Dripping paint’ plots for SH.	10
2-1	SAM and eddy momentum flux convergence power spectra.	19
2-2	SAM and eddy momentum flux convergence power spectra - low frequencies.	20
2-3	Synthetic cross-correlation plots.	22
2-4	Seasonal cross-correlation plots.	23
2-5	Eddy power spectrum - statistical significance.	27
2-6	SAM power spectrum - statistical significance.	27
2-7	SAM power spectrum - second half of data record.	28
3-1	EDJ snapshots.	32
3-2	EDJ climatology from October 15 - January 15.	33
3-3	Stratospheric vortex breakdown date time series.	35
3-4	Vortex breakdown anomaly composite - no separation.	35
3-5	Vortex breakdown anomaly composite - early and late separation.	36
3-6	Vortex breakdown EDJ composite along with EDJ climatologies for early and late years separately.	38
3-7	Jet transition schematic.	40
3-8	SAM persistence timescales.	42
3-9	SAM EOF.	43
3-10	Long-term circulation changes during austral summer.	45
3-11	Confidence intervals for long-term austral summer changes.	45
3-12	ENSO SH zonal mean teleconnection.	47

4-1	Correlation plot between DJF 500hPa geopotential height anomalies and stratospheric vortex breakdown date.	55
4-2	30hPa polar cap averaged geopotential height seasonal cycle and EOF1.	59
4-3	Principal component time series of EOF1.	59
4-4	Monthly-mean composite differences for zonal-mean zonal wind between weak and strong stratospheric vortex years.	60
4-5	Monthly-mean zonal-mean zonal wind for S and W years.	61
4-6	Correlation coefficients between polar cap averaged 30 hPa geopotential height at a given month and subsequent months.	62
4-7	Predictor model for stratospheric vortex breakdown date using strength of winter/spring stratospheric vortex.	63
4-8	Yearly time series of 30hPa polar cap averaged geopotential height anomalies.	64
4-9	Monthly-mean differences in zonal-mean zonal wind between westerly and easterly QBO phase.	67
4-10	EDJ climatology.	68
4-11	Climatology of SH zonal index along with climatologies for weak and strong stratospheric vortex years separately.	69
4-12	EDJ climatology along with climatologies for weak and strong stratospheric vortex years separately.	69
4-13	Correlation coefficients between polar cap averaged 30 hPa geopotential height at a given month of the year and SH zonal index in subsequent months, and between SH zonal index at a given month of the year and SH zonal index in subsequent months.	71
4-14	Graphical representation of correlation table results for month of October.	72
4-15	'Dripping paint' plots as a function of lag and calendar day of the year.	73

List of Tables

4.1	Yearly values of PC1 index, midwinter QBO index and stratospheric vortex breakdown date index.	66
-----	--	----

Chapter 1

Introduction

As a result of contrasting surface boundary conditions north and south of the equator, a hemispheric asymmetry is observed in the seasonal cycle of the Earth's atmospheric circulation. In the troposphere, stronger westerly winds are found in the Southern Hemisphere (SH) mid-latitudes throughout the year; these westerly winds also undergo a semi-annual oscillation (SAO) in latitude, with the strongest winds located closest to the pole around the time of the equinoxes (Karoly and Vincent, 1998). In contrast, the Northern Hemisphere (NH) winds exhibit something closer to an annual cycle, with the strongest mid-latitude winds generally found in winter (Kallberg et al., 2005). In the stratosphere, even larger contrasts are observed. One widely highlighted difference is that the SH winds are stronger and exhibit much reduced intraseasonal variability relative to their NH counterparts (Hartmann et al., 1984). Less widely-appreciated is that the SH stratospheric westerlies shift downward as part of their seasonal cycle, with the strongest winds progressing from the upper stratosphere in August to eventually reach the upper troposphere sometime in austral summer (Hartmann et al., 1984). This systematic downward progression is not usually seen in the NH (Hardiman et al., 2011).

Models of atmospheric variability typically attempt to account for these seasonal variations of the circulation by constructing a long-term average for each day or month of the year (Trenberth, 1984). Year-to-year variability can then be treated as some form of stochastic process about this long-term average. In general, the stochastic processes are assumed to be statistically stationary (invariant under time translation), sometimes with a seasonal dependence. However, for a non-linear system such as the Earth's atmosphere, multiple seasonal evolutions may be possible for the same external forcing (e.g., Scott and Haynes, 2000, 2002). In the presence of such

a multiplicity of solutions, the identification of a seasonal cycle with a long-term average may not be the optimal procedure. Evidence that such a scenario may be applicable to the SH circulation has previously been presented by Kuroda and Kodera (1998).

The central goal of this thesis is to build on the work of Kuroda and Kodera (1998) and to present evidence for different seasonal evolutions of the SH mid-latitude circulation. This evidence is initially presented using the concept of a non-stationary stochastic process. Following this, an alternative model of circulation variability is proposed that explicitly references various stages of the seasonal cycle (like the downward shift and the breakdown of the stratospheric polar vortex) in a deterministic manner. The potential benefits of this alternative perspective are then considered by revisiting several previous results in the literature.

The remainder of this chapter gives a more thorough background to the thesis, focusing in Section 1.1 on a purely phenomenological description of SH mid-latitude circulation variability. Section 1.2 reviews some common paradigms of this variability. Section 1.3 introduces the concept of a non-stationary stochastic process along with a discussion on the duality between non-stationary and deterministic models of variability. Finally, the chapter closes with an outline of the work carried out that forms the original content of the thesis.

1.1 Mid-latitude circulation variability in re-analyses

1.1.1 The troposphere

One of the most prominent features of the circulation of the troposphere is the presence of a broad belt of westerly winds in the mid-latitudes of both hemispheres. Rossby (1939) introduced the concept of the zonal index cycle to describe the varying strength and location of these westerlies in the NH. He defined this index as the zonally-averaged surface pressure difference between 35 and 55 N. A similar index was subsequently introduced for the SH using the zonally-averaged surface pressure difference between 50 and 65 S (see Bracegirdle, 2011, and references therein). Larger values of these indices tend to occur during periods of strong westerly flow and/or when the westerlies are found closer to the poles. Inspection of long-term monthly averages of the zonal index for the SH reveal that the SH westerlies undergo a twice-yearly vacillation in latitude and strength as part of their seasonal evolution, with

the strongest westerlies generally located closer to the pole around the time of the equinoxes (Figure 1-1). This twice-yearly vacillation of the SH westerlies is commonly referred to as the semi-annual oscillation (SAO). In contrast, the seasonal evolution of the zonal index in the NH exhibits more of an annual cycle, with largest values generally found in the cold season (Figure 1-1).

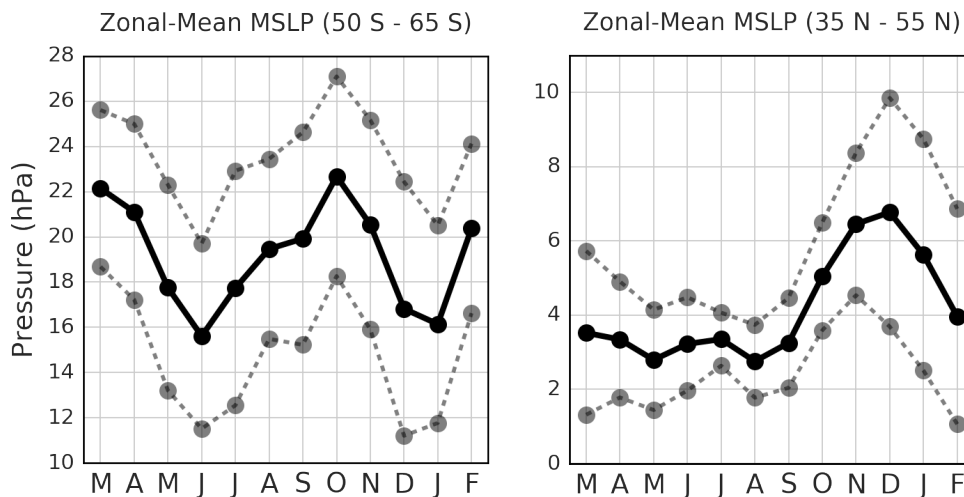


Figure 1-1: (Left) Climatology of monthly-mean difference in zonally-averaged sea level pressure between 50 and 65 S (solid line) along with interannual standard deviation (dashed line). (Right) Climatology of monthly-mean difference in zonally-averaged sea level pressure between 35 and 55 N (solid line) along with interannual standard deviation (dashed line). Note the different scales on the y-axis used for both plots. ERA-Interim, 1979-2017.

Previous studies have regularly noted that the westerly winds of the SH tend to be more zonally symmetric than their NH counterparts, where localised jets are more prevalent (Hartmann and Lo, 1998). This has led to the introduction of zonal averages as a useful approximation for analysing SH mid-latitude circulation variability. Furthermore, studies of the zonally-averaged flow of the SH tend to emphasise the approximately equivalent barotropic nature of the mid-latitude westerlies. This zonally-averaged equivalent barotropic structure is frequently referred to as the SH eddy-driven jet (EDJ; see section 1.2.1 for an explanation of this term) and represents an important metric for much of the work in this thesis.

The SH EDJ is present in all seasons, with the strongest winds invariably located somewhere between 40 and 60 S (Hartmann and Lo, 1998). These winds are generally stronger than those found in the NH, and differences between the hemispheres can often exceed 10 m/s in the middle and upper troposphere (Karoly and Vincent, 1998). To a first approximation, variability of the SH EDJ can be characterised as a wandering in the meridional plane. This wandering of the jet is found to occur on all timescales and is regularly approximated as a Gaussian red-noise process with an e-folding timescale of about 10 days (Hartmann and Lo, 1998). Previous research has not found evidence for any preferred periodicities in this wandering of the jet.

1.1.2 The stratosphere

The seasonal cycle of the mid/high-latitude stratosphere of both hemispheres is characterised by the formation of a band of strong circumpolar westerlies each winter (often referred to as the stratospheric polar vortex), and the development of easterlies each summer. However, while the winter westerlies of the Northern Hemisphere are characterised by intermittent vacillations in their strength and location that can occasionally lead to their reversal altogether, the winter westerlies of the Southern Hemisphere are considerably stronger and exhibit much less daily variability (Karoly and Vincent, 1998). The distinct behaviour between the hemispheres also extends to the spring and early summer seasons and is associated with contrasting evolutions in the final breakdown of the stratospheric polar vortex.

The final breakdown of the stratospheric polar vortex is an annual phenomenon that leads to the development of summer easterlies throughout much of the stratosphere. Perhaps the most striking difference between the two hemispheres in the evolution of this event is that the strongest westerlies gradually progress downward in height in the Southern Hemisphere, before shifting entirely to the upper troposphere in association with the breakdown event (see Figure 1-2). This systematic downward progression is not usually seen in the NH (Hardiman et al., 2011).

The timing of the downward shift in the Southern Hemisphere can be influenced by the strength of the stratospheric vortex in the preceding winter (Gerber et al., 2010). It is also subject to a variety of other influences including anthropogenic effects (e.g., ozone depletion); these mechanisms of variability will be considered in greater detail in the next subsection. The net result of these various effects is a considerable year-to-year variability in the phase of the seasonal cycle of the vortex during austral spring.

They also necessarily result in a considerable year-to-year variability in the timing of the final breakdown event, with this event generally occurring anytime between November and January in the Southern Hemisphere. Interannual variability in the timing of the final breakdown event is also large in the Northern Hemisphere, with the event generally occurring anytime between March and June. The larger interannual variability in the Northern Hemisphere can in part be traced to larger vacillations in the vortex in the preceding winter (Hardiman et al., 2011).

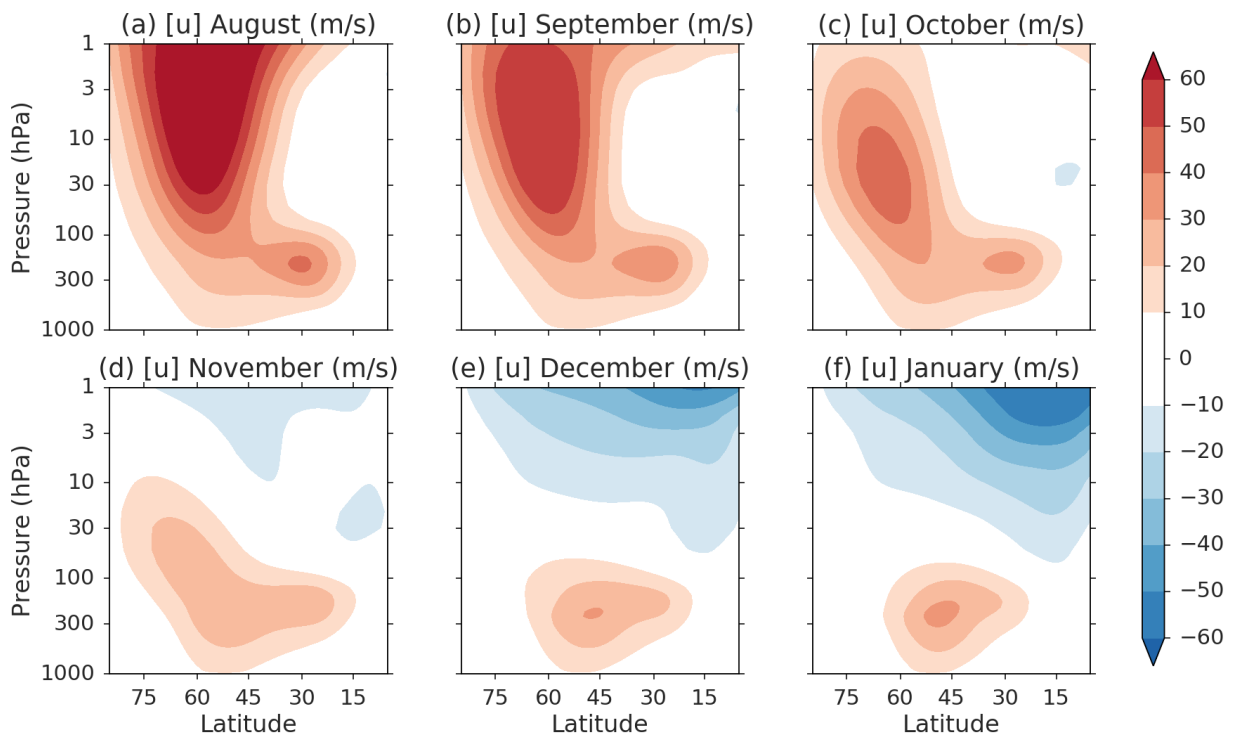


Figure 1-2: Monthly-mean climatologies of $[u]$. ERA-Interim, 1979-2017.

1.2 Factors relevant to mid-latitude circulation variability

1.2.1 Baroclinic lifecycles

A theory for the maintenance and variability of the EDJ is a classical problem of geophysical fluid dynamics. A comprehensive review of the history and developments

in this field is beyond the scope of this thesis; instead, a brief review of one well-established paradigm will be presented following Held and Hoskins (1985). Observations suggest that the dominant forcing of the EDJ comes from meridional angular momentum transport by eddies (hence the term ‘eddy-driven jet’; see also Figure 1-3). From consideration of the zonally and vertically integrated quasi-geostrophic momentum equation, this leads to an equation for the EDJ of the form:

$$\frac{\partial \langle [u] \rangle}{\partial t} = -\frac{1}{\cos^2\phi} \frac{\partial(\langle [u'v'] \rangle \cos^2\phi)}{a\partial\phi} - F \quad (1.1)$$

In this equation ¹, variations of the EDJ are described by the terms on the left hand side of the equation and variations in the eddy forcing are described by the first term on the right. A theory for a parametrisation of the variations in the eddy forcing begins with the concept of a baroclinic lifecycle.

An important source of eddies (or waves) in the mid-latitude troposphere is considered to be baroclinic instability in the lower troposphere. Theory and observations suggest that irreversible mixing due to these instabilities can be divided into two distinct parts: that in the source region near the surface in mid-latitudes and that in the region where the waves are dissipated in the (sub-tropical) upper troposphere. Furthermore, a link between these two parts can be made via the notion of (Rossby) wave radiation from the lower tropospheric source. Large poleward transports of westerly momentum into the mid-latitudes (‘eddy momentum flux convergence’) are associated with the equatorward propagation and dissipation of such Rossby waves in the upper troposphere. These eddy momentum fluxes determine the surface stress and, therefore, the surface wind distribution in the mid-latitudes, since the convergence of the eddy flux in these regions can only be balanced in the time mean by surface drag.

Thus the problem of the maintenance of the westerlies is seen to be essentially one of a parametrisation of the sources and sinks of Rossby waves. This paradigm also allows for the potential for tropical (e.g., L’Heureux and Thompson, 2006) or stratospheric influence (see subsection 1.2.3) on the westerlies via influence from these regions on the wave propagation characteristics of the upper troposphere.

¹Here $\langle [u] \rangle$ represents the vertically and zonally integrated zonal wind, $(.)'$ represents a deviation from a zonal mean, ϕ represents latitude, a represents the radius of the Earth and F represents a residual momentum forcing term.

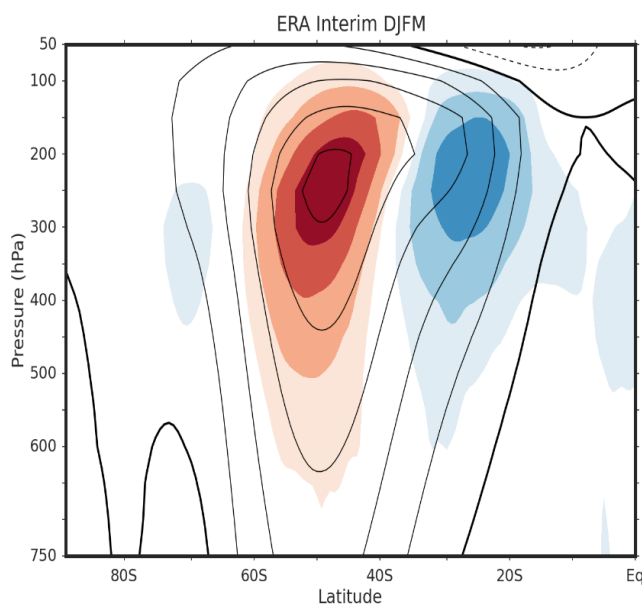


Figure 1-3: DJFM climatology of eddy momentum flux convergence (shading) and zonal-mean zonal wind (contours). Intervals for shading are $0.5 \text{ m s}^{-1} \text{ day}^{-1}$; red represents positive values (convergence). Contour intervals are 6 m s^{-1} ; the bold line represents the zero contour. ERA-Interim, 1979-2014.

1.2.2 Variations in the stratospheric circulation

At least three separate mechanisms for interannual variability in the extratropical stratosphere have been suggested. The first is associated with interannual variability of the tropospheric circulation, in particular the wave sources. The sharply contrasting behaviour between the NH and SH tropospheric wave sources is the principal reason for such different winter evolutions of the NH and SH extratropical stratospheres. It should be noted that the wave sources need not be restricted to the mid-latitude troposphere as there is evidence that variations in the tropical troposphere such as the El-Nino Southern Oscillation (ENSO) may also play an influential role (e.g., Polvani et al., 2017, and references therein). A second important mechanism for interannual variability in the extratropical stratosphere arises from the equatorial quasi-biennial oscillation (QBO, Anstey and Shepherd, 2014). Both this mechanism and variability of the tropospheric wave sources might be regarded as externally forced influences on the extratropical stratosphere.

The third potential mechanism represents variability internal to the stratosphere itself (e.g., Scott and Haynes, 2000, 2002). Multiple-flow equilibria have previously

been found to exist in two-dimensional latitude-height primitive equation models of the stratosphere under the same external forcing. This multiplicity of solutions emerges as a result of the inherently non-linear nature of the system. This can subsequently lead to a multiplicity of seasonal evolutions of the stratospheric polar vortex. Variability in the stratospheric circulation has also been found to emerge as a result of a persistence of perturbations to the sub-tropical stratospheric circulation from one winter to the next (Scott and Haynes, 1998). This persistence arises because the smaller Coriolis parameter at low latitudes results in longer radiative damping times of perturbations compared to the extra-tropics. This so-called low-latitude ‘flywheel’ effect imprints a distinct two-year periodicity to variability in the mid-latitude stratosphere.

1.2.3 Stratosphere-troposphere coupling

Investigations of coupled variability of the stratospheric and tropospheric circulations are a comparatively recent phenomenon in the meteorological literature. Much of this work can be traced to a study by Kodera et al. (1990), which noted that lag-correlations of monthly zonal-mean zonal wind anomalies (deviations from a long-term monthly average) near the NH subtropical upper stratosphere appeared to migrate poleward and then downward over the course of 2-3 months. The dynamics of this poleward and downward migration are discussed in Hitchcock (2012). A similar behaviour was documented for the SH by Kuroda and Kodera (1998) using a multiple empirical orthogonal function analysis (EOF) on zonal-mean zonal wind. The overall features of this progression were found to be similar to the NH except that the entire sequence of evolution was closely locked to the annual cycle and that it required a longer period of 6 months. In a follow-on study, Kuroda and Kodera (2001) referred to the SH progression as ‘an interannual phenomenon with a well-defined intraseasonal structure’ - or equivalently, the coupled variability exhibited a seasonal march. This march of the circulation anomalies was further investigated by Hio and Yoden (2005) who distinguished between two types of seasonal evolutions based on the state of the winter stratospheric polar vortex. Broadly speaking, their first type of seasonal evolution was associated with a weak winter vortex and their second type of seasonal evolution was associated with a strong winter vortex. In both Kuroda and Kodera (1998) and Hio and Yoden (2005) it was noted that perturbations to the winter stratospheric vortex could propagate downward into the troposphere in

spring and subsequently persist until the vortex breakdown event in early summer at least. The coherency and long timescale of the SH circulation anomalies found in both of these studies is suggestive of a multiplicity of seasonal evolutions of the SH mid-latitude circulation.

Coupled variability around the time of the stratospheric vortex breakdown event was explored by Black et al. (2006) and Black and McDaniel (2007). In both of these studies the concept of an organising influence of the vortex breakdown event on the EDJ was considered. These authors found that this influence was substantially stronger in the NH, with the effects apparently restricted to the upper troposphere and lower stratosphere in the SH. The apparent influence in the SH was of particular interest in light of the previously documented influence of ozone depletion on the SH tropospheric circulation (see subsection on Annular Modes for more details); SH ozone depletion maximises in austral spring and has been widely implicated in changes in the evolution of the SH breakdown event in the stratosphere. More recently, Sun et al. (2014) used both re-analyses and a hierarchy of models to argue that long term changes in the vortex breakdown evolution were responsible for the influence of ozone depletion on the SH tropospheric circulation.

The dynamical understanding of exactly how the stratosphere couples to the troposphere is currently an active area of research and a variety of theories have been proposed. One such theory suggests that this coupling is via the mechanism of planetary wave breaking in the stratosphere (see Sun et al., 2014, and references therein). The changes in stratospheric planetary wave breaking can drive changes in atmospheric vertical motion that extend to the surface of the earth via downward control (Haynes et al., 1991; Thompson et al., 2006). A second theory proposes that it is changes to the lower stratospheric flow and wave fluxes of momentum at the tropopause level that are important. Both numerical experiments (Kushner and Polvani, 2004; Wittman et al., 2007; Simpson et al., 2009) and theory (Chen and Held, 2007) suggest that changes to the circulation in the lower stratosphere can impact the fluxes of momentum by synoptic waves in the upper troposphere. These changes in upper tropospheric momentum fluxes directly impact on the strength of the prevailing westerlies which can subsequently influence the near-surface climate. However, a consensus has yet to emerge in the literature on the exact mechanism(s) involved in this coupling.

1.2.4 Annular modes of the circulation

A complementary perspective of the coupled variability between the stratosphere and troposphere is offered by the Annular Mode (AM) diagnostics (Thompson and Wallace, 1998, 2000; Kushner, 2010). These diagnostics can be interpreted as measuring the large-scale variations of the extratropical zonal-mean circulation in both hemispheres. In the troposphere, the AM is most often defined as the leading principal component (PC) time series of zonal-mean geopotential height and reflects the meridional wanderings of the EDJ. In the stratosphere, the AM is defined in a similar manner and it reflects both a pulsing in strength and a shifting in latitude of the stratospheric polar vortex. One of the most compelling pieces of evidence for the influence of the stratosphere on the troposphere is found in the so-called ‘dripping-paint’ plots (Baldwin and Dunkerton, 2001; Thompson et al., 2005, see Figure 1-4). These plots show composites of the AM in both the troposphere and stratosphere following weak or strong index events in the stratosphere. In both weak and strong events, a coherent signal is seen to propagate down into the troposphere following the peak of the event in the stratosphere, sometimes persisting for up to several months.

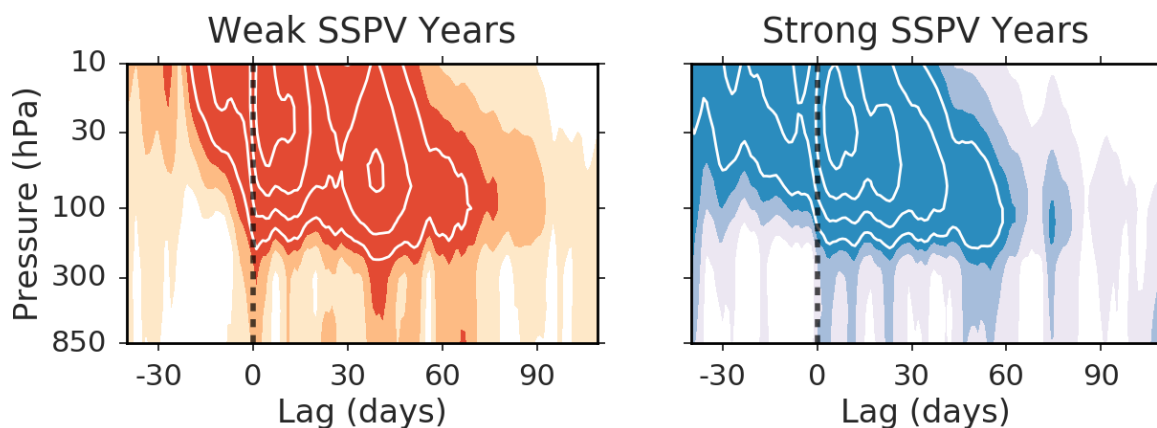


Figure 1-4: (Top) Composite plots of Annular Mode indices for 13 weakest and 13 strongest SH stratospheric polar vortex years (SSPV). Weak and strong years are defined using Annular Mode index at 30 hPa. Dashed vertical line represents onset date (see Chapter 4). Shading and contour intervals are 0.25 and 0.5 standard deviations respectively. Shading is drawn for values greater than ± 0.25 standard deviations. ERA-Interim, 1979-2017.

A variety of statistical measures for analysing AM behaviour have been developed for both hemispheres. These offer further circumstantial evidence of coupled

variability between the stratosphere and troposphere (Gerber et al., 2010). Perhaps the most widely remarked upon of these measures are the AM persistence timescales. These timescales are usually computed as a function of calendar day of the year and it has previously been noted that the longest timescales in the troposphere appear to emerge around the same time of the calendar year in both hemispheres (November to January). This is also the same time of the year where some of the longest timescales are seen in the stratosphere. That some of the longest stratospheric timescales occur at similar times of the calendar year in both hemispheres has been partially understood by the contrasting seasonal evolutions of the stratospheric vortex in both hemispheres (see subsection 1.1.2). That the longest timescales in the troposphere are also seen to emerge during this time has been interpreted as further evidence of a stratospheric influence on the tropospheric circulation. Several mechanistic theories have been proposed to explain this increase in tropospheric timescales, most of which involve the notion of an eddy feedback in the troposphere, but a consensus has yet to emerge.

Long-term trends in the AM have been documented in both hemispheres (Thompson et al., 2000), with those in the SH receiving particular attention in recent years. In the SH, the trends in the Southern Annular Mode (SAM) have been strongly linked to the process of ozone depletion in the stratosphere (Thompson et al., 2011). In the stratosphere, trends in the SAM are associated with a long-term tendency toward a colder and stronger stratospheric vortex in austral spring, due to reduced absorption of solar radiation by ozone. These trends are also associated with a later date of the final vortex breakdown. In the troposphere the trends are less clearly understood. The largest signal is found to emerge in austral summer and is regularly interpreted as a poleward shift of the EDJ. It has been viewed as a response to ozone depletion in the stratosphere, with support for this view emerging independently from both modelling work and observations. It is also consistent with a variety of other studies (for both hemispheres and across a range of timescales) which have linked shifts of the EDJ to perturbations to the strength of the stratospheric vortex (Kidston et al., 2015). However, a theoretical explanation for these tropospheric effects remains elusive.

1.3 Stochastic and deterministic models of circulation variability

The first step in any time series analysis is to remove known regularities in the data (e.g., Trenberth, 1984). For geophysical time series, in order to account for the deterministic variations associated with the annual march of the sun's declination, an annual cycle is usually removed. This is traditionally done by constructing a long-term average for each day or month of the year and subtracting this long-term average from the original time series. The resulting data (often referred to as anomalies) is then treated as some form of stationary stochastic process i.e., the statistics of the anomalies are modelled as being invariant under time translation. This assumption allows the construction of an ensemble (e.g., in determining autocorrelation times). Time series of circulation anomalies traditionally represent the starting point for most statistical investigations of circulation variability.

A pioneering treatment of the stochastic approach to modelling circulation variability was introduced by Hasselmann (1976). He considered a simple forced-damped system which contained two timescales - a fast 'weather' component (m) and a slow 'climate' component (z), along with a damping timescale τ :

$$\frac{dz}{dt} = m - \frac{z}{\tau}. \quad (1.2)$$

He then outlined how this system could produce statistics very similar to those observed for the Earth's climate by parametrising the influence of the weather component on the climate component as a (stationary) stochastic process. An analogy with 'Brownian Motion' from statistical physics was proposed insofar as the climate component was considered to act as an integrator of the stochastic forcing by the weather component. In a follow-on paper (Frankignoul and Hasselmann, 1977), a statistical framework was introduced for diagnosing potential feedback behaviour in such systems. A basic assumption underpinning this framework was that the weather component could again be accurately modelled as a stationary stochastic process.

A more recent example of the stochastic approach that is also relevant to the content of this thesis (see Chapter 2) can be found in Lorenz and Hartmann (2001). Here the authors considered the variability of the SH EDJ and its interaction with mid-latitude eddy momentum flux convergences (EMFC) in re-analysis data. They began by analysing circulation anomalies and presented evidence that the EMFC and

EDJ could be approximately viewed as fast and slow components of the mid-latitude troposphere respectively (see also the close correspondence between equation 1.1 and equation 1.2; this correspondence is exact if the residual momentum forcing term in equation 1.1 is parametrised by a Newtonian damping term). This enabled these authors to employ the stochastic framework of Frankignoul and Hasselmann (1977). They subsequently argued for the existence of a feedback between the EMFC and the EDJ. This feedback is now a well-accepted concept in the literature and represents an important paradigm for interpreting mid-latitude jet variability (e.g., Kushner, 2010). For example, longer persistence timescales for EDJ anomalies are generally identified with stronger positive eddy feedbacks.

Implicit in the stationary stochastic description of circulation anomalies is that all deterministic influences (such as the seasonal cycle) have been removed from the original time series. Time series where significant deterministic components still remain are more appropriately described using a non-stationary model. This duality between deterministic components of a time series and non-stationarity is discussed extensively in Koutsoyiannis (2011) where, as a simple illustration, the problem of modelling streamflow downstream of a dam is considered. For this problem, a non-stationary model is considered most appropriate, as a result of a shift in the statistical characteristics of the streamflow before and after the dam construction.² For geophysical time series in general, non-stationary models of variability are appropriate wherever causative relationships between forcing and climate can be established.

Viewed from this (deterministic) perspective, the stationary stochastic description of mid-latitude circulation anomalies might be regarded as somewhat problematic - there is ample evidence for externally forced influences on this region of the climate system (see Section 1.2). Furthermore, it is also conceivable that the circulation anomalies may still contain a deterministic component related to the phase of the seasonal cycle. This is because for a non-linear system like the Earth's mid-latitudes, multiple seasonal evolutions of the system may be possible, and modelling the seasonal cycle as a long-term average may be overly simplistic (see Section 1.2.2). In the simplest case of two seasonal evolutions which differ by a translation in phase, 'anomalies' can be expected to exhibit a persistent bias, the sign of which depends on whichever seasonal evolution is selected for a given year. Such 'anomalies' will not be most parsimoniously described using a stationary stochastic model.

²However, by accounting for this shift in the statistics in some deterministic manner, perhaps via numerical simulations, the residual data might subsequently be modelled as a stationary process.

In this thesis an alternative deterministic model of the seasonal cycle in the SH mid-latitudes is considered. This model exploits the fact that in the SH, the stratospheric polar vortex progresses downwards and breaks up between austral winter and summer every year. It is proposed that circulation variability in the stratosphere is best viewed as variability about these deterministic components of the seasonal cycle i.e., the shift-down and the break-up of the vortex. Coupled variability between the stratosphere and the troposphere during austral spring and summer is then used to develop a related model for the tropospheric seasonal cycle. Both of these models are deterministic insofar as the shift-down and the breakup of the stratospheric vortex is expected to occur every year.

1.4 Outline and contributions

Following this introductory chapter, Chapter 2 of this thesis revisits the work of Lorenz and Hartmann (2001, 2003) from the perspective of externally forced influence on the mid-latitude tropospheric circulation. It is based on Byrne et al. (2016). The chapter begins by presenting evidence of a distinct quasi-two-year periodicity to EMFC variability in the troposphere. This quasi-two-year periodicity is interpreted as evidence for externally-forced influence on the mid-latitude circulation. The consequences of this external forcing are then considered for the results of Lorenz and Hartmann (2001, 2003). It is argued that positive lagged correlations previously attributed to the existence of an eddy feedback are more plausibly attributed to non-stationary interannual variability external to any potential feedback process. Furthermore, the lagged correlations are found to be largely restricted to austral spring and summer, suggestive of an influence from the stratosphere (see Section 1.2.3).

Chapter 3 builds on this notion of a stratospheric influence on the tropospheric jet during austral spring and summer. It is based on Byrne et al. (In press). A deterministic model of the mid-latitude circulation around the time of the stratospheric vortex breakdown is first proposed. It is then shown how this model is consistent with previous results in the literature if a non-stationary model of circulation anomalies is permitted. Finally, the implications of this perspective of circulation variability for several previous results in the literature are considered. For example, the summer-time poleward shift of the SAM in response to the ozone hole is interpreted instead as a delayed equatorward shift.

Chapter 4 extends the results of the previous chapters by incorporating the down-

ward shift of the stratospheric vortex into the deterministic model from chapter 3. The chapter begins by investigating the extent to which the stratospheric vortex breakdown event can be predicted in a seasonal forecasting sense. The impact of the QBO on the timing of the downward shift of the vortex is then briefly considered. Next, the extent to which the EDJ in the troposphere is coupled with the vortex in the stratosphere during austral spring and summer is considered, along with the impact of this coupling on the SAO in the troposphere. Finally, an assessment is made of the potential for skilful seasonal forecasting in the troposphere during this time of the year. The material of this chapter has been submitted as a journal article to *Journal of Climate*.

Chapter 5 concludes the thesis by summarising the results and discussing the implications of the work for the broader field. Possible future work stemming from the results of the thesis is also presented.

1.4.1 Methods

A small subset of standard statistical methods is used for analysing the data in this thesis. In Chapter 2 a spectral analysis is performed following the procedures outlined in Bloomfield (2000). A discussion on the degrees of freedom involved in this analysis, the statistical significance of the analysis and the robustness of the analysis to splitting the data into various subsets can be found in 2.C. All correlation calculations in this thesis are performed following the procedures outlined in 2.A. These calculations include the SAM persistence timescales in Chapter 3 as well as the correlation calculations of Chapter 4. EOF analysis is employed throughout the thesis and follows the procedures outlined by North et al. (1982). A variant of EOF analysis (referred to as ‘multiple EOF analysis’) is employed in Chapter 4; further details can be found in 4.3.1. Unless otherwise stated, all statistical significance tests in this thesis involve a one or two-sided Student’s t-test.

Chapter 2

Annular modes and apparent eddy feedbacks

2.1 Introduction

Fluctuations in the strength and location of the zonally averaged westerlies have long been recognised as an important pattern of atmospheric low-frequency variability. Such fluctuations are also seen across a wide hierarchy of numerical models.

The study of these variations is frequently investigated with the use of Empirical Orthogonal Function (EOF) analysis. This has the effect of significantly reducing the dimensionality of the data to be analysed while arguably preserving the underlying physical mechanisms. In the Southern Hemisphere the leading EOF of the zonal wind anomalies is referred to as the Southern Annular Mode (SAM). It is the dominant pattern of climate variability affecting the Southern Hemisphere extratropics, is present in every season and is interpreted as a poleward/equatorward shift of the westerlies (Hartmann and Lo, 1998).

It is well established from physical principles that momentum flux convergence anomalies (hereafter referred to as ‘anomalous eddy flux convergence’) force the zonal wind anomalies. This can be seen by considering the zonally and vertically integrated quasi-geostrophic momentum equation:

$$\frac{dz}{dt} = m - \frac{z}{\tau}. \quad (2.1)$$

Here z represents an index for the zonal wind anomalies, m an index for the anomalous eddy flux convergence and τ a timescale approximating damping of the zonal wind

anomalies by frictional processes (see Chapter 1, Section 1.3).

As a result of the equivalent barotropic structure of the SAM, equation (2.1) is often used as a conceptual model for studying SAM dynamics. In this case z represents SAM variations and m represents an index for the anomalous eddy flux convergence projected onto the SAM. This approximation is found to hold well in re-analysis data (Lorenz and Hartmann, 2001).

In the presence of white-noise forcing by m (anomalous eddy flux convergence) such a system is known to exhibit low-frequency variability in z (SAM) (e.g., Hasselmann, 1976). For the true climate system it is of considerable interest whether the low-frequency variability in the SAM is also modified by the existence of a feedback process on the anomalous eddy flux convergence, behavior which has previously been shown to exist in idealised numerical models (e.g., Robinson, 1996). Such a (positive) feedback could act to increase the persistence of the SAM and could thus account for much of the low-frequency variability in the extratropics.

An understanding of the relationship between the SAM and the anomalous eddy flux convergence is thus important for the problem of predicting the intraseasonal variability of the zonal wind in the extratropics. It is also of considerable importance for quantifying the long-term response to climate forcing (e.g., Ring and Plumb, 2007, 2008).

To diagnose potential feedback behavior a framework has been developed using the method of lagged regression analysis (Hasselmann, 1976; Frankignoul and Hasselmann, 1977). This framework requires that there be a clear timescale separation between the components of the system (in this case between the anomalous eddy flux convergence and the SAM) and assumes the feedback to be a linear process. Such a timescale separation between the anomalous eddy flux convergence and the SAM has been previously verified in re-analysis data (Lorenz and Hartmann, 2001).

In the lagged regression framework, for those lags where the anomalous eddy flux convergence leads the SAM, increasing correlation values have been found from about twenty days up to two days (e.g., Feldstein, 1998). This is as expected theoretically for a system that obeys equation (2.1). More significantly, positive correlations at lags where the SAM leads the anomalous eddy flux convergence have also been documented and these have been attributed to the presence of an eddy feedback mechanism (e.g., Lorenz and Hartmann, 2001). This eddy feedback mechanism is now a well-accepted concept in the literature (e.g., Kushner, 2010).

Causal attribution in this lagged regression framework is subject to the additional

assumption that the low-frequency portion of the power spectrum of the anomalous eddy flux convergence is white in the absence of a feedback (Frankignoul and Hasselmann, 1977) i.e., that the anomalous eddy flux convergence is not influenced by non-stationary interannual variability. This is a significant assumption as there is ample evidence of interannual variability in the mid-latitude troposphere of both hemispheres that is externally forced e.g., from the tropics or the stratosphere (L’Heureux and Thompson, 2006; Lu et al., 2008; Simpson et al., 2011; Anstey and Shepherd, 2014). In light of this we revisit earlier results to see if they can be more naturally explained in terms of non-stationary interannual variability in the extratropics.

2.2 Data and methods

We use four-times-daily wind data from the ERA-Interim re-analysis dataset for the period January 1980 - December 2013 (Dee et al., 2011). Data was available on an N128 Gaussian grid and on 27 pressure levels (1000 - 100 hPa). The indices for the SAM and for the anomalous eddy flux convergence were computed using daily mean values as per Lorenz and Hartmann (2001).

The cross-correlation plots were estimated following Von Storch and Zwiers (2002) (see 2.A). To assess significance of the cross-correlation values a formula suggested by Bartlett (see section 12.4.2 of Von Storch and Zwiers, 2002) was used throughout (see 2.B).

For the spectral analysis the year-round indices for the SAM and for the anomalous eddy flux convergence were first windowed by a Hanning window. The raw periodogram was then computed from this windowed data. Finally a smoothed estimate of the spectrum was calculated by successive application of modified Daniell filters of length 6, 12 and 12 to the raw periodogram following Bloomfield (2000).

2.3 Results

2.3.1 SAM and anomalous eddy momentum flux convergence power spectra

To investigate the hypothesis of externally forced influence on the SAM and the anomalous eddy flux convergence, power spectra from re-analysis data were computed (Figure 2-1 and Figure 2-2). The power spectrum of the SAM is shown in Figure

2-1a and Figure 2-2a. It offers evidence that there is considerable variability on interannual timescales with increasing power at lower frequencies. This increase of power at lower frequencies is in qualitative agreement with theoretical predictions from equation (2.1) (Hasselmann, 1976).

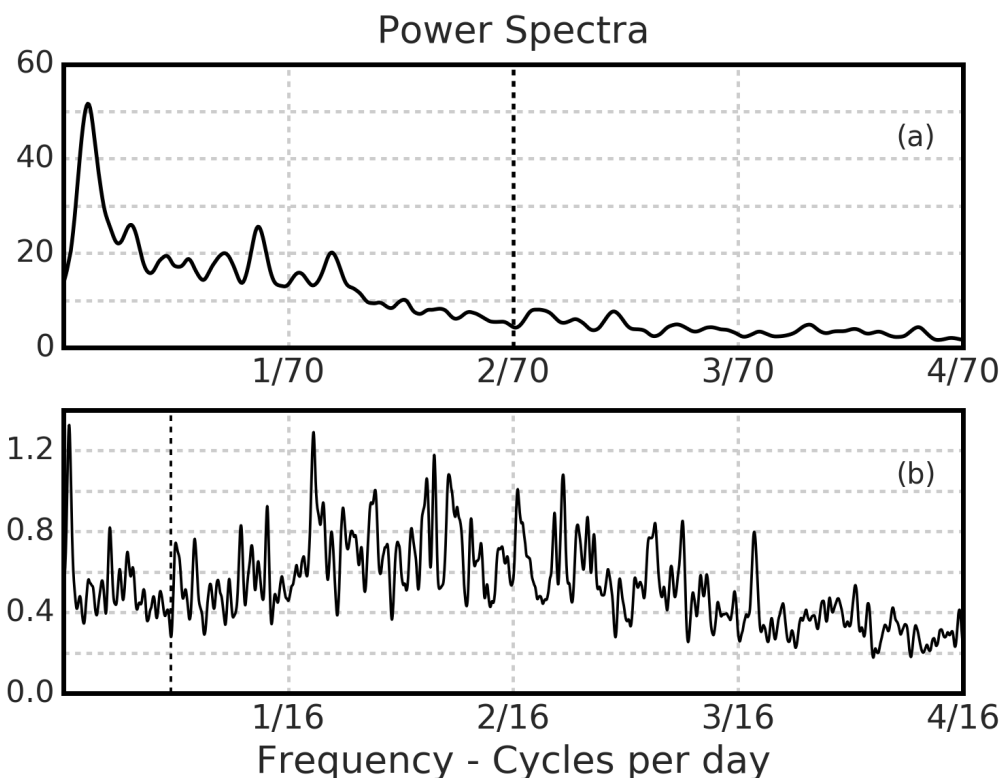


Figure 2-1: Power spectral density plots for (a) z and (b) m . Different limits are used for the x axis in (a) and (b) for visual purposes. The black dashed vertical lines correspond to the cutoff period of 35 days used in Figure 2-2. Units are (a) $\Delta\omega^{-1}$ and (b) $s^{-2} \Delta\omega^{-1}$, where $\Delta\omega = (34 \text{ years})^{-1}$.

We find that the power spectra of both the anomalous eddy flux convergence and the SAM exhibit a pronounced quasi-two-year peak (see Figure 2-1b and Figure 2-2b and also see 2.C). In contrast to the inherent high-frequency variability of the eddies (Figure 2-1b), this low-frequency peak occurs on climate timescales.

To determine whether this peak is consistent with an eddy feedback or in fact represents non-stationary interannual variability, we consider here whether the spectral peak can be reproduced by assuming a linear model of the feedback. Specifically

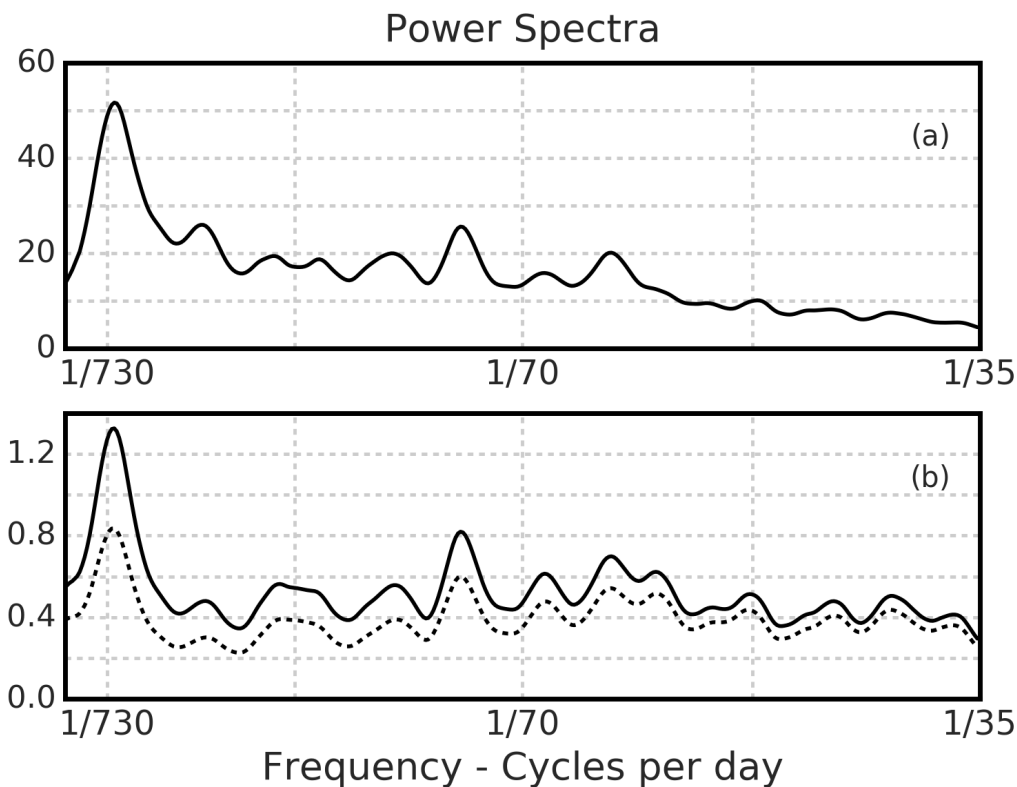


Figure 2-2: Power spectral density plots for the low-frequency segments (periods greater than 35 days) of (a) z and (b) m . The black dashed line in (b) represents the power spectral density plot of $m - bz$ for a value of $b = 0.035 \text{ s}^{-1}$. Units are (a) $\Delta\omega^{-1}$ and (b) $\text{s}^{-2} \Delta\omega^{-1}$, where $\Delta\omega = (34 \text{ years})^{-1}$.

we assume that the anomalous eddy flux convergence index m can be written as:

$$m \equiv \tilde{m} + bz \quad (2.2)$$

where \tilde{m} represents a moving average process of order seven and b represents a constant feedback parameter that can be estimated from re-analysis data. This is consistent with previous work in the literature (e.g., Frankignoul and Hasselmann, 1977; Lorenz and Hartmann, 2001). As mentioned in Section 2.1 a necessary condition for this model to be valid is that, in the absence of a feedback, the low frequency portion of the anomalous eddy flux convergence power spectrum is white i.e. that $m - bz$ has no low frequency peaks.

To test the validity of this assumption, power spectra for $m - bz$ were constructed from re-analysis data for a range of values of b . Previous work has estimated a

value of $b = 0.035 \text{ s}^{-1}$ for the feedback parameter (Lorenz and Hartmann, 2001) and the power spectrum for this value is shown in Figure 2-2b. It is clear that the assumption of ‘white-noise’ behavior is not appropriate as there is still a noticeable peak at a quasi-two-year timescale. This is also the case for other plausible values of b (not shown).

Monte Carlo simulations were performed to provide a more quantitative confirmation of this result. Synthetic models of \tilde{m} were generated and the maximum amplitude of the low-frequency peaks in each synthetic model was compared against that from re-analysis data. For all values of b considered the results are statistically significant at the 1% level at least i.e. the simulations were unable to reproduce a low-frequency peak of similar amplitude to that seen in Figure 2-2b. This leads us to conclude that linear feedback models are unable to explain the low-frequency behavior of the anomalous eddy flux convergence.

2.3.2 Causal attribution and lag regression

Some insight can be gained into how non-stationarity of the data affects causal attribution in the lag regression framework by constructing synthetic time series for m and z that explicitly include external influence. Specifically we consider a model of the anomalous eddy flux convergence of the form:

$$m \equiv \tilde{m} + \alpha F \quad (2.3)$$

Here \tilde{m} is taken as a moving average process of order seven as before and F as an autoregressive process of order one to crudely approximate some general external forcing. The e-folding time of F and the constant α were chosen so that the power spectrum of the synthetic m matched well with that from re-analysis data (not shown). A time series z can then be generated using equation (2.1). Note that this model has no feedback by construction and is distinct from the previous linear feedback model as F is not a function of z .

A sample cross-correlation plot for this model is shown in Figure 2-3b and can be compared with the corresponding plot from re-analysis data in Figure 2-3c. For reference, a sample cross-correlation plot for a model with no external forcing (i.e. with $\alpha = 0$) is also shown in Figure 2-3a. Positive correlations at positive lags are seen to be present in both Figure 2-3b and Figure 2-3c and are of a similar magnitude. In the model simulations we are able to definitively attribute the positive correlations

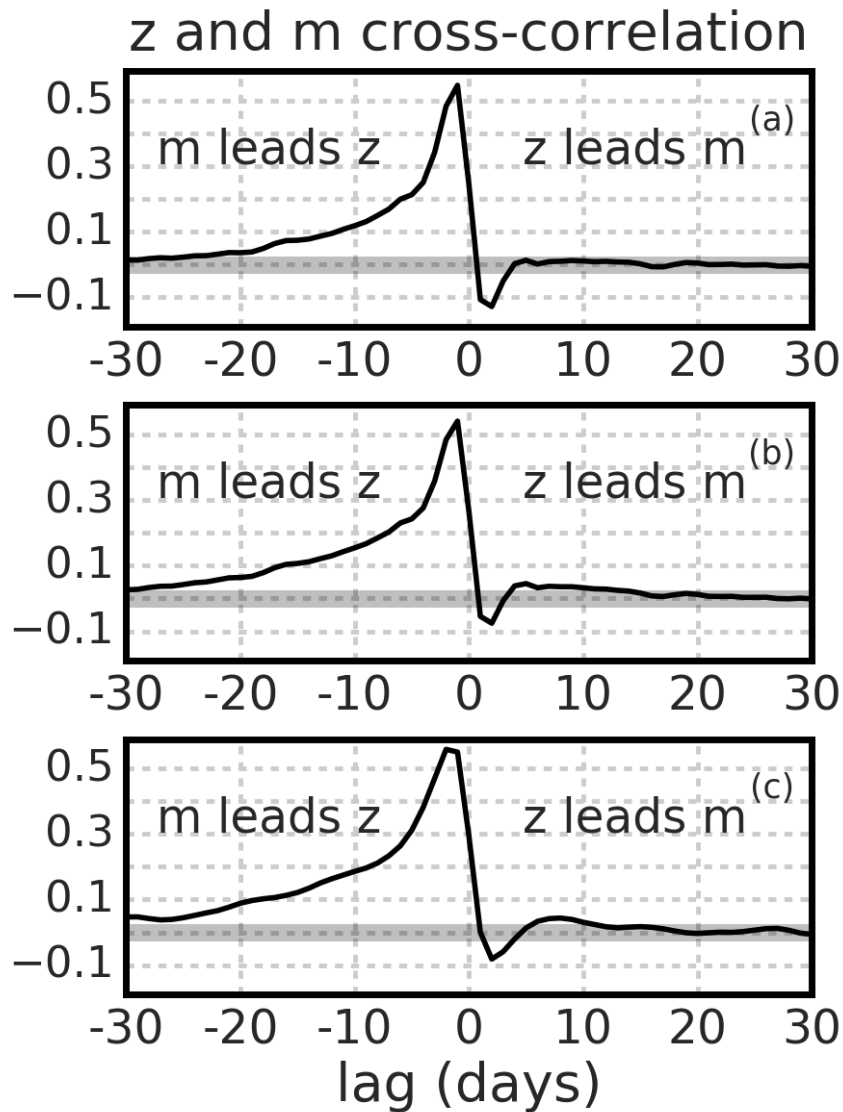


Figure 2-3: (a) Synthetic time series cross-correlation plot for z and m with no external forcing term F . (b) Synthetic time series cross-correlation plot for z and m with external forcing term F . See text for details. (c) Cross-correlation plot of z and m using year-round reanalysis data. Update of Figure 5 from Lorenz and Hartmann [2001]. Grey shading represents 5% significance level according to the test of Bartlett (see 2.B).

to external influence on m rather than to the presence of eddy-zonal flow feedbacks. This provides quantitative evidence that lag regression plots alone are not sufficient to distinguish between external forcing or a potential feedback.

2.3.3 Seasonality of the lag regression plots

Further evidence that the positive correlations at positive lags in re-analysis data represent non-stationary interannual variability rather than a feedback is provided by analysis of seasonal cross-correlation plots of the SAM and the anomalous eddy flux convergence. The cross-correlation plots for various seasons in the Southern Hemisphere are shown in Figure 2-4 along with the cross-correlation plot for year-round data.

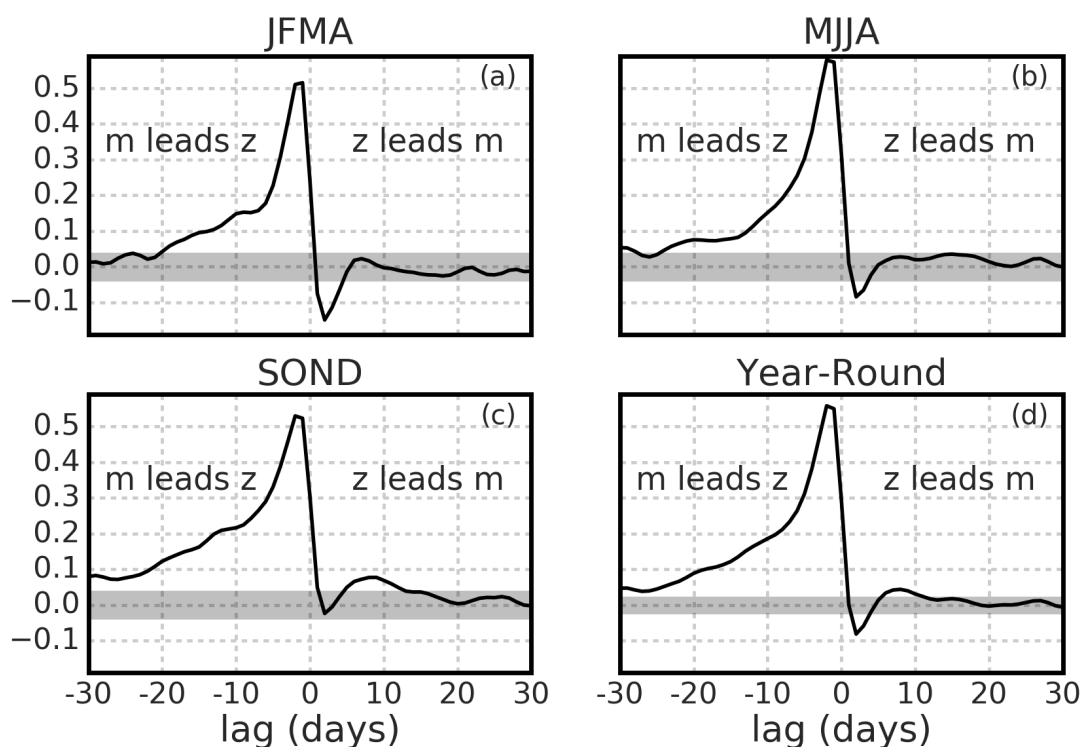


Figure 2-4: Seasonal cross-correlation plots of z and m for (a) JFMA (b) MJJA (c) SOND (d) year-round data. Grey shading as in Figure 2-3.

It is immediately clear that statistically significant positive correlations at positive lags are visible only in austral spring (primarily between September and December) and that this time of year makes the dominant contribution to the positive correlations in year-round data in Figure 2-4d. Austral spring is the relevant time

period for Southern Hemisphere stratospheric interannual variability which, through stratosphere-troposphere coupling, is a known source of tropospheric interannual variability (e.g., Simpson et al., 2011; Anstey and Shepherd, 2014). It is also the relevant time-period for coupling between the extratropics and ENSO in the Southern Hemisphere (e.g., L’Heureux and Thompson, 2006). This seasonal synchronization, combined with the fact that there is no a priori reason why a feedback should be most evident in Southern Hemisphere spring, leads us to conclude that the positive correlations at positive lags most likely represent the influence of non-stationary interannual variability external to any potential feedback process.

2.4 Discussion and conclusion

We have revisited the apparent eddy feedback on SAM persistence inferred from lagged correlation analysis of re-analysis data. The SAM power spectrum also suggests that interannual variability might be organised in a very particular way as there is a distinct peak at a quasi-two-year period. The statistical significance and robustness of these peaks are discussed in 2.C. Linear models of eddy feedback are unable to account for this low-frequency peak which ultimately leads to a breakdown of the statistical assumptions required to infer causality from re-analysis data. We also show through a synthetic time series argument that positive lagged correlations very similar to that seen in re-analysis data can be induced by a slowly-varying forcing that provides long-term memory to the anomalous eddy flux convergence, without an eddy feedback process. We conclude that the lagged correlation approach cannot distinguish between an internal eddy feedback mechanism and the presence of non-stationary (i.e. externally forced) interannual variability.

Additionally we find that the inflated lagged correlations have a particular seasonal dependence. They are only seen in austral spring which is a period of known stratosphere-troposphere coupling and tropical-extratropical coupling. All of the above features, together with the known influence of externally forced interannual variability, lead us to conclude that the simplest and most robust explanation of the positive lagged correlations at positive lags seen in re-analysis data is not eddy feedback but non-stationary interannual variability. Note that our results do not disprove the existence of an eddy feedback in the real atmosphere. We argue only that the positive observed lagged correlations should not be interpreted as evidence in favour of an eddy feedback or used to quantify the strength of a purported eddy feedback.

A companion study has also been performed for Northern Hemisphere winter (Lorenz and Hartmann, 2003) which likewise relies on the lagged correlation approach for inferring causality. Whilst the present analysis approach relies on year-round data and hence cannot be applied to Northern Hemisphere winter, the same caveats over causal inference from lagged correlations still apply. In particular, stratospherically forced influence on the Northern Hemisphere extratropical troposphere during the winter season has been well documented (e.g., Baldwin and Dunkerton, 2001; Anstey and Shepherd, 2014) and it is unclear what effect these influences will have on the lagged correlations.

These results illustrate that lagged correlations are not a reliable indicator of causal inference when the time series is non-stationary. Such non-stationary behavior also appears to be present in several global climate models (Aditi Sheshadri, personal communication, 2016). The results have implications for the estimation of Annular Mode timescales from autocorrelations in both observations and models, especially when used in the context of the fluctuation-dissipation theorem.

2.A

For a sample (X_t, Y_t) , the estimator of the cross-covariance function was constructed as

$$c_{xy}(\tau) = \frac{1}{T} \sum_{t=1}^{T-\tau} (x_t - \bar{x})(y_{t+\tau} - \bar{y}), \tau \geq 0 \quad (2.4)$$

$$= \frac{1}{T} \sum_{t=1}^{T-|\tau|} (x_{t+|\tau|} - \bar{x})(y_t - \bar{y}), \tau < 0 \quad (2.5)$$

where the bar represents the sample mean (e.g. for the seasonal cross-correlation plots $\bar{x} = \frac{1}{NL} \sum_{j=1}^N \sum_{i=1}^L x_{i,j}$, where i represents the day of the season and j represents the year). For the seasonal cross-correlation plots, the sample cross-covariance functions for each year were averaged together to arrive at a final estimate for the sample cross-covariance function. The cross-correlation function was then estimated as

$$r_{xy}(\tau) = \frac{c_{xy}(\tau)}{[c_{xx}(0)c_{yy}(0)]^{\frac{1}{2}}} \quad (2.6)$$

2.B

For stationary normal processes (X_t, Y_t) with true cross-correlation function $\rho_{xy}(\tau)$ zero for all τ outside some range of lags $\tau_1 \leq \tau \leq \tau_2$ then

$$\text{Var}(r_{xy}(\tau)) \approx \frac{1}{T - |\tau|} \sum_{l=-\infty}^{\infty} \rho_{xx}(l)\rho_{yy}(l) \quad (2.7)$$

for all τ outside the range.

To determine whether an estimated cross-correlation $r_{xy}(\tau)$ is consistent with the null hypothesis that $\rho_{xy}(\tau)$ is zero an appropriate test at the 5% significance level is performed as follows. The estimated variance s^2 of r_{xy} is obtained by substituting the estimated auto-correlation functions for X_t and Y_t into equation (2.7). If $|r_{xy}(\tau)| > 2s$ then the null hypothesis is rejected at the 5% significance level.

2.C

Lorenz and Hartmann (2001) proposed that the anomalous eddy flux convergence time series could be modelled as a moving average process (see their Appendix B). This was also the approach that was adopted in this thesis. The parameters of the moving average model were chosen so that the generated synthetic time series had a similar autocorrelation to that of the observational time series. Using the moving average model, 10000 synthetic time series of length 12410 were generated. These synthetic time series were then normalised to have identical variance to the anomalous eddy flux convergence time series from observations. Finally, a power spectrum for each of these time series was calculated in an identical manner to the observational power spectrum, and 95%, 99% and 99.9% confidence intervals were calculated for each frequency bin estimate. All of these calculations, along with the ensemble mean power spectrum, are shown by the red lines in Figure 2-5. The black line represents the observational power spectrum. The quasi-two-year peak is seen to be significant at the 0.1% level.

To test the statistical significance of the quasi-two-year peak in the SAM, a null hypothesis of variability consistent with an autoregressive process of order 1 (a so-called ‘red-noise’ process) was considered. Analysis was performed in a similar manner to the anomalous eddy flux convergence power spectrum analysis, by first generating an ensemble of synthetic time series with the appropriate statistical properties, and

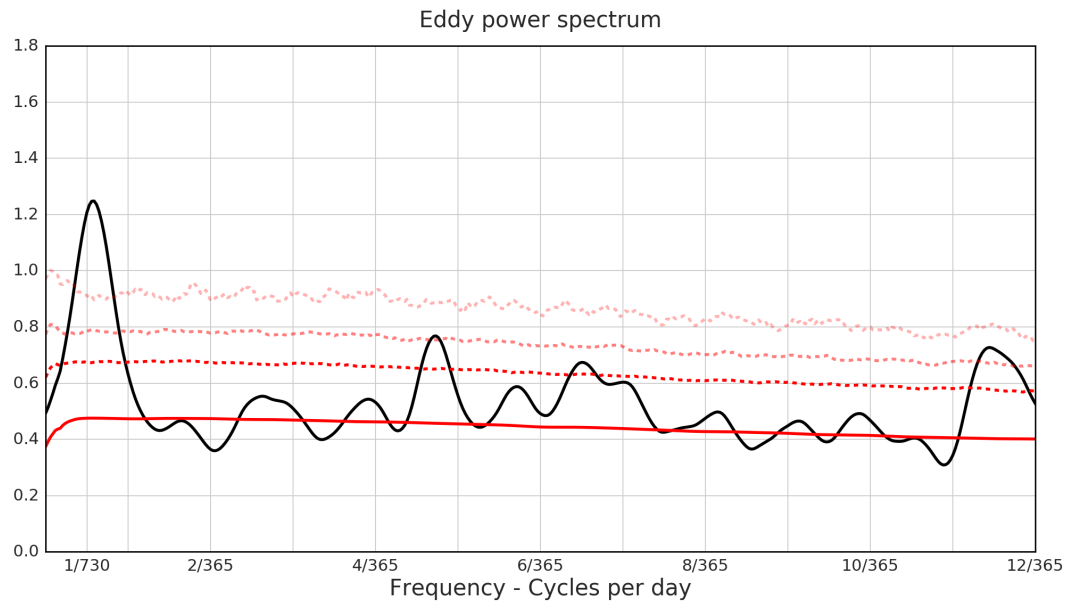


Figure 2-5: Anomalous eddy momentum flux convergence power spectrum from observations, along with simulated (red) confidence intervals (see text for details).

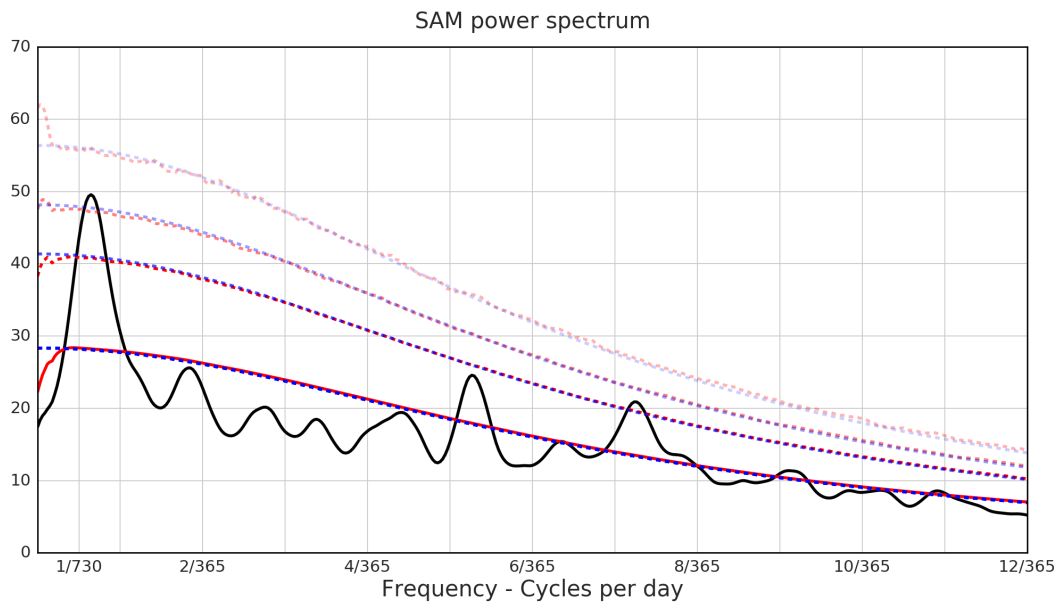


Figure 2-6: SAM power spectrum from observations, along with simulated (red) and theoretical (blue) confidence intervals (see text for details).

then estimating power spectra for each of these time series. The results are shown in Figure 2-6. Theoretical estimates of the various confidence intervals were also calculated assuming an F-distribution of the test statistic and 30 degrees of freedom in the

sample. These are indicated by the blue lines in Figure 2-6. In both the synthetic and theoretical calculations, the quasi-two-year peak is seen to be significant at the 1% level. Similar calculations for the first and second half of the observational record are also shown in Figure 2-7. It should be noted that the null hypothesis cannot be rejected during the first half of the record.

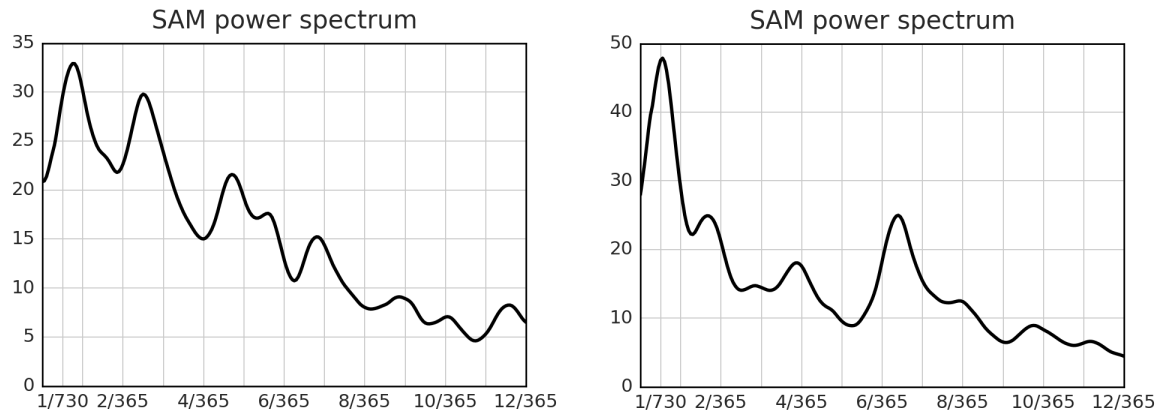


Figure 2-7: SAM power spectrum during the first half (left) and second half (right) of the observational record.

Chapter 3

The seasonal breakdown of the SH stratospheric polar vortex

3.1 Introduction

The interval encompassing late spring and summer represents a timeframe of uncommon interest for Southern Hemisphere (SH) climate variability. The stratosphere-troposphere coupling evident in the Southern Annular Mode (SAM) pattern of variability maximizes during this period (Thompson and Wallace, 2000). There is a concomitant increase in SAM persistence timescales, which suggests potential for skilful seasonal forecasting (Baldwin et al., 2003; Kidston et al., 2015). The teleconnection between the El Niño-Southern Oscillation (ENSO) and SH high-latitude climate also maximizes during this period (Seager et al., 2003; L’Heureux and Thompson, 2006). Finally, the largest changes in the SH circulation over the past half-century have occurred during the summer season (Fogt et al., 2009). Modelling studies have implicated stratospheric ozone depletion as the most likely driver of these changes (see Thompson et al., 2011, and references therein), and indeed they represent the only observed circulation changes so far attributable to human influence (IPCC, 2013). Despite much study of these various phenomena, the responsible mechanisms have yet to be conclusively identified.

In all these studies, the approach has been to regard the intraseasonal and inter-annual variability, and the long-term changes, as anomalies about the climatological seasonal cycle. The statistical methods used then generally treat those anomalies in the usual way as a stationary stochastic process (i.e. with statistics that are invari-

ant under time translation) plus a long-term seasonally-dependent trend. However, Chapter 2 has argued that the variability of the SH zonal-mean circulation should not be treated as a stationary stochastic process because of the presence of non-stationary interannual variability, which exhibits a strong two-year peak in the EMFC. The effect is most pronounced between late spring and early summer. These two features point to the role of the stratosphere.

Black and McDaniel (2007) suggested that the annual spring breakdown of the stratospheric polar vortex acts as an organising influence on the variability of the SH zonal-mean circulation, although they found only a weak influence on the zonal-mean tropospheric circulation. More recently, Sun et al. (2014) used both re-analyses and a hierarchy of models to argue that the long-term changes in the vortex breakdown dates were responsible for the long-term changes in the zonal-mean tropospheric circulation. That the vortex breakdown event can act as an organising influence on tropospheric variability implies that a stationary model of tropospheric variability is suspect, given that the vortex breakdown is a singular event within the seasonal cycle which breaks time symmetry. Moreover, the breakdown event itself is known to be affected by non-stationary sources of variability such as the Quasi-Biennial Oscillation (QBO) and solar cycle (e.g., Anstey and Shepherd, 2014). Rather than viewing variability (and long-term changes) of SH late spring and early summer circulation as anomalies to a climatological seasonal cycle, it may be more useful to regard it as variability in the seasonal transition between spring and summer, which is organised around the date of the stratospheric vortex breakdown. The purpose of this chapter is to explore the implications of this perspective for the various topics mentioned earlier.

3.2 Data and methods

The basic data input for our study is four-times daily zonal wind data from the ERA-Interim re-analysis dataset (Dee et al., 2011) for the period June 1 1979 to May 31 2016. This period encompasses 37 years in the SH in total. Data was available on an N128 Gaussian grid and on 37 pressure levels (1000 - 1 hPa). Before analysing the data we first processed it by forming a daily and zonal average of the data. This processed data formed the input for all of our subsequent analysis. We define a climatology of our data as the long-term daily average that is subsequently smoothed by retaining the first six Fourier harmonics (Black et al., 2006; Black and McDaniel,

2007). We define a daily jet latitude index by mass-weighting our data, vertically averaging it between 1000 and 250hPa and subsequently computing the latitude of the maximum daily value of this average between 0° and 90° S. We identify the date of the vortex breakdown as the final time that the zonal-mean daily-mean zonal wind at 60° S drops below 10m s^{-1} ; we apply this criterion to running 5-day averages at 50hPa (Black and McDaniel, 2007). We define early and late breakdown events as the 18 earliest and latest breakdown events (separated by one median event, 1993).

We define a SAM index for each pressure level of our data in a similar manner to Simpson et al. (2011). First we compute daily anomaly data by removing a daily climatology. Next we perform an empirical orthogonal function (EOF) analysis between 20° and 90° S and at each individual level; we weight our data to account for the decrease in area toward the pole (North et al., 1982). Finally we define our SAM index as the normalised principal component time series that results from our EOF analysis. To compute our SAM autocorrelation function e-folding timescale we follow the method of Mudryk and Kushner (2011) (see also Simpson et al., 2011). We obtained our time series for effective equivalent stratospheric chlorine (EESC) from the Goddard automailer. Our EESC time series was generated by specifying a mean age-of-air of 5.5 years (Newman et al., 2006), which is appropriate for the ozone hole. Linear trends and EESC regression values are calculated for each day of the year after the daily data are first smoothed using a Gaussian window with a 7-day half-width (Sun et al., 2014).

Variations in ENSO are defined using the Niño 3.4 sea-surface temperature index obtained from the NOAA Earth System Research Laboratory website. This index was detrended and standardised using the same time period as our re-analysis data prior to analysis. ENSO episodes are defined using the Oceanic Niño Index (ONI), according to the NOAA Climate Prediction Center definition. Specifically, El Niño episodes are defined as 5 consecutive overlapping 3-month periods at or above the $+0.5^\circ$ anomaly relative to the base period chosen for the ONI, while La Niña episodes are defined as 5 consecutive overlapping 3-month periods below the -0.5° anomaly relative to the base period. Periods where neither of these criteria are met are referred to as neutral episodes. We do not distinguish between the strength of ENSO episodes.

3.3 Composite analysis

3.3.1 Climatology

We employ zonal-mean zonal wind ($[u]$) as a measure of the large-scale extra-tropical circulation. From late October until the following May, the dominant feature in $[u]$ in the SH troposphere is an approximately equivalent barotropic jet in the extra-tropics which extends to the surface (e.g., Hartmann and Lo, 1998). Snapshots of this structure, for the months of November and December, are shown in Figure 3-1 for reference.

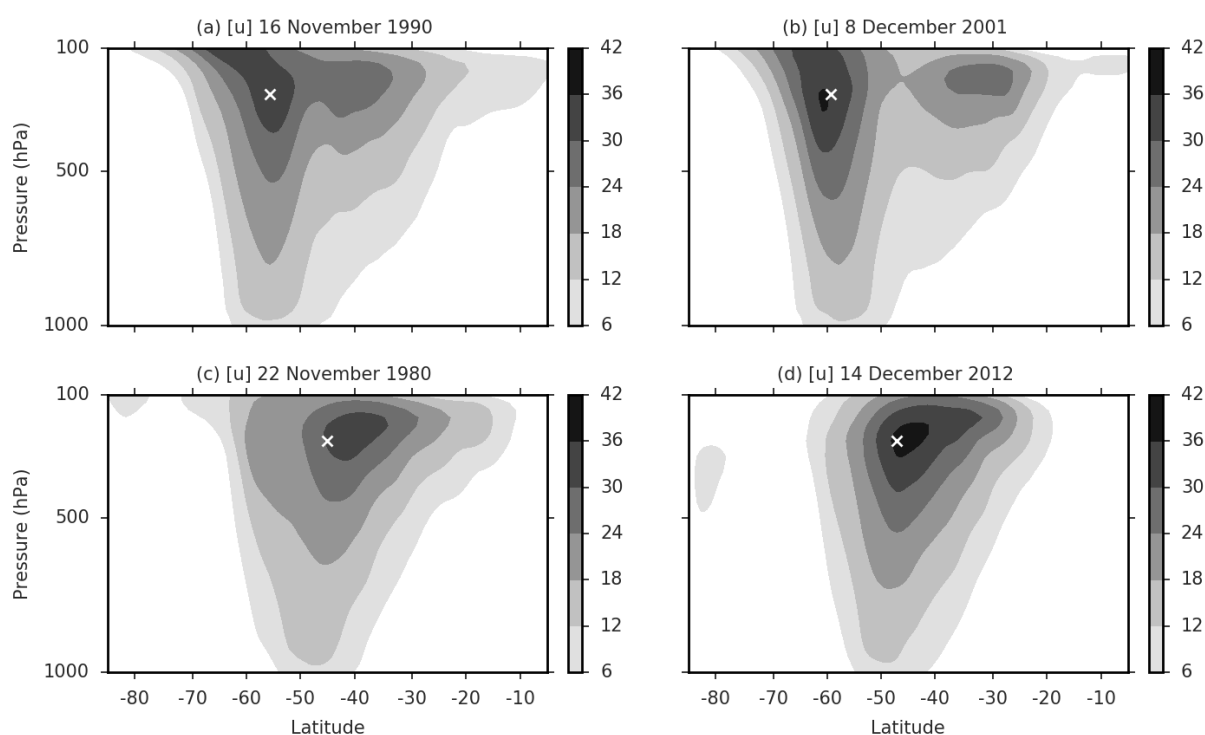


Figure 3-1: Daily-mean snapshots of $[u]$. Units are m s^{-1} . Values below 6 m s^{-1} have been masked for presentation purposes. Crosses denote the daily latitude of the jet according to our jet latitude index.

This structure is frequently referred to as the eddy-driven jet and hereafter we refer to it simply as the jet. Definitions for the daily latitude of the jet commonly exploit either its lack of vertical tilt (equivalent barotropic property) or the strength of the near-surface winds in the region of the jet (surface extension property). We make use of the equivalent barotropic property and define the latitude of the jet as the latitude

of the maximum value of the mass-weighted vertical average of $[u]$ between 1000 and 250 hPa. For the remainder of the paper we denote this vertical average as $\langle[u]\rangle$.

Figure 3-2 shows the climatological seasonal cycle of $\langle[u]\rangle$ from the middle of October (mid/late spring) until the middle of January (mid summer). In a climatological sense, the jet is seen to exist at a more poleward latitude in mid/late spring compared to early summer. This description also appears valid

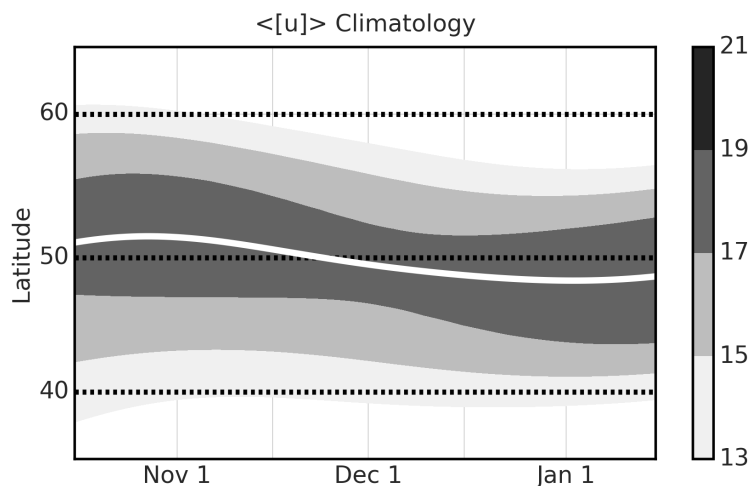


Figure 3-2: Climatology of $\langle[u]\rangle$ (shading) and jet latitude index (white line) from October 16 until January 15. Units are m s^{-1} .

in a more deterministic sense: inspection of individual years reveals that the picture of a more poleward jet in mid/late spring relative to early summer offers a fair description of 33 out of the 37 years considered. The years where this description does not appear appropriate include the spring seasons of 1988 and 2002 along with, to a lesser extent, 1996 and 2007. The climatological plot suggests an equatorward transition between the two states from early November until late December, with a change in jet latitude of the order of 5 degrees over a timescale of the order of 50 days. There is also a hint of a weakening in the strength of the jet during the transition period, as evidenced by the narrowing of the highest contour level. From inspection of individual years there does appear to be some evidence to support this notion of a weakening during the transition period, with some years exhibiting an occasional loss of jet coherence resulting in a relatively broad band of westerlies and weaker surface winds. However, this phenomenon appears to be limited to at most 8 out of the 37 years considered and so for purposes of simplicity, in the remainder of this study we consider the transition between spring and summer to reflect purely a shift in jet

latitude.

A feature that emerges more clearly from inspection of individual years is that the timing of this transition in jet latitude appears to exhibit significant interannual variability. Particular examples of this variability can be seen in Figure 3-1: the top panels represent snapshots of the jet taken from years where the seasonal transition has yet to occur and the bottom panels represent snapshots of the jet in years where the seasonal transition has already taken place. This variability in the timing of the seasonal transition is highlighted in greater detail in the next subsection.

3.3.2 Breakdown date composites

To quantify the organising influence of the breakdown of the stratospheric polar vortex on the variability of the SH circulation, Black and McDaniel (2007) introduced composite plots of the zonal-mean circulation centered around the breakdown date for each year. The breakdown date is subject to substantial interannual variability (see Figure 3-3 for a measure of this variability) and so composite plots were used as a means of isolating the recurring features of the circulation associated with the breakdown event. In several of these composites, circulation anomalies about the climatological seasonal cycle were used as the primary data input (hereafter, unless otherwise stated, we refer to anomalies about a climatological seasonal cycle simply as anomalies). Figure 3-4 is an example of such an anomaly composite; it has been vertically integrated to allow for comparison across latitude bands. At high latitudes in the weeks either side of the breakdown event there is a hint of an organising influence, as suggested by the sharp change in sign of the anomalies around lag 0. However, the anomaly magnitudes are relatively small and cannot clearly be distinguished from natural variability, consistent with Black and McDaniel's finding of a weak influence on the troposphere.

We now construct composite plots of (i) breakdown events that occur either prior to or after the median climatological vortex breakdown event and (ii) the ten earliest and ten latest breakdown events, which represent respectively the lower and upper quartiles of breakdown dates. Hereafter we refer to events prior to and after the vortex breakdown as early and late events, and to the lower and upper quartiles as extreme early and extreme late events. The plots for all of these subgroups are shown in Figure 3-5 and from inspection, it is immediately clear that they all contain very different anomaly patterns to that shown in Figure 3-4. The strengths are also

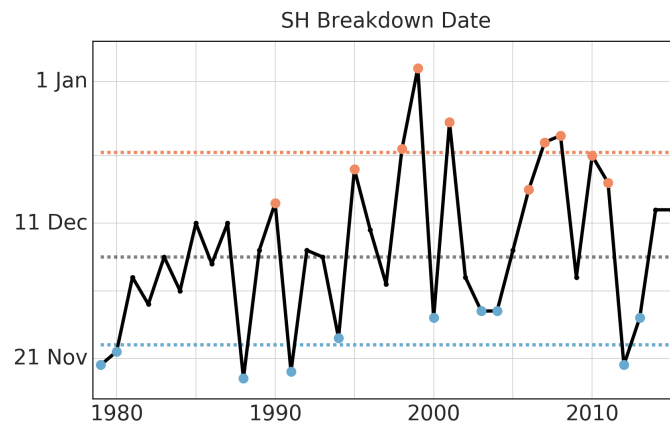


Figure 3-3: Time series of the annual SH stratospheric vortex breakdown date (solid line). The median date is December 6 (grey dashed line). The extreme late and extreme early breakdown years (red and blue dots) along with the median dates for these years (red and blue dashed lines) are also plotted. The breakdown date has been subject to a long-term trend that has been attributed to SH ozone depletion (see Thompson et al., 2011). Updated from Figure 1 of Black and McDaniel (2007).

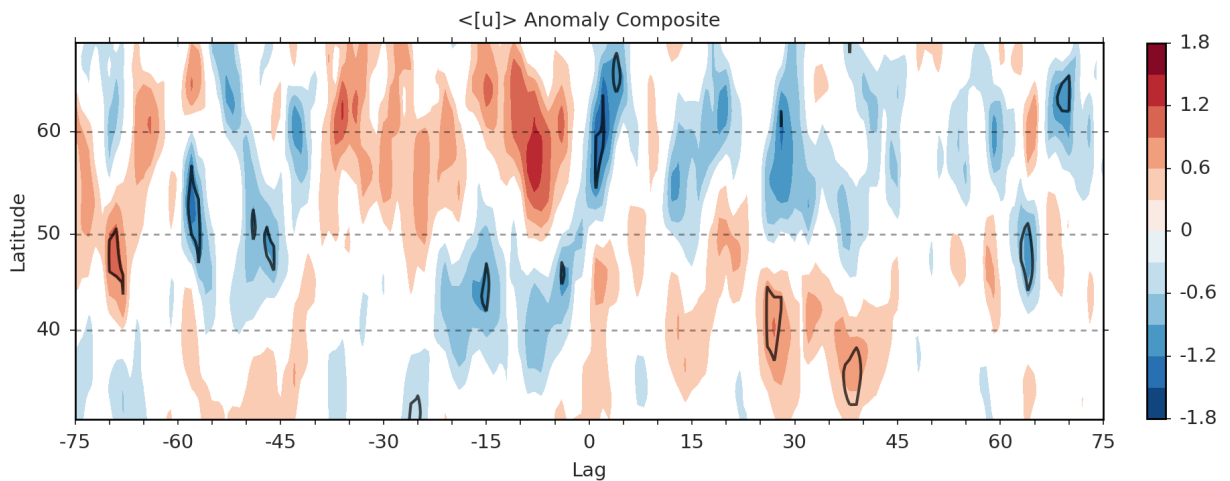


Figure 3-4: Composite plot of $\langle [u] \rangle$ anomalies (shading) centered about the stratospheric vortex breakdown date. Black contours indicate anomalies that are significant at the 5% level, based on a two-sided one-sample Student's t -test for a reference mean value of zero. Units are m s^{-1} . Values between -0.3 and 0.3 m s^{-1} have been masked for presentation purposes.

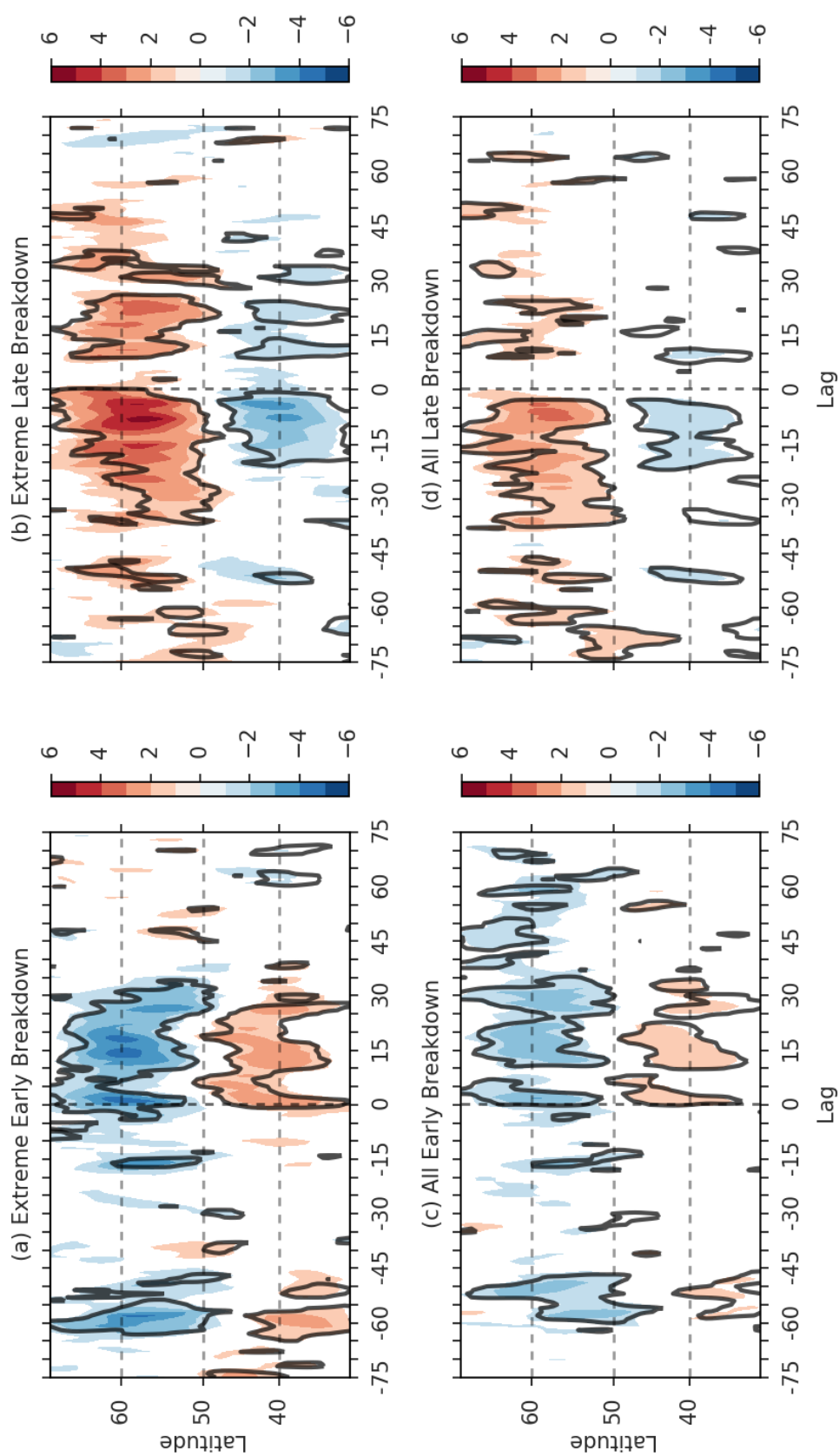


Figure 3-5: Composite plots of $\langle [u] \rangle$ anomalies (shading) relative to the actual stratospheric vortex breakdown date for (a) extreme early years, (b) extreme late years, (c) all early years and (d) all late years. Black contours indicate anomalies that are significant at the 5% level, based on a one-sided one-sample Student's t -test for a reference mean value of zero. Units are m s^{-1} . Values between -1 and 1 m s^{-1} have been masked for presentation purposes.

very different - note the very different colour scale - and clearly distinguishable from natural variability. Early breakdown years are seen to be associated with persistent high-latitude negative anomalies that are particularly prominent between lags 0 and +30. Late breakdown years are seen to be associated with persistent high-latitude positive anomalies that are particularly prominent between lags -40 and 0, and to a lesser extent between lags +10 and +30. Opposite-signed anomalies are seen in mid-latitudes. Anomaly magnitudes for both early and late breakdown years are seen to be enhanced for extreme breakdown events, which offer an illustration of how different the actual circulation can be compared to that predicted by the climatology around the time of the vortex breakdown date. Figure 3-4 can be approximately recovered by combining Figure 3-5c and Figure 3-5d, but the dilution of the two very different signals means that the structure can no longer be distinguished from the noise. This distinct difference between anomaly patterns for early and late breakdown events is *prima facie* evidence for treating anomalies around the time of the vortex breakdown as a non-stationary process.

That the anomalies around the time of the vortex breakdown should be modelled as a non-stationary stochastic process implies that the physical relevance of a climatological seasonal cycle is suspect. To explore this issue further, we compute early and late composites of $\langle [u] \rangle$ i.e., we do not remove a climatological seasonal cycle prior to computation of the composite plots (see Figure 3-6a and Figure 3-6c). In both of these plots the jet transitions equatorward, commencing several weeks prior to the vortex breakdown date and concluding shortly afterwards¹. Also evident is the apparent tendency for early breakdown events to be associated with a more equatorward jet transition. Rather than viewing the climatological seasonal cycle as a relatively slow equatorward transition of the jet, the composite plots suggest that it should instead be interpreted as an average of yearly equatorward jet transitions, organised about the vortex breakdown date, which diffuses the sharpness of the transition seen in individual years. This interpretation is further supported by calculating a climatological seasonal cycle for early and late breakdown years separately (see Figure 3-6b and Figure 3-6d). The two climatological cycles are seen to be quite different, consistent with an organising influence from the vortex breakdown event. Such an organising influence of the vortex breakdown on the jet has recently

¹It should be noted that for individual years there will be day-to-day variability superimposed on this transition. ‘Wiggles’ in our jet-latitude index should not necessarily be interpreted as coherent jet variability and may be an artefact of our limited sample size.

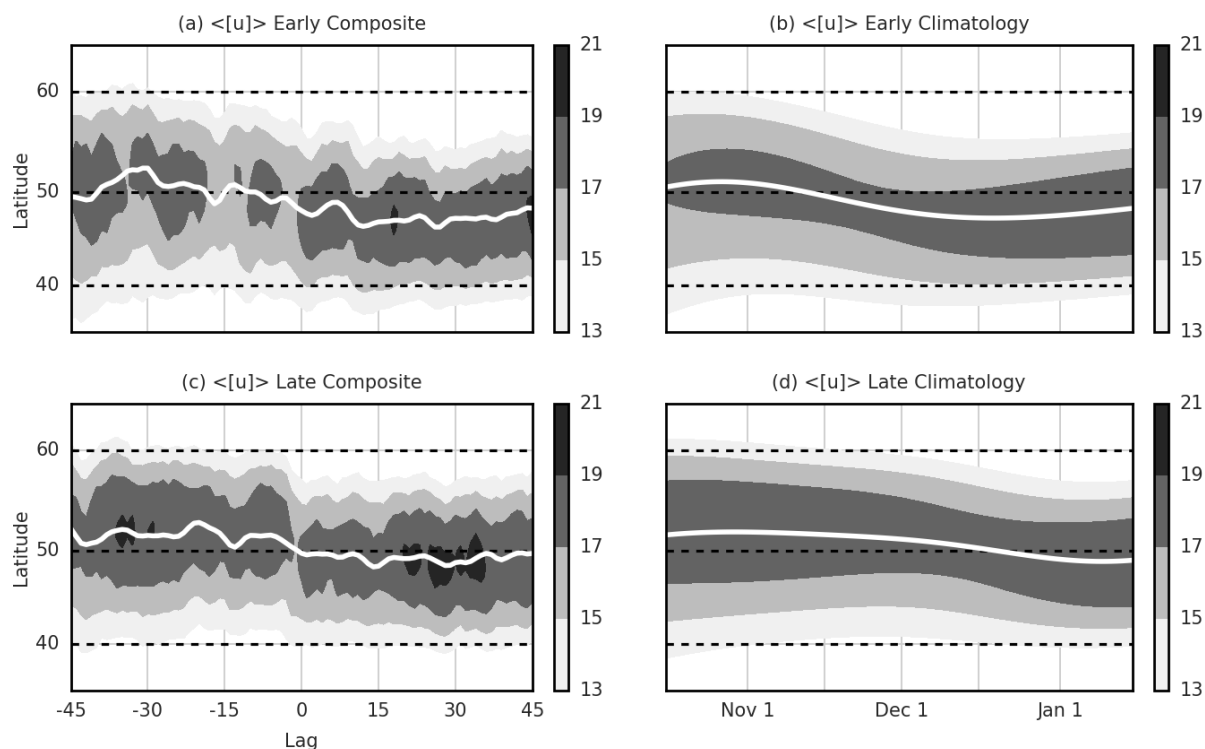


Figure 3-6: (a, c) Composite plots of $\langle [u] \rangle$ (shading) and jet latitude index (white line), centered about the stratospheric vortex breakdown date, for (a) all early years and (c) all late years. Jet latitude index has been smoothed with a binomial filter of order 4 for presentation purposes. (b, d) Climatology of $\langle [u] \rangle$ (shading) and jet latitude index (white line) from October 16 until January 15 for (b) all early years and (d) all late years. Units in all plots are m s^{-1} and values below 13 m s^{-1} have been masked for presentation purposes.

been documented across a hierarchy of models by Sun et al. (2014). These authors also noted that early and late vortex breakdown events appeared to exhibit somewhat distinct evolutions, beyond a simple translation in time of the breakdown dates. They hypothesised that both the timing and type of breakdown event are important for characterising the organising influence on the troposphere, consistent with the results from our jet composites.

To try to understand the impact of variations in the timing of the breakdown date on anomaly composites, we introduce a schematic of the seasonal jet transition in Figure 3-7. This schematic is motivated by the results of our composite plots in Figure 3-6 and neglects any potential evolutionary differences between early and late breakdown events, in an attempt to isolate the influence of breakdown date

variability. We also restrict the schematic to extreme years, as these are the years where we expect the impact from variations in the timing of the event to be most pronounced.

In extreme early years in our schematic, as a result of the earlier circulation transition, circulation anomalies can be expected to exhibit a persistent dipolar structure that is negative on the poleward flank of our jet latitude index and positive on the equatorward flank (Figure 3-7c). In extreme late years, we can expect the opposite behaviour to emerge (Figure 3-7d). As a result of the stronger meridional gradients on the poleward flank of our idealised jet profile (Figure 3-7b), the circulation anomalies are larger on the poleward flank than on the equatorward flank for a given latitude shift. Furthermore, in the distribution of early years in our schematic, we find that anomalies emerge from about fifteen days prior until almost thirty days after the vortex breakdown date of that year. In the distribution of late years, we note that anomalies exist from about fifty days up until five days prior to the vortex breakdown date of that year. In the schematic, we see that very different anomaly structures are expected for early and late breakdown events; in this simplified setting, we can attribute the different anomaly structures to the differences in the date of the circulation transition for each individual year. We also see that the anomalies can be characterized by very long persistence timescales, even though the transition is itself a comparatively rapid event. This has implications for the understanding of SAM persistence timescales, as discussed in Section 3.4.1.

The predictions of our schematic are in good qualitative agreement with the anomaly patterns in Figure 3-5. In particular, the sign and temporal structure of the anomalies share a close correspondence. We also note that anomaly amplitudes decrease somewhat when all years are considered, consistent with the idea that extreme variability in the breakdown date is associated with large anomalies about the climatological seasonal cycle. Not all features of the anomaly composites are predicted by our schematic; the re-emergence in extreme late years of persistent positive anomalies, from about lag +10, is perhaps the most obvious example. This suggests that this feature is associated with differences in the type of breakdown event. Inspection of individual years reveals that the persistence of positive anomalies beyond the breakdown date appears restricted to a relatively small subset of exceptionally late breakdown years - the five latest breakdown years along with the summers of 2011/2012 and 2015/2016 (we note the disappearance of this feature when all late years are considered as quantitative evidence of this statement). These exceptionally

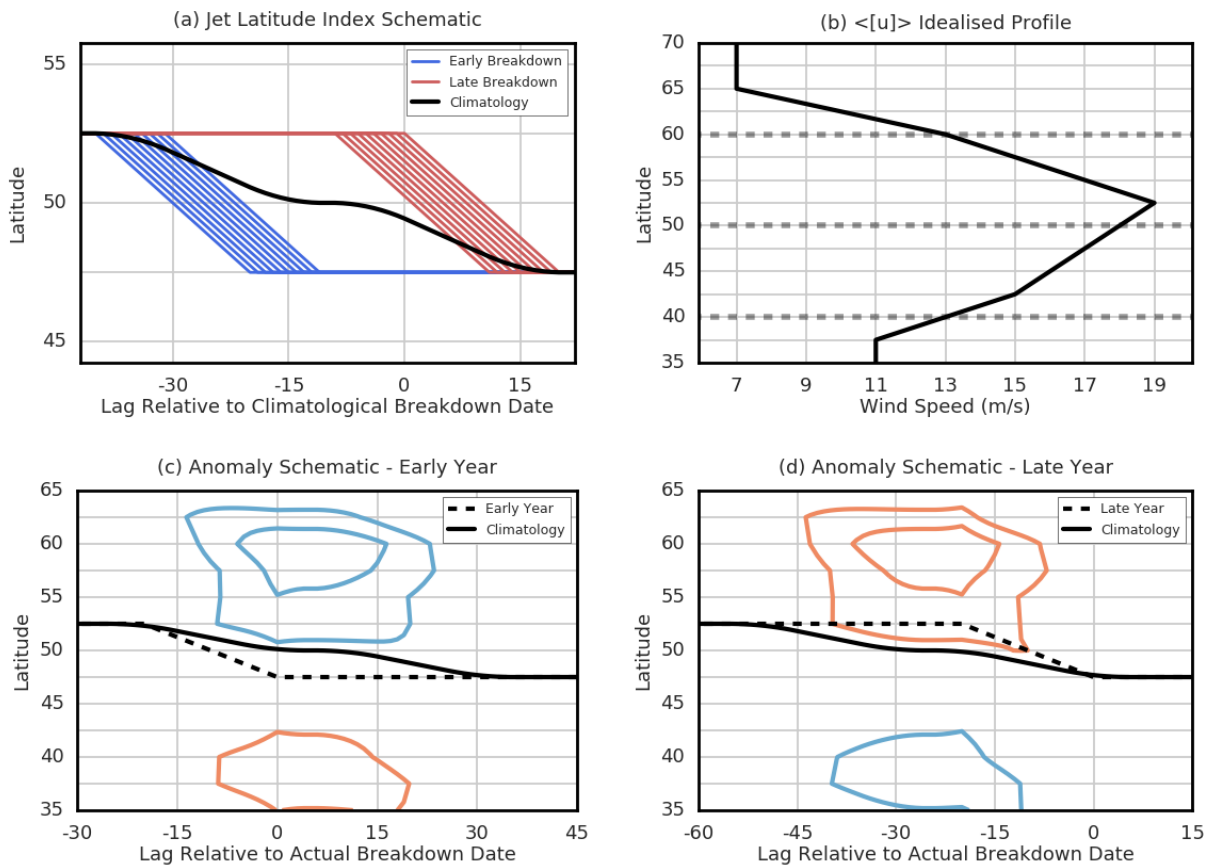


Figure 3-7: (a) Schematic for jet latitude index. Individual lines represent an idealised jet latitude index for individual years. Extreme early breakdown years are defined as years where the vortex breakdown occurs between 11 and 20 days prior to the climatological vortex breakdown date (we consider a uniform distribution between lags -11 and -20) and extreme late years are defined in a similar manner. For each year we imagine our jet to exist at a fixed latitude until 20 days prior to the vortex breakdown date of that year. At 20 days prior to the breakdown date we then imagine it to transition equatorward in a linear fashion and, subsequent to this breakdown date, to again persist at a fixed, relatively more equatorward, latitude. The transition timescale and breakdown dates are taken as representative of the re-analysis data (see Figure 3-3 and Figure 3-6). We form a climatology by averaging the jet behaviour across all years i.e., by averaging the blue and red lines. (c, d) Schematic for zonal-mean zonal wind anomalies. The schematic is an extension of (a) by also incorporating an idealised profile for $\langle[u]\rangle$ (see (b)). For each event in (a), we align the maximum value in the idealised jet profile with the location of the jet-latitude index. We construct a climatology for $\langle[u]\rangle$ by averaging over all breakdown events. We then plot the jet-latitude index for breakdown events that are 15 days earlier and 15 days later than the climatological breakdown date (dashed lines), along with the difference between $\langle[u]\rangle$ for these breakdown events and the climatology of $\langle[u]\rangle$ (contours). The contour interval is 1 m s^{-1} . Red and blue contours indicate positive and negative values respectively; the zero contour is not plotted.

late years appear to be associated with a reduced equatorward jet transition around the vortex breakdown date and, consequently, a more poleward jet in January. Thus, it appears likely that a combination of both the timing and type of breakdown is necessary to account fully for circulation anomalies around the vortex breakdown, as argued by Sun et al. (2014). Nevertheless, we derive some confidence from the fact that our schematic appears consistent with the preponderance of features seen in the anomaly composites.

The combined evidence of the composite plots, climatologies and schematic leads us to propose that during late spring and early summer, zonal-mean tropospheric SH circulation variability is most naturally viewed as variability in the seasonal transition of the jet, and that this transition is organised about the date of the breakdown of the stratospheric vortex. In the next section we consider the implications of this perspective for the various topics mentioned in Section 3.1.

3.4 Applications

3.4.1 Southern Annular Mode persistence timescales

A peculiar property of the large-scale extra-tropical SH circulation between November and January is that anomalies (as measured by the SAM index) appear to persist for longer than at other times of the year (Baldwin et al., 2003). Previous work has implicated stratospheric variability in this increase in tropospheric persistence timescales (e.g., Baldwin et al., 2003; Gerber et al., 2010), and this feature has generated interest as indicating a potential time of year where skilful long-range forecasts may be possible (see Kidston et al., 2015, and references therein). Usually the calculation is performed using zonal-mean geopotential height anomalies; however, balance considerations associated with the large-scale circulation (e.g., McIntyre, 2015) suggest that this is also likely to be a feature of the zonal-mean zonal wind field. Figure 3-8 represents evidence in favour of this statement; it has been computed using zonal-mean zonal wind anomalies rather than geopotential height. The temporal and structural similarity between Figure 3-8 and the earlier calculation of Baldwin et al. (2003) suggests that both plots are isolating the same feature of the circulation, and that we can use zonal-mean zonal wind timescales as a proxy for geopotential height. The benefit of this transformation is that we can directly employ the results of the previous section to further our understanding of why this increased persistence feature

emerges.

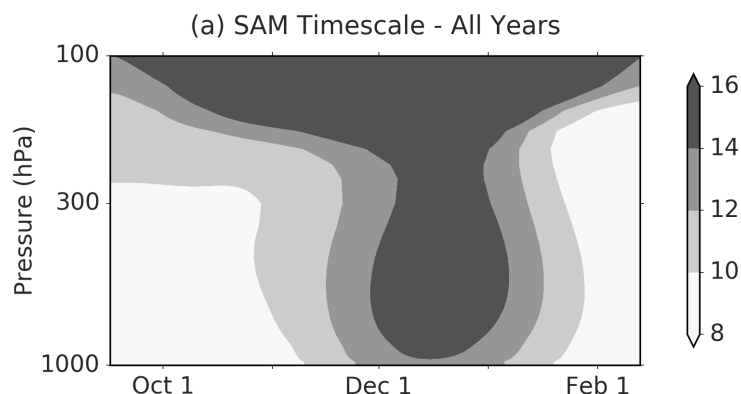


Figure 3-8: SAM autocorrelation function e-folding timescale as a function of day of the year and pressure level. Figure is analogous to Figure 1 of Baldwin et al. (2003).

A complicating factor in applying our results is that the computational procedure for constructing Figure 3-8 is somewhat involved (see 3.A of Mudryk and Kushner, 2011). Nevertheless, a key component of the calculation involves projecting circulation anomalies onto a leading EOF structure. Figure 3-9 represents the leading EOF for $\langle [u] \rangle$ between 20° and 90° S². The EOF is plotted in m s^{-1} to illustrate typical anomaly magnitudes associated with one standard deviation of the SAM index. Comparison of this structure with the anomaly patterns in Figure 3-5 reveals a close correspondence, and suggests that the composite anomalies are of the correct amplitude to provide a substantial contribution to the SAM index. This motivates the following interpretation for the increased SAM timescales between November and January: variability in the seasonal transition of the jet associated with variability in the date of the breakdown of the stratospheric vortex.

As evidence in favour of this interpretation, several recent modelling studies (e.g., Simpson et al., 2011; Kim and Reichler, 2016) have highlighted an important role for zonal-mean stratospheric variability in lengthening tropospheric SAM timescales. As an alternative means of quantifying the influence of interannual variability in the vortex breakdown date on tropospheric jet variability, we have developed a linear predictor model for the November–December mean jet-latitude, using the date of the

²The leading EOF for $\langle [u] \rangle$ is closely associated with the leading EOF for $[u]$ at each level in the troposphere, as a result of the equivalent barotropic property of the jet. The SAM index at each level in the troposphere has a temporal correlation > 0.95 with the SAM index formed using $\langle [u] \rangle$, based on a 37 year daily time series.

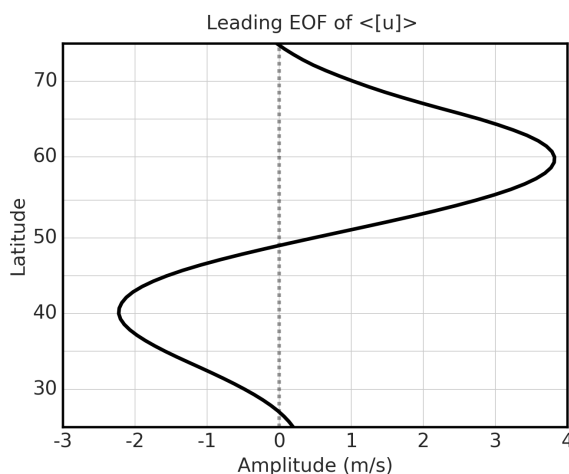


Figure 3-9: Leading EOF of $\langle [u] \rangle$ between 20° and 90° S. Values are presented in m s^{-1} .

vortex breakdown as our predictor (see Appendix A; $r \sim 0.73$). The relative success of this simple linear model is further evidence of the substantial organising influence of the vortex breakdown event on the jet at this time of year. The combination of all these results leads us to conclude that the increase in SAM timescales between November and January can be largely interpreted as variability in the seasonal transition of the jet. This interpretation supports the idea that long-range skill in the prediction of the latitude of the tropospheric jet is possible at this time of year (see also Baldwin et al., 2003), although the source of such skill is attributed to the organizing influence of the stratospheric vortex breakdown rather than to enhanced persistence of SAM variability.

3.4.2 Southern Hemisphere high-latitude climate change

The positive trend of high-latitude circulation anomalies in austral summer has been a well-documented feature of the satellite era; it has been largely attributed to stratospheric ozone depletion (see Thompson et al., 2011, and references therein). This positive trend is commonly diagnosed using monthly-mean geopotential height anomalies and has been interpreted as a poleward shift of the mid-latitude jet. Here we perform a related calculation and diagnose decadal linear trends in $\langle [u] \rangle$ (see Figure 3-10a). To confirm the qualitative robustness of the features of this plot to the potentially compensating effect of an ozone recovery since 2000 (Solomon et al., 2016), we have also performed a regression analysis against EESC (see Figure 3-10b). In both of

these figures, the plotted contours are largely representative of regions that are statistically significant at the 5% level, and it is clear that they both share very similar features. As an alternative means of quantifying the significance of these features, we have also plotted the long-term means and standard errors for $\langle[u]\rangle$ for both the ozone depletion and ozone recovery eras (see Figure 3-11).

Inspection of all three of these figures reveals that there appear to be at least two distinct components to high-latitude changes in $\langle[u]\rangle$. Of primary interest to the present work are those changes that emerge around the December 1 period; the difference between the long-term means for the ozone depletion and recovery eras is particularly striking for this period. Based on our analysis in Section 3.3, we propose that these apparent changes can be interpreted as a delayed equatorward transition of the jet, as a result of a long-term trend in the vortex breakdown date associated with ozone depletion (e.g., Thompson et al., 2011), rather than the more common interpretation of a poleward shift of the jet. Late breakdown years are associated with positive tropospheric circulation anomalies in the lead-up to the breakdown date (see Figure 3-5b and Figure 3-5d), and any trend toward later breakdown dates will therefore be associated with a trend toward positive tropospheric circulation anomalies. This behaviour is illustrated in an idealised setting in Figure 3-7d. In this schematic, for a year where the vortex breakdown date occurs approximately two weeks later than the climatological breakdown date, positive anomalies are seen to emerge on the poleward flank of the jet, centered around the time of the climatological vortex breakdown date. The circulation anomalies are subsequently seen to disappear following the seasonal transition of the jet. This highlights how a long-term delay in the seasonal transition will show up as an apparent poleward shift of the circulation, even though the physical interpretation is of course quite different.

The second apparent component to high-latitude trends is associated with changes to the mid/late summer circulation. From inspection of both panels in Figure 3-10, it appears that in years with large ozone depletion the jet remains in its summer configuration for a reduced period of time, and that it transitions poleward into its autumn profile at an earlier date. Previous work (e.g., Neff, 1999; Sun et al., 2014) has linked changes in the tropospheric summer circulation with changes to the evolution of the stratospheric vortex breakdown process. In that respect it is worth noting that extreme late breakdown years, which occur preferentially in the later part of the record (Figure 3-3), are associated with positive high-latitude zonal-wind anomalies at positive lags of 10-30 days (Figure 3-5b), which would reach into January. Thus,

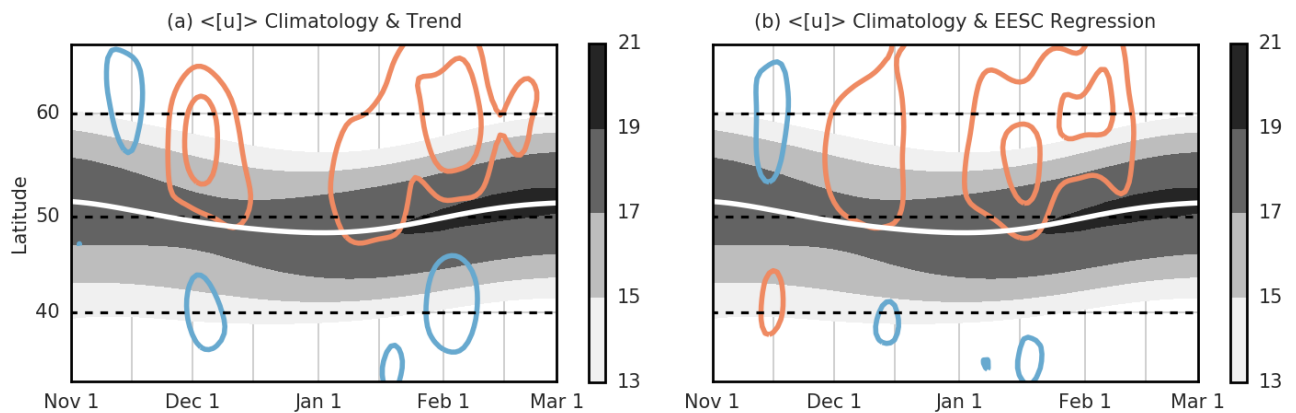


Figure 3-10: (a) Climatology (shading) and linear trend (contours) for $\langle [u] \rangle$, along with jet latitude index (white line), from November 1 until March 1. Units for $\langle [u] \rangle$ are m s^{-1} . Contour interval is 0.6 m s^{-1} per decade. Negative trends are indicated by blue contours and positive trends by red contours; the zero contour is not plotted. (b) As (a) but with EESC regression values (contours). Contour interval is now 1 m s^{-1} per decade; we display trends in these units by scaling m s^{-1} per pptv by the total change in EESC across the 1980s, a decade where EESC increased approximately linearly.

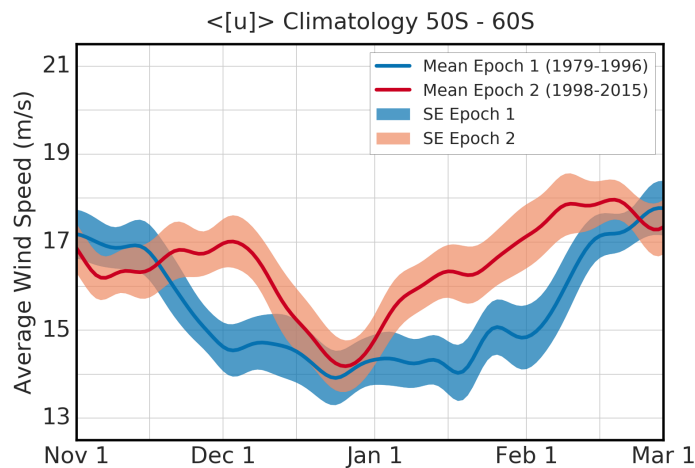


Figure 3-11: Mean value for $\langle [u] \rangle$ as a function of day of the year, averaged across the latitude band $50^\circ - 60^\circ \text{ S}$, for the years 1979 - 1996 (blue solid line) and 1998 - 2015 (red solid line). Shading indicates ± 1 standard error interval for each set of years. Units are m s^{-1} . Data is smoothed using a Gaussian window with a 7-day half-width prior to calculation of statistics.

these two features that are not accounted for by our schematic may in fact be linked. However, the period from mid-January onwards is outside the scope of the present work, and so we do not attempt to explore these features further.

3.4.3 High-latitude ENSO teleconnection in austral summer

A prominent teleconnection that has been documented for the zonal-mean circulation is that between ENSO and the SH mid-latitude jet during austral summer (Figure 3-12a; see shaded region near 60° S during November and December in particular). This teleconnection has previously been interpreted as a direct response of the jet to tropical forcing; its seasonality has been argued to arise from a seasonally-varying waveguide effect (Seager et al., 2003; L’Heureux and Thompson, 2006). Here, we instead hypothesize that this teleconnection may be interpreted as the result of a correlation between the strength of the stratospheric vortex and the phase of ENSO, and that its seasonality occurs as a result of the timing of the vortex breakdown (i.e., between November and January; see also Hurwitz et al., 2011).

As a preliminary step in testing our hypothesis we note that the measure used for the zonal-mean circulation in Figure 3-12a is interchangeable with $\langle [u] \rangle$ for the months November through February - the time series of monthly-mean $[u]$ at 300 hPa has an interannual correlation > 0.98 with monthly-mean $\langle [u] \rangle$, across the latitude band 50° to 60° S, for each of the months November through February. This allows us to use our earlier results to interpret the high-latitude features of Figure 3-12a. We next note that during the satellite-era, nine out of twelve El Niño episodes have been associated with early vortex breakdown years and six out of ten La Niña episodes have been associated with late vortex breakdown years³. This would appear to be an unusually close association between the strength of the vortex and the phase of ENSO; we have made an attempt at quantifying this statement further in 3.B, where we provide evidence for an apparent statistical relationship between these two quantities. Next, we highlight the summer of 2015/2016 as a year where the relationship between ENSO and jet latitude appeared to fail (L’Heureux et al., 2016); this summer was also anomalous in the sense that an El Niño occurred in association with a late breakdown of the vortex. The structure of the jet anomalies for this summer was relatively well-explained by our anomaly composites for late

³We associate each ENSO episode with the breakdown event that occurred during the episode. For example, the large El Niño episode of 1982/1983 is associated with the (early) breakdown event of 1982.

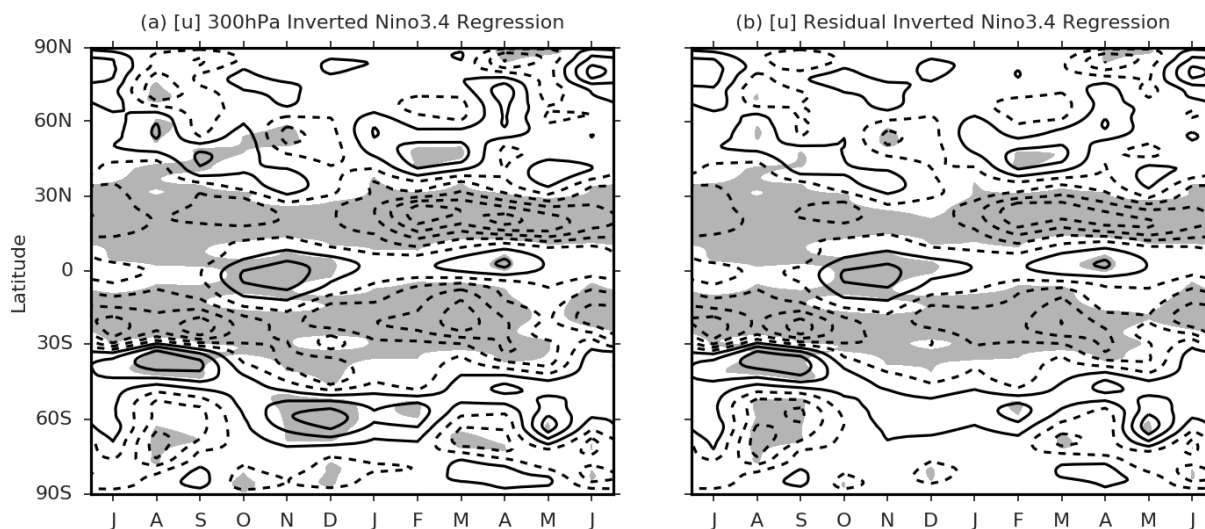


Figure 3-12: (a) Monthly-mean 300 hPa [u] anomalies and (b) monthly-mean 300hPa [u] residual anomalies regressed onto inverted values of the Niño 3.4 index. Residual time series formed by using the regression model in Appendix A to remove the linear influence of the vortex breakdown event at each spatial point. Values of the Niño 3.4 index have been standardized and detrended prior to regression. Contour interval is 0.5 m s^{-1} (-0.75, -0.25, 0.25). Shading denotes relationships that are significant at the 5% level, based on a one-sided one-sample Student's t-test for a reference mean value of zero. Panel (a) is adapted from Figure 1 of L'Heureux and Thompson (2006).

breakdown years but was in opposition to that expected from Figure 3-12a. This is despite 2015 being one of the strongest El-Niño episodes on record (e.g., L'Heureux et al., 2016). Finally, we have repeated the regression analysis used to produce Figure 3-12a using a residual time series formed by removing a regression model similar to 3.A. The high-latitude teleconnection is seen to vanish when the linear influence of the vortex breakdown event is accounted for (Figure 3-12b).

We therefore argue that a parsimonious interpretation of the observed ENSO / mid-latitude jet teleconnection during austral summer is a correlation between the strength of the stratospheric vortex and the phase of ENSO. The organising influence of the vortex breakdown on the tropospheric jet subsequently leads to a correlation between the phase of ENSO and the latitude of the jet. We acknowledge that this interpretation is somewhat speculative for the behaviour suggested by the January and February regression values (i.e., these months are somewhat outside the scope of our results in Section 3.3). However, we note that the apparent tendency for circulation anomalies to persist beyond the breakdown date in very late breakdown

years offers a plausible explanation as to why regression values might persist weakly until February.

3.5 Summary and discussion

We have proposed that during SH late spring and early summer, high-latitude circulation variability is more usefully viewed as variability in the seasonal transition, which is organised around the date of the stratospheric vortex breakdown, rather than as anomalies to a climatological seasonal cycle. We have subsequently explored the implications of this perspective for previous results in the literature. We argue that there are at least four clear examples where this perspective appears to shed new light.

First, we have illustrated how anomaly composites must be interpreted with care when statistical models of circulation variability exhibit non-stationary behaviour. We have used our proposed perspective on circulation variability to offer a different interpretation of the anomaly composites that were originally introduced by Black and McDaniel (2007), and find a much stronger relationship between vortex breakdown and tropospheric circulation than they did. This interpretation is argued to be consistent with the more recent results of Sun et al. (2014).

Second, we have presented evidence that the SH high-latitude ENSO teleconnection can be interpreted as a correlation between the phase of ENSO and the strength of the stratospheric vortex, rather than as a direct effect from the tropics. According to this hypothesis, the organising influence of the vortex breakdown on the high-latitude circulation would then lead to the emergence of this teleconnection in SH late spring/summer. An important caveat attached to our analysis is that we have only considered zonal-mean teleconnections; traditionally, it is the zonal asymmetries that have been the focus of teleconnection studies. Our results make no conclusions about high-latitude teleconnections associated with the SH zonally-asymmetric circulation. However, we caution that in the absence of a greater understanding of (for example) mid-latitude stratosphere-troposphere coupling mechanisms, the causal nature of any such teleconnections should be treated with care. Furthermore, if robust, the correlation between the phase of ENSO and the strength of the SH stratospheric vortex warrants further attention as to the precise nature of this relationship.

Third, we have argued that the increased SAM timescales encompassing late spring and summer can be viewed as reflecting variability in the timing of the seasonal

transition, rather than as weakened damping of SAM anomalies by eddy feedbacks. This increase in SAM timescales has often been interpreted as a potential time of year where long-range forecast skill may be possible (see Kidston et al., 2015, and references therein). Our interpretation is consistent with this suggestion, although for different reasons than generally believed. In particular, our proposed interpretation of the ‘source’ of these increased timescales (variability in the date of the breakdown of the stratospheric vortex) suggests that long-range forecast skill associated with the stratospheric vortex should also lead to a realisation of long-range forecast skill in the prediction of the latitude of the tropospheric jet; the recent results of Seviour et al. (2014) offer some promise in this respect. However, it should also be acknowledged that there is still much to be improved in the current generation of climate models (Wilcox and Charlton-Perez, 2013); the diagnostic used in this study ($\langle [u] \rangle$) may represent a helpful tool for assessing model fidelity. It is unclear how instructive, if at all, our results may be for improving understanding of the increased timescales of the Northern Annular Mode (NAM) in boreal winter (Baldwin et al., 2003).

Fourth, we have presented evidence that SH high-latitude climate change can be separated into at least two distinct time periods, and that for the earliest of these time periods (December), changes are more physically interpreted as a delayed equatorward transition of the jet, rather than a poleward shift. From inspection of the anomaly patterns at positive lags for extreme late breakdown years, which occur preferentially in the later part of the record, it would appear that a deeper understanding of the dynamics of this transition may also be beneficial for an improved understanding of changes in the later time period (January/February).

Understanding why the jet transitions equatorward in association with the breakdown of the stratospheric vortex is perhaps the outstanding question that emerges from this analysis. That the stratospheric vortex can exert a persistent influence on the tropospheric jet appears to be a characteristic feature across a wide range of models (e.g., Sun et al., 2014); furthermore, it would appear that the tropospheric jet can shift seasonally even when the only imposed seasonality is in the stratosphere (e.g., Sun and Robinson, 2009; Sheshadri et al., 2015). To understand this behaviour further, it would appear pertinent to revisit theories for the maintenance of the westerlies and what ‘sets’ the latitude of the jet.

In the absence of a complete theory for jet latitude, the concept of a circulation regime (e.g., Palmer, 1999) may offer a complementary perspective for predicting the SH circulation response to external forcing (e.g., anthropogenic forcing). In this

chapter we have argued that the response of the SH zonal-mean circulation to external forcing (ozone depletion) may be partly interpreted as an increased residency time in the spring regime, consistent with the results of Lee and Feldstein (2013). Recent work (Ivy et al., 2017) has documented apparent long-term changes to the SH jet in May, which share qualitative similarities with changes to the jet in austral spring/summer. May is notable as the climatological month where the zonal-mean SH circulation transitions to a winter regime (e.g., Neff, 1999), hinting that SH circulation responses to external forcing may emerge most clearly around the time of a seasonal (regime) transition. Whether or not such a perspective offers a helpful re-formulation of the SH jet changes in May is unclear at the present time.

Finally, we argue that the combined evidence of these four examples demonstrates that the traditional paradigm of decomposing circulation variability into anomalies about a long-term climatological seasonal cycle may not always be the optimal approach; such a decomposition is perhaps traditionally motivated by analogy with linearised perturbations to a ‘basic state’, with the implicit assumption of a timescale separation. In the four examples outlined above, we have shown how a non-stationary model of circulation variability, which incorporates a deterministic representation of the organising influence of the vortex breakdown, represents a simpler means of viewing circulation variability (see also Koutsoyiannis (2011) for a discussion on the correspondence between non-stationary processes and deterministic behaviour). Furthermore, the concept of a basic state may have limited physical meaning in this non-stationary model of circulation variability. Such non-stationary models of circulation variability need not be restricted to intraseasonal timescales: Chapter 2 highlighted a pronounced quasi-two year timescale to SH high-latitude eddy variability, which is most likely linked to stratospheric processes. This suggests that the organising influence of the vortex can lead to high-latitude tropospheric circulation variability on both the intraseasonal and the interannual timescales.

The concept of an organising influence of the vortex breakdown (Black et al., 2006; Black and McDaniel, 2007) appears to be a powerful paradigm within which to interpret high-latitude tropospheric variability. It has previously been applied to the NH circulation, within a framework that models variability as (statistically stationary) anomalies to a long-term climatological seasonal cycle (Black et al., 2006). The results of this analysis suggest that it may be of benefit to revisit the results of that study, within a modelling framework of non-stationary variability. Related applications that may likewise benefit from the perspective of circulation variability

proposed here include, but are not limited to: detection and attribution methodologies that are restricted by large internal variability at high-latitudes, the assessment of forecast skill in the presence of an artificial climatology (e.g., Hamill and Juras, 2006), and the use of statistical tests that treat the population parameters as fixed in time.

3.A

As an attempt at quantifying the organising influence of the breakdown of the stratospheric vortex on the variability of the tropospheric jet, we construct a linear statistical model between the vortex breakdown date and the November-December (ND) mean of daily tropospheric jet latitude, following the procedures outlined in Wilks (2011). We denote our time series for vortex breakdown date $x(t)$ and our time series for ND jet latitude $y(t)$. We have thirty-seven data points for each index and prior to construction of our statistical model we linearly detrend each index. The statistical model is given by:

$$y(t) = \beta x(t) + \epsilon(t)$$

where β represents the regression coefficient estimated using an ordinary least-squares method and $\epsilon(t)$ is a residual error. For our entire dataset we find a correlation value of $r \sim 0.73$ and a regression coefficient of $\beta(t) \sim 0.14$ degrees per day i.e., a delay of one week in the breakdown date is associated with an increase of one degree in ND jet latitude. We have confirmed the robustness of this relationship by repeating the procedure for only the first half and only the second half of our dataset, for only the early breakdown years and only the late breakdown years, and by employing a ‘leave-one-out’ method. We have also checked for any possible non-linearity in the relationship by inspection of a scatterplot and have analysed a box plot and a q-q plot to confirm that the residual appears to be normally distributed.

3.B

There have been twelve El Niño (EN) and ten La Niña (LN) episodes during the satellite era (see Data and Methods section for how we define the phase of ENSO). Nine EN episodes have been associated with early (E) breakdown years and six LN episodes have been associated with late (L) breakdown years. For brevity, we introduce the

notation $(9, 6)$ to represent this combination. We are interested in quantifying how likely it is that at least nine EN episodes occur in association with E years as well as at least six LN episodes in association with L years. For the purposes of this calculation, we consider the year associated with the median breakdown date (1993) as an E year. Our conclusions do not change if we instead classify it as an L year.

First we note that there are $\binom{37}{12} \cdot \binom{25}{10}$ possible ways of distributing EN and LN episodes among the thirty-seven years of our satellite record. Next we note that we require at least nine EN episodes to occur in E years ($\binom{19}{9}$) and at least six LN episodes to occur in L years ($\binom{18}{6}$). We now consider all possible combinations that satisfy this criterion and calculate the number of ways of selecting each combination. For example, $(10, 8)$ represents a valid combination; there are $\binom{19}{10} \cdot \binom{18}{8} \cdot \binom{10}{2} \cdot \binom{9}{2}$ ways of selecting this combination. Code has been written that sums the number of ways of selecting each of the twenty possible valid combinations (x, y) and subsequently computes the ratio of this sum to $\binom{37}{12} \cdot \binom{25}{10}$. This ratio is found to be 0.034 i.e., the relationship between ENSO phase and vortex strength is found to be statistically significant at the 5% level, according to our measures of ENSO phase and vortex strength.

Chapter 4

Seasonal persistence of stratospheric circulation anomalies

4.1 Introduction

Seasonal climate prediction is distinct to conventional weather forecasting in that it does not attempt to forecast the day-to-day evolution of weather. Instead it attempts to provide estimates of time-mean statistics, typically several months in advance (Palmer and Anderson, 1994). The theoretical basis for such extended-range prediction is attributed to two fundamental constraints on the evolution of the climate: the surface boundary conditions and the atmospheric initial conditions. Traditionally it has been the lower boundaries of the atmosphere that have been the primary focus of attention. In particular, the phenomenon of El Niño-Southern Oscillation (ENSO) has formed the key paradigm for the design and implementation of many modern seasonal forecast systems (National Research Council, 2010). More recently, evidence has been offered for the importance of the atmospheric initial conditions (Stockdale et al., 2015), with the role of the stratospheric polar vortex receiving much attention. Much of this work has focused on the Northern Hemisphere (NH) and on the influence of sudden stratospheric warmings (SSW) on the tropospheric circulation in particular. However, there also exists a related body of work for the Southern Hemisphere (SH; Son et al., 2013; Seviour et al., 2014). SSW events are exceedingly rare in the SH (e.g., Thompson et al., 2005) and so the source of this apparent skill requires a somewhat different explanation to that proposed for the NH.

As discussed in Chapter 1, the seasonal evolution of the SH stratospheric polar

vortex (SSPV) exhibits several distinct features compared to its NH counterpart. In particular, the SSPV undergoes an annual downward shift in its location relative to its midwinter position (Hartmann et al., 1984). The ‘shift-down’ behaviour of the SSPV typically proceeds from mid-late August and culminates in the vortex breakdown event sometime between mid-November and mid-January. The seasonal evolution of the SH tropospheric mid-latitude jet/eddy-driven jet (EDJ) also exhibits several distinct features compared to its NH counterpart. In particular, the EDJ undergoes a semi-annual oscillation (SAO) in latitude with the strongest winds closest to the pole in autumn and spring (van Loon, 1967). The interannual variability of both of these components of the large-scale SH circulation was previously investigated by Kuroda and Kodera (1998), who documented an apparently coupled relationship between the SSPV and EDJ from midwinter until the vortex breakdown event in summer. These authors noted that during this period the variability of the coupled system appeared to be an ‘interannual phenomenon with a well-defined intraseasonal structure’. This work was further extended by Hio and Yoden (2005), who noted two distinct configurations for the late winter SSPV and who referred to a ‘seasonal march’ of the coupled variability. These authors conditioned their analysis on the late winter configuration of the SSPV and presented evidence that between August and December, the time-mean statistics of the large-scale extra-tropical tropospheric and stratospheric circulations were a function of this late winter configuration. A potential link between the stratospheric quasi-biennial oscillation (QBO) and the configuration of the winter SSPV was also investigated by both Kuroda and Kodera (1998) and Hio and Yoden (2005).

In Chapter 3, evidence has been presented of an equatorward transition of the EDJ in association with the vortex breakdown event in the stratosphere, with the timing of this transition representing a leading-order influence on large-scale circulation variability during this time of year. Figure 4-1 illustrates the extent of this influence - 500hPa geopotential height anomalies averaged over the summer months are regressed against the date of the stratospheric vortex breakdown for each year during the satellite era. The significant correlation values at high-latitudes are indicative of the impact of year-to-year variability in the timing of the vortex breakdown event in the stratosphere on tropospheric circulation anomalies. A natural question that emerges from this work is to ask how predictable (in a seasonal forecasting sense) the timing of this event might be, and how it relates to the earlier work of Kuroda and Kodera (1998) and Hio and Yoden (2005). It is also of interest to try to understand

500hPa Geopotential Height (DJF 1979 - 2016)

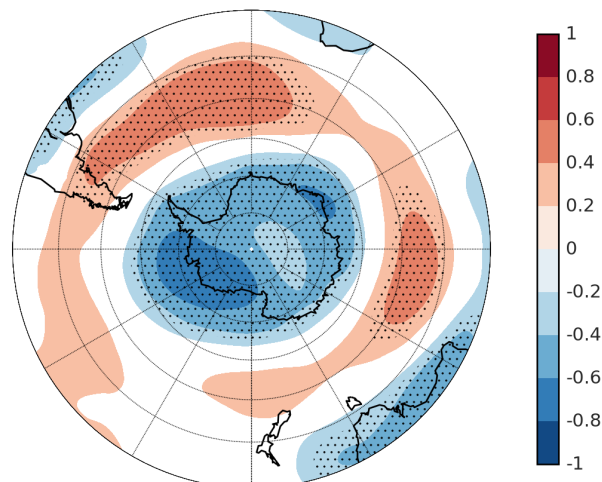


Figure 4-1: Correlation values between DJF 500 hPa geopotential height anomalies and the date of the stratospheric vortex breakdown during the satellite era. All data has been linearly de-trended prior to calculation of correlation values. Stippled regions represent correlation values that are statistically significant at the 5% level, based on a two-tailed test of the Student's *t* statistic. Correlation values between -0.2 and 0.2 are colored white for presentation purposes.

how these results might relate to the 'Annular Modes' of the circulation, which in recent years have become the de-facto choice for diagnosing stratosphere-troposphere coupling and the associated prospects for seasonal forecasting (e.g., Kidston et al., 2015, and references therein).

The present chapter is an attempt at investigating these questions. It begins by exploring the extent to which the date of the vortex breakdown in the stratosphere is predictable. This is done by relating interannual variations in the timing of the breakdown event to persistent variations of the SSPV in the previous winter and spring. Coupled variability between the stratosphere and troposphere is then considered, and an argument is made for the concomitant potential for skilful seasonal forecasting in the troposphere. Based on these results, an alternative perspective of large-scale extra-tropical SH circulation variability between late winter and summer is proposed.

4.2 Data and methods

The basic data input for our study is four-times daily zonal wind and geopotential data from the ERA-Interim re-analysis dataset for the period Mar 1 1979 to Feb 28 2017 (Dee et al., 2011). This period encompasses 38 years in the SH in total. Data was available on an N128 Gaussian grid and on 37 pressure levels (1000 - 1 hPa). Before analysing the data we first processed it by forming a daily and zonal average of the data. This processed data formed the input for all of our subsequent analysis. We define a climatology of our data as the long-term daily average that is subsequently smoothed by retaining the first six Fourier harmonics (Black and McDaniel, 2007). We define a daily jet latitude index by mass-weighting our zonal-mean daily-mean zonal wind data, vertically averaging it between 1000 and 250hPa and subsequently computing the latitude of the maximum value of this average between 0 and 90 S (Chapter 3). We identify the date of the stratospheric vortex breakdown as the final time that the zonal-mean daily-mean zonal wind at 60 S drops below 10m s^{-1} ; we apply this criterion to running 5-day averages at 50hPa (Black and McDaniel, 2007). We use 60 S as the boundary for our polar-cap average. We define the phase of the QBO using the sign of July monthly-mean zonal-mean zonal wind at 20hPa averaged between 5 N and 5 S (Anstey and Shepherd, 2014). We define our SAO index as the difference between monthly-mean zonally-averaged sea-level pressure at 50 S and 65 S (Bracegirdle, 2011). We define our Annular Mode index for each pressure level of our data in a similar manner to Baldwin and Thompson (2009). First we compute daily anomaly data by removing a daily climatology. Next we perform an empirical orthogonal function (EOF) analysis between 20 and 90 S and at each individual level; we weight our data to account for the decrease in area toward the pole (North et al., 1982). Finally we define our Annular Mode index as the normalised principal component time series that results from our EOF analysis. For our Annular Mode composite analysis we consider years with the 13 largest positive and 13 largest negative values in our Annular Mode index at 30hPa. These represent approximately the upper and lower terciles of our data. We composite about an onset date which is defined as the day when anomalies in the Annular Mode index at 30hPa cross the two-standard deviation threshold for the final time prior to the peak of the event (Thompson et al., 2005).

4.3 Stratospheric circulation variability

4.3.1 Climatology and interannual variability

The shift-down of the SSPV typically proceeds from mid-late August (Hartmann et al., 1984). Long-term monthly average plots of zonal-mean zonal wind ($[u]$) are plotted from August in Figure 1-2. Clear evidence of the downward progression and a general weakening of the winds can be seen in this figure.¹ There is also a suggestion of something of a merger with the tropospheric EDJ and a tilting of the SSPV from late September onwards. The downward progression of the SSPV continues until the final vortex breakdown event, which occurs every year sometime between mid-November and mid-January. The year of 2002 is a notable exception to this description as it was associated with the only documented SSW in the SH during the observational record; in 2002 the downward progression of the SSPV was substantially accelerated relative to its usual behaviour (e.g., Hio and Yoden, 2005). Interannual variations in the SSPV lifecycle, such as those of 2002, were previously investigated by Kuroda and Kodera (1998) and Hio and Yoden (2005) by means of a multiple empirical orthogonal function (EOF) analysis on zonal-mean zonal wind. We employ a similar method using polar cap averaged geopotential height at 30hPa. The use of polar cap averaged geopotential height allows us to relate our results more directly to the Annular Mode indices that are considered later in the chapter.

Figure 4-2 shows the seasonal evolution of polar cap averaged geopotential height at 30hPa. It is plotted from March as the vortex occasionally persists into January in the lower regions of the stratosphere. Interannual variability is seen to be largest from August until January. The exceptional year of 2002 is also plotted for comparison. To perform a multiple EOF analysis on our 38 year dataset we proceed by combining 12 months of data (starting from March) in a vector \mathbf{x}^i as

$$\mathbf{x}^i = [Z^i(1), \dots, Z^i(12)]^T \quad (4.1)$$

where $Z^i(m)$ is the anomalous monthly averaged polar cap averaged geopotential height at 30hPa for the m th month of the i th year. The leading modes of variability

¹Inspection of individual years reveals that the downward progression occurs concurrently with transient vacillations in the magnitude of $[u]$, which are associated with the development of eastward-travelling anticyclones about the polar vortex (e.g., Hio and Yoden, 2004, and references therein). As the present analysis is primarily concerned with an analysis of the zonal-mean circulation, we do not document this three-dimensional behaviour further.

are then extracted as the eigenvectors of the covariance matrix calculated from \mathbf{x}^i . The leading mode (EOF1) is shown in Figure 4-2. This leading mode explains over 73% of the total variance and is clearly separated from the second EOF (North et al., 1982). Its monopolar structure suggests that for a year where a strong or weak SSPV develops in winter (negative or positive polar cap average geopotential height anomalies respectively), it will tend to persist for the remainder of the SSPV lifecycle until the vortex breakdown event in summertime (see also Gerber et al., 2010). The principal component (PC1) time series of EOF1 is shown in Figure 4-3. Weak (W) SSPV years are associated with a positive PC1 value and strong (S) SSPV years are associated with a negative value. Inspection of this plot reveals that the extreme values of PC1 (defined as the upper and lower quartiles of the data) are distributed in a somewhat specific manner. In particular, the extreme values are clustered in the second half of the dataset, and there is a tendency for extreme positive years to directly follow extreme negative years. We have made an attempt at quantifying the significance of these features in 4.A ($p \sim 0.02$ and $p \sim 0.06$ respectively); we discuss potential explanations in Section 4.5.

To explore how the EOF picture of interannual variability relates to the long-term average behaviour described earlier, we follow Hio and Yoden (2005) and perform a composite analysis on zonal-mean zonal wind using the W and S years of our PC1 index. We do this by forming monthly averages of $[u]$ for W and S years separately and then calculating the difference between them. The results are presented in Figure 4-4. The principal difference between the composites is that the entire downward progression of the SSPV is delayed in S years compared to W years. This delay results in a later average stratospheric vortex breakdown date in S years (16 December versus 30 November). It has been suggested that the dynamics of late breakdown events differ from those of early breakdown events (e.g., Sun et al., 2014, see also Chapter 3) and this may explain the differences in January. A more modest difference between the composites is that the SSPV appears stronger in S years (as measured by inspection of the meridional gradients of $[u]$ on the equatorward flank of the SSPV). This difference in strength is beyond that which can be accounted for by a simple translation in time between the composites. The most noticeable impact of this difference in strength is on the tilting of the SSPV during October. This can be seen more clearly in Figure 4-5, where monthly-average plots for W and S years are shown separately. During October, the SSPV undergoes a relatively rapid weakening and tilting of the winds in W years, whereas it is more resilient to this

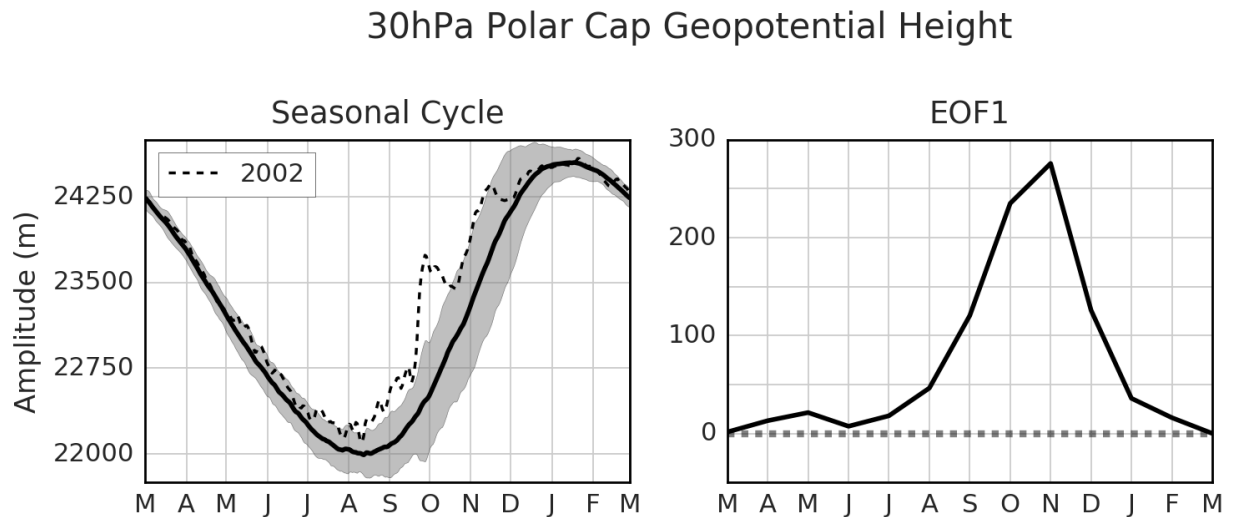


Figure 4-2: (Left) Seasonal cycle of polar cap averaged geopotential height at 30 hPa (thick black line). Shading represents ± 2 standard deviation interval for each day of the year. Dashed line represents daily values during year of 2002. (Right) EOF1 from multiple EOF analysis on polar cap averaged geopotential height at 30hPa (see text). EOF is plotted in m and represents anomaly associated with 1 standard deviation of principal component time series.

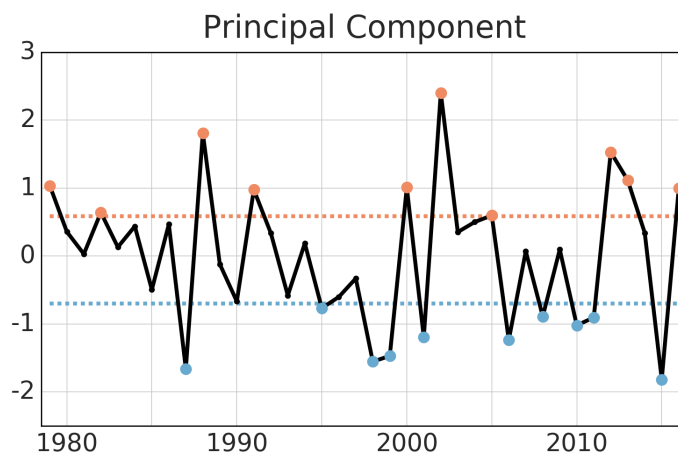


Figure 4-3: Principal component time series of EOF1. The 10 largest positive (red dots) and negative (blue dots) years are also plotted.

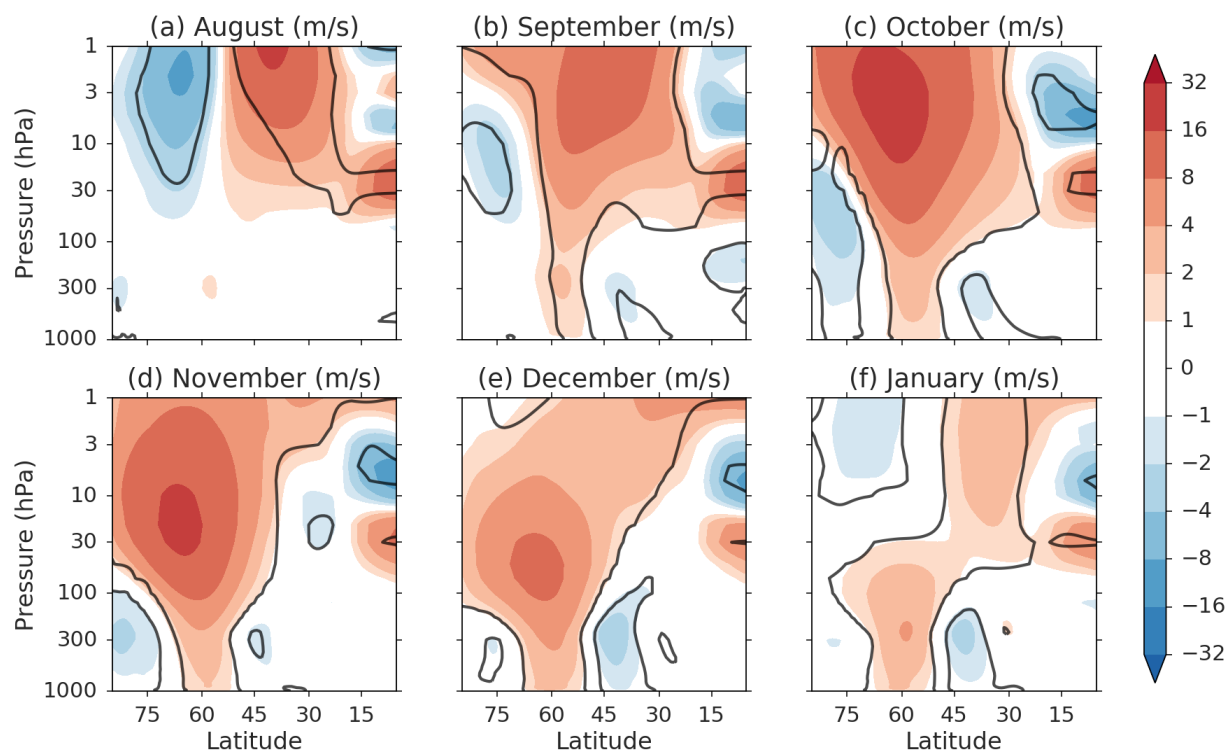


Figure 4-4: Monthly-mean differences in $[u]$ between S and W years (shading). Black contours represent regions where differences are statistically significant at the 5 % level, based on a one-sided two-sample Student's t test. Note the non-linear colour scale required for including tropospheric and stratospheric differences in the same figure.

weakening and tilting in S years. S years are also associated with an extension of the strongest winds of the SSPV into the upper troposphere. This extension into the upper troposphere gives the appearance of something of a merger between the SSPV and the tropospheric EDJ; we return to the tropospheric impacts in more detail in Section 4.4. Overall, it would appear that interannual variations between August and February can be largely described as a phase delay of the SSPV lifecycle in S years, with changes to the amplitude of the lifecycle (SSPV strength) a non-negligible secondary effect.

4.3.2 Seasonal persistence of SSPV anomalies

The results of the previous section suggest that perturbations to the SSPV during winter can persist until the vortex breakdown event in summer. To investigate this

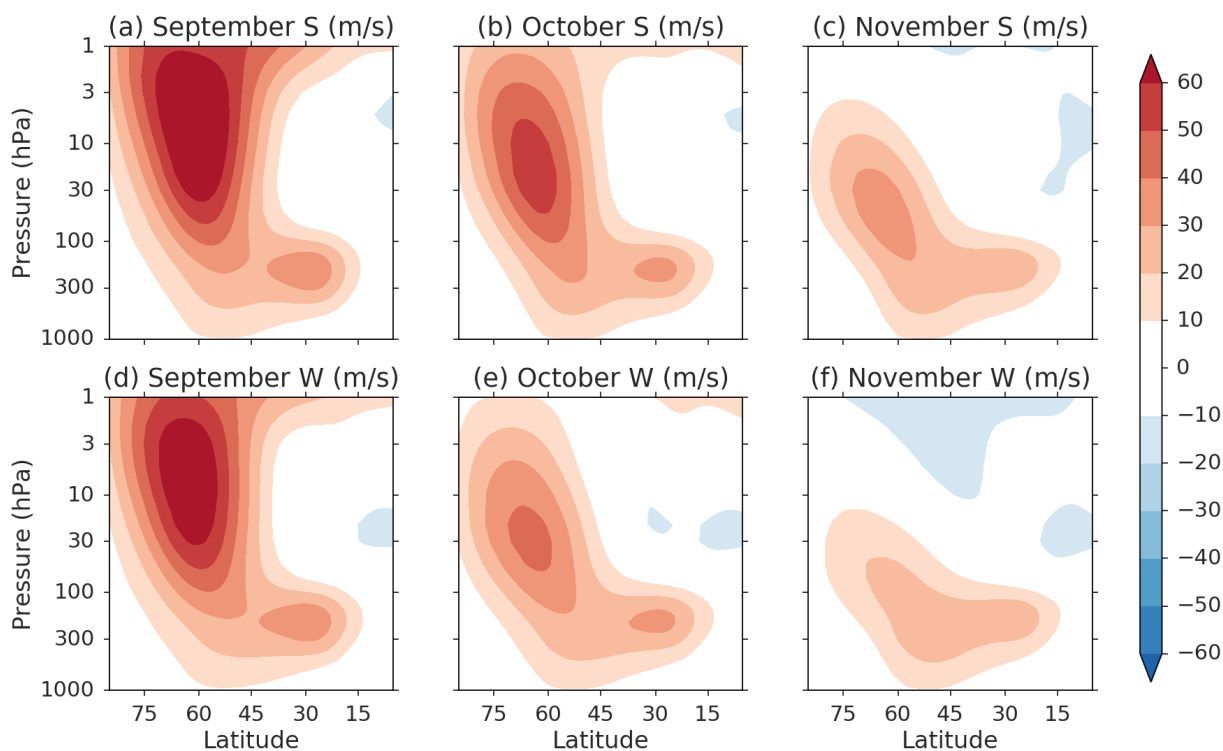


Figure 4-5: (Top) Monthly-mean $[u]$ for S years. (Bottom) Monthly-mean $[u]$ for W years.

potential predictive capability of the SSPV we employ a procedure suggested by Fioletov and Shepherd (2003) for total column ozone and compute correlation coefficients between a measure of the SSPV at a given month of the year and at subsequent months (see Figure 4-6). We use polar cap averaged geopotential height at 30hPa as our SSPV measure and we neglect the year of 2002 from this correlation analysis due to its outlier nature. Inspection of Figure 4-6 suggests that SSPV predictability is considerable, particularly between the months of September and January. Predictability is seen to develop from August, with the longest period of predictability emerging around October, consistent with the peak of EOF1 in Figure 4-2. Correlation values above 0.6 are found for November, December and January during this time. Predictability then decays following this October peak. These results are consistent with an hypothesis that perturbations to the SSPV in winter can lead to a shift in the statistics of the vortex breakdown event in the following summer. A separate attempt has also been made at quantifying this statement in 4.A, although the power of the analysis is somewhat limited by the sample size. Nevertheless, a shift in the statistics would appear detectable from at least as early as September. Furthermore,

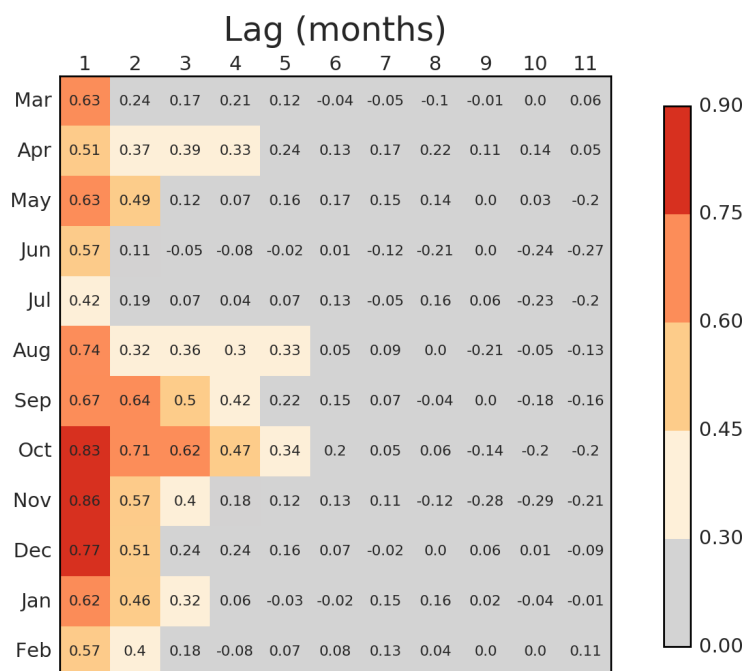


Figure 4-6: Correlation coefficients between polar cap averaged 30 hPa geopotential height at a given month of the year with values in the subsequent months. For example, the correlation coefficient between polar cap averaged geopotential height in March and in the subsequent April is shown in the first column for March. Data has been linearly de-trended for each month prior to calculation. Shaded cells represent values that are statistically significant at the approximate 5 % level based on a one-tailed test of Student's *t* statistic. 2002 is not included in the correlation analysis (see text).

it would also appear possible to detect an increased likelihood in the occurrence of extremely early or late vortex breakdown events from September, based on the emergence of large perturbations to the SSPV lifecycle at this time of year. This is of interest as extreme events are expected to have the largest impact on tropospheric circulation statistics (Chapter 3). These results can also be seen in Figure 4-7, where monthly-mean polar cap averaged geopotential height is used as a predictor of the vortex breakdown date for each year.

Another means of exploring the association between perturbations to the SSPV lifecycle and the vortex breakdown date involves the use of a graphical method previously suggested by Hirano et al. (2016). Polar cap averaged geopotential height anomalies at 30hPa are computed for each day between September 1 and February 1, and these are used to construct yearly time series. The yearly time series are then

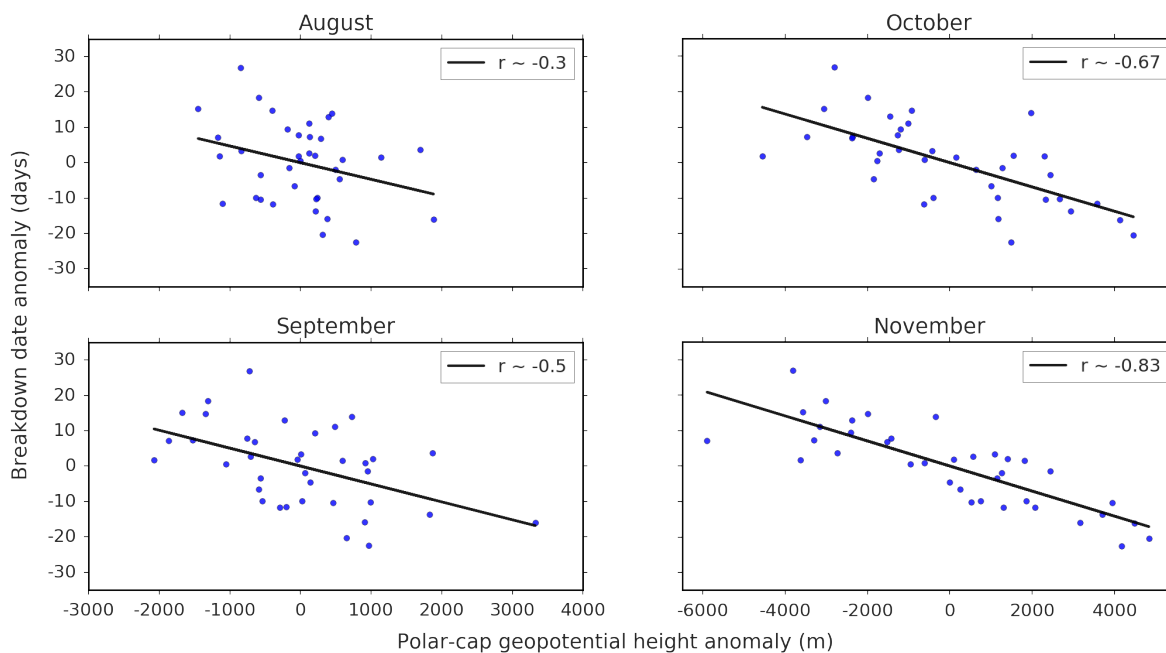


Figure 4-7: Regression of stratospheric vortex breakdown date anomaly against monthly-mean polar cap averaged geopotential height anomaly at 30hPa for August - November. Correlation coefficients for each month are indicated by the label in the top right corner of each plot. All correlation coefficients are significant at the 5% level at least. 2002 is not included in the correlation analysis (see text).

arranged chronologically by breakdown date. The result is plotted in Figure 4-8. To a first approximation the figure is seen to be in reasonable agreement with the previous analysis: the latest breakdown dates are associated with a strong SSPV in the preceding months, while the opposite is found for the earliest breakdown dates. Closer inspection suggests two further features of interest. Firstly, evidence of a strong SSPV is often seen to emerge at 30 hPa by September 1, and this behaviour would appear to largely persist until the vortex breakdown event in summer; in contrast, evidence of a weakened SSPV is occasionally not seen to emerge until late September. It may be the case that some weak SSPV years are more clearly understood in terms of a single dynamical event (e.g., 1982; see Newman, 1986). This may be suggestive of a fundamental asymmetry between weak and strong vortex years, perhaps related to the inherently dynamical nature of weak vortex years, with subsequent implications for the predictability timescale of the vortex breakdown event in weak SSPV years. However, confirmation of this statement is likely to be outside the scope of what is

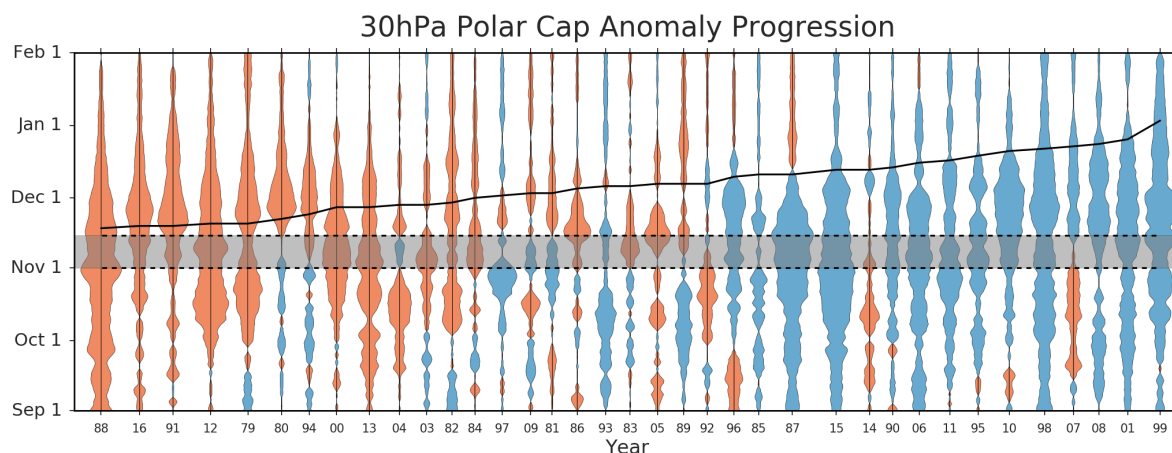


Figure 4-8: Yearly time series of polar cap averaged geopotential height anomalies at 30hPa. Positive anomalies are red and negative anomalies are blue. Units are m. For reference, anomaly on November 1 1988 is approximately + 700 m. Shaded region indicates suggested period for re-initialisation of forecast model (see text). Black line indicates stratospheric vortex breakdown date for each year. 2002 is not included (see text).

possible based on re-analyses.

The second feature that emerges from inspection of Figure 4-8 is that occasionally years with a weak SSPV are associated with a somewhat delayed vortex breakdown date, with opposite behaviour for years with a strong SSPV. From inspection of the particular examples for weak SSPV events, it appears that years with a large vortex weakening can occasionally be associated with a brief recovery of the vortex in late spring. The years of 2007 and 2014 are the outstanding examples of this behaviour. From inspection of the particular examples for strong SSPV events, it appears that as the SSPV nears the end of its lifecycle it can occasionally break down rather dramatically. The years of 1980 and 1997 are the outstanding examples of this behaviour. While these exceptional years are not sufficient to affect the qualitative conclusions of our analysis, they may be of interest for seasonal forecasting applications, where a quantitative assessment is more important. Figure 4-8 suggests that re-initialisation of a forecast model sometime in early November may be sufficient to account for the unusual behaviour of these years. It should be noted that the potential benefits of such a re-initialisation need not be restricted to short-medium term forecasts, as the timing of the breakdown event represents a leading-order influence on large-scale circulation variability during November, December and even January (Sun et al., 2014,

see Chapter 3 and Figure 4-1).

Before concluding this section we also consider the role of the QBO, as previous research has suggested a potential for the QBO to perturb the SSPV lifecycle during winter (e.g., Baldwin and Dunkerton, 1998; Anstey and Shepherd, 2014). We proceed by repeating our composite analysis from the previous section using July monthly-mean winds at 20hPa to define the phase of the QBO (Anstey and Shepherd, 2014, see Table 4.1); we again neglect the year of 2002 from our analysis due to its outlier nature. The results of our analysis are shown in Figure 4-9. Based on inspection of the individual months of this figure it would appear that there is indeed an association between perturbations to the SSPV lifecycle and the phase of the QBO, with weak SSPV years associated with an easterly winter QBO and strong SSPV years associated with a westerly winter QBO. As an alternative measure of this association we also test whether there is evidence of a statistical relationship between our PC1 index from Section 3 and the phase of the QBO (see 4.A). The results are suggestive of an association ($p \sim 0.06$), although our sample size again limits the statistical power of our analysis. Thus it would appear likely that there is an association between the phase of the QBO and perturbations to the SSPV lifecycle, although the strength of this association is not so large that it can be clearly detected in small sample sizes.

4.4 Stratosphere-troposphere coupling

4.4.1 Interannual variations

The results of the previous section suggest that there is the potential for skilful seasonal forecasting in the SH stratosphere between August and February at least. As was highlighted in the references in Section 4.1, stratosphere-troposphere coupling in the SH has been regularly documented for this time of year. Thus we now consider whether there is also evidence for the potential for skilful seasonal forecasting in the troposphere, based on knowledge of the initial stratospheric state. We begin by describing the long-term behaviour of the tropospheric EDJ using two separate measures. For our first measure we use vertically averaged zonal-mean zonal wind, denoted $\langle [u] \rangle$ (Chapter 3). For our second measure we use the difference in zonal-mean sea level pressure between 50 and 65 S, denoted ZI (Bracegirdle, 2011); this difference in sea level pressure can be viewed as the SH equivalent to the NH zonal index (Kidson, 1988). Long-term averages for both of these measures are shown in

Table 4.1: Classification of 38 yr based on PC1 (Figure 4-3) along with classifications for the QBO and the breakdown date of the SSPV. For PC1, W is a weak SSPV year and S is a strong SSPV year. For the QBO, E represents easterly monthly-mean zonal wind values for July at 20hPa and W represents westerly values. The brackets denote actual monthly-mean values according to the ERA-Interim re-analysis product. For the SSPV breakdown date (Chapter 3) E represents extreme early years, L represents extreme late years, e represents years before the median breakdown date and l represents years after the median breakdown date. Breakdown dates for each year are shown in brackets.

<i>Year</i>	79	80	81	82	83	84	85	86	87	88	89	90	91
PC1	W	W	W	W	W	W	S	W	S	W	S	S	W
QBO (20hPa)	E (-33)	W (16)	E (-28)	W (6)	E (-26)	E (-29)	W (12)	E (-30)	W (6)	E (-28)	E (-36)	W (17)	E (-27)
BD	E (20 Nov)	E (22 Nov)	e (3 Dec)	e (29 Nov)	e (6 Dec)	e (1 Dec)	l (11 Dec)	e (5 Dec)	l (11 Dec)	E (18 Nov)	l (7 Dec)	L (14 Dec)	E (19 Nov)
<i>Year</i>	92	93	94	95	96	97	98	99	00	01	02	03	04
PC1	W	S	W	S	S	S	S	S	W	S	W	W	W
QBO (20hPa)	W (8)	E (-23)	E (-26)	W (1)	E (-35)	W (14)	E (-29)	W (8)	E (-37)	E (-11)	W (6)	E (-29)	W (8)
BD	l (7 Dec)	l (6 Dec)	E (24 Nov)	L (19 Dec)	l (10 Dec)	e (2 Dec)	L (22 Dec)	L (3 Jan)	E (27 Nov)	L (26 Dec)	e (3 Dec)	e (28 Nov)	E (28 Nov)
<i>Year</i>	05	06	07	08	09	10	11	12	13	14	15	16	
PC1	W	S	W	S	W	S	S	W	W	W	W	S	W
QBO (20hPa)	E (-34)	W (13)	E (-33)	W (11)	E (-33)	W (8)	E (-26)	E (-20)	W (16)	E (-29)	W (15)	W (9)	
BD	l (7 Dec)	L (16 Dec)	L (23 Dec)	L (24 Dec)	e (3 Dec)	L (21 Dec)	L (17 Dec)	E (20 Nov)	E (27 Nov)	l (13 Dec)	l (13 Dec)	E (19 Nov)	

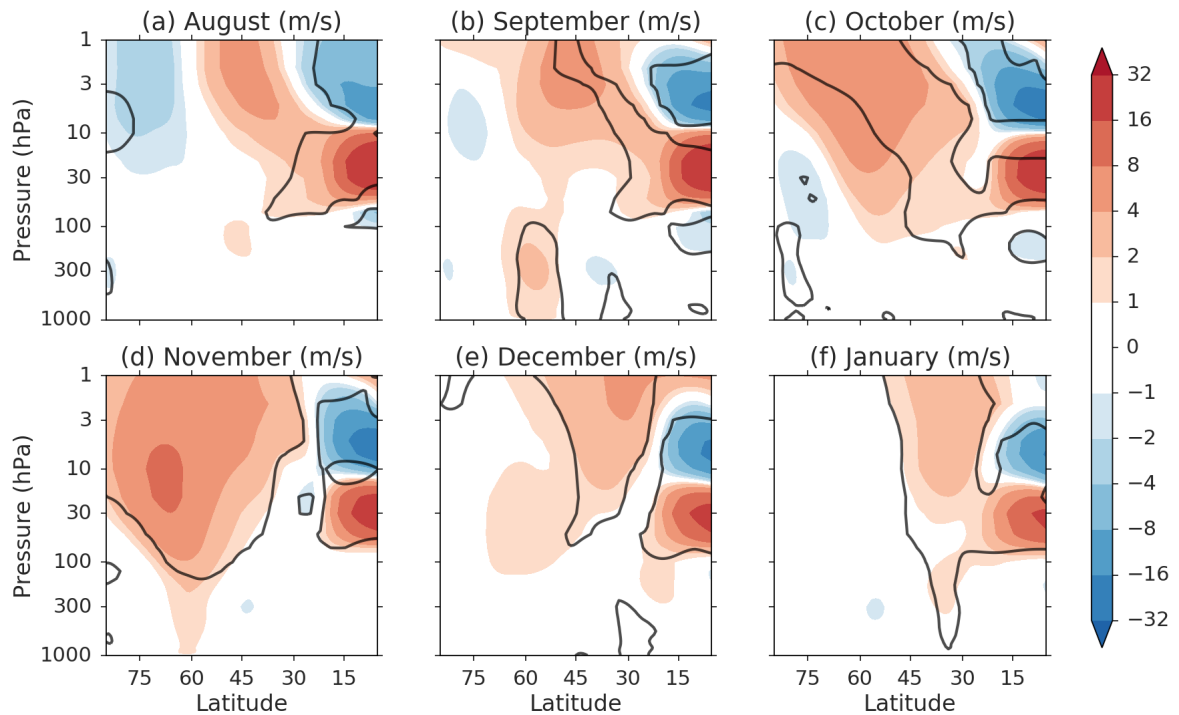


Figure 4-9: Monthly-mean differences in $[u]$ between westerly and easterly QBO phase (shading). 2002 is not included in the analysis (see text). Black contours represent regions where differences are statistically significant at the 5 % level, based on a one-sided two-sample Student's t test. Note the non-linear colour scale required for including tropospheric and stratospheric differences in the same figure.

Figure 4-10 and Figure 4-11. Inspection of these figures reveals a clear semi-annual oscillation in the location of the EDJ, with the strongest winds closest to the pole in late March and October. As the present chapter is concerned primarily with coupled stratosphere-troposphere behaviour from late winter, we now restrict our attention to describing EDJ behaviour between August and February.

From August until late September the long-term average location of the EDJ undergoes little change. Starting from about late September, the EDJ transitions poleward until early November. This poleward transition of the EDJ is also associated with an intensification of the winds. Inspection of individual years suggests that this picture of a more poleward and intense EDJ in October is a reasonable description, although the intensification of the winds is more pronounced in some years than in others. The years of 1988 and 2002 are two clear exceptions to this description, both having very clearly defined equatorward jets. These years are also notable as having the two largest values in our PC1 index of stratospheric variability (Figure 4-

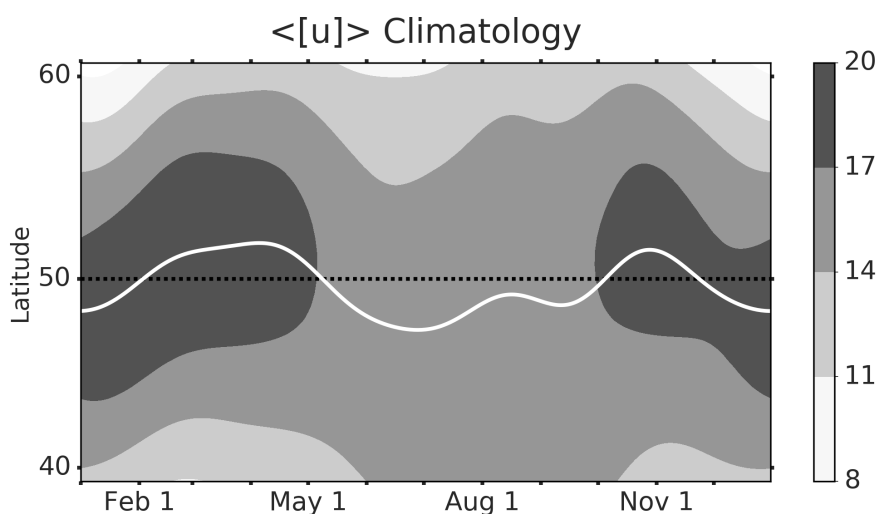


Figure 4-10: Climatology of $\langle [u] \rangle$ (shading) and jet-latitude index (white line). Units are m s^{-1} .

3). Large stratospheric variations during these years were associated with a vigorous minor warming (Hirota et al., 1990) and an SSW event respectively. From about mid-November onwards the EDJ undergoes an equatorward transition. This equatorward transition was the focus of Chapter 3, to which the reader is referred for more details. Broadly speaking, it reflects a shift in latitude of the EDJ in association with the vortex breakdown in the stratosphere.

To investigate the potential for interannual variations in the stratosphere to impact the troposphere, we begin by revisiting Figure 4-4. In the troposphere, statistically significant differences between W and S years are present from September until the beginning of February, consistent with the earlier results of Hio and Yoden (2005). To examine these differences in greater detail, we have computed long-term averages of $\langle [u] \rangle$ and ZI for W and S years separately (Figure 4-11 and Figure 4-12). We begin by discussing the September and October differences. In both W and S years a poleward transition and intensification of the winds is seen from about late September, consistent with the long-term average behaviour in Figure 4-10. However, in S years this intensification and shift of the winds is of larger amplitude. This is particularly clear during October, where changes in ZI are found to be dominated by a reduction in zonally-averaged sea level pressure at 65 S (not shown), consistent with a more poleward and intense EDJ in S years. This enhanced poleward shift of the EDJ during S years is associated with a stronger and deeper SSPV in the stratosphere (see previous section). Thus, while the SSPV lifecycle is accelerated in

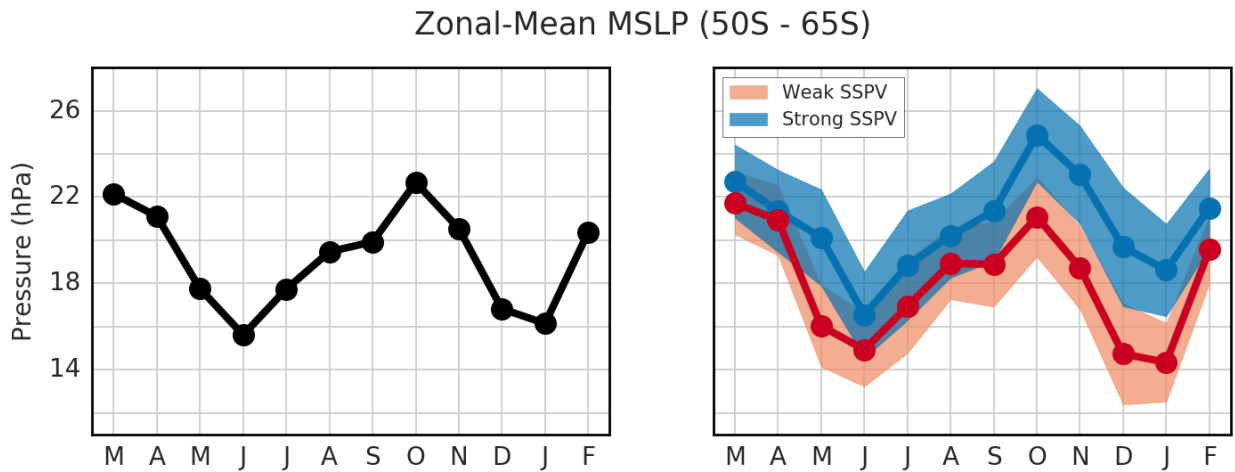


Figure 4-11: (Left) Climatology of monthly-mean difference in zonally-averaged sea level pressure between 50 and 65 S. (Right) Similar calculation for W years (red line) and S years (blue line). Shading represents ± 1.96 standard error interval for each set of years.

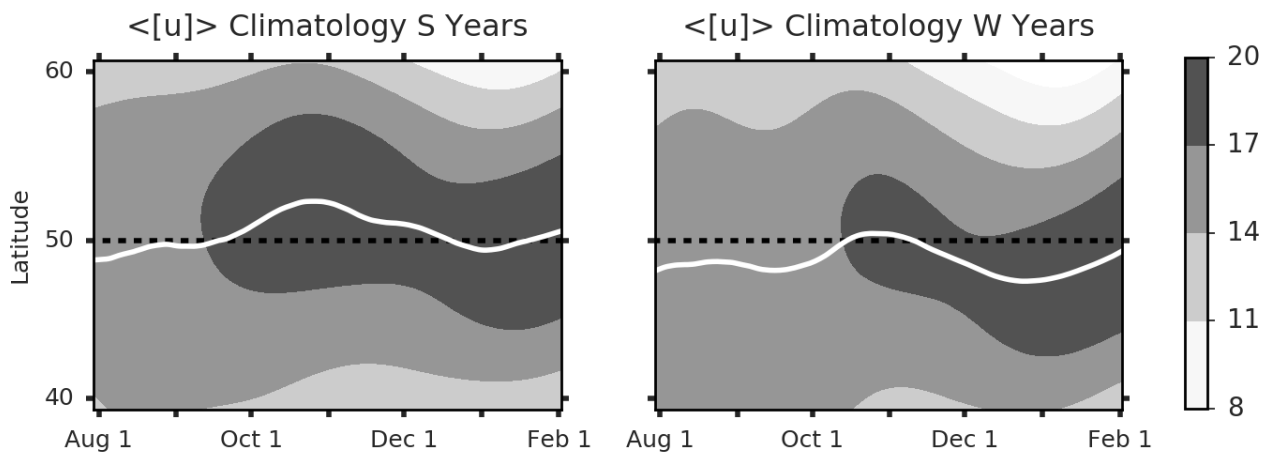


Figure 4-12: (Left) Climatology of $\langle [u] \rangle$ (shading) and jet-latitude index (white line) for S years between August 1 and February 1. (Right) Similar calculation for W years. Jet-latitude index climatologies have also been smoothed using a moving-average filter for presentation purposes. Units are m s^{-1} .

W years on average, it is also weaker and smaller in size, and it is the combination of these features that apparently explains why an approximate phase delay in the SSPV lifecycle in the stratosphere emerges as an approximate change in amplitude (i.e, a poleward transition and intensification) in the EDJ lifecycle in the troposphere during October.

Between November and early February the difference in tropospheric statistics can be largely understood in terms of the results of Chapter 3. Broadly speaking, this difference reflects a difference in the timing of the summer equatorward transition of the EDJ, which is closely tied to the vortex breakdown event in the stratosphere. This is because there is a relationship between the winter strength of the SSPV and the timing of the vortex breakdown event each year (see previous section). As a result, S years are on average expected to have a delayed, and somewhat reduced, equatorward transition of the EDJ compared to W years. Thus it would appear that the difference in tropospheric statistics between September and February can be approximately described as a combination of a change in amplitude (September/October/January) and a phase delay (November until January) of the EDJ lifecycle, and that these differences are closely tied to the state of the SSPV in the stratosphere.

4.4.2 Alternative circulation perspective

The results of the previous section suggest at least two components to skilful seasonal forecasting in the SH troposphere during spring and summer. The first component represents a change in the September/October EDJ statistics in association with the apparent downward merger of the SSPV and the EDJ. The second component represents a change in the November - February EDJ statistics in association with the timing and type of vortex breakdown event in the stratosphere. Based on our analysis in Section 4.3, this would suggest that skilful seasonal forecasts of the troposphere might be possible based on knowledge of the state of the winter SSPV. To test this hypothesis, we repeat a similar analysis from Section 4.3 and compute correlation coefficients between a measure of the SSPV at a given month of the year and a measure of the troposphere at subsequent months. We use polar cap averaged geopotential height at 30hPa and the ZI time series as our respective measures. The results of this calculation for August - February are presented in Figure 4-13. Statistically significant correlations are seen to emerge for forecasts of the troposphere from October until February. Furthermore, when this calculation is repeated using the troposphere

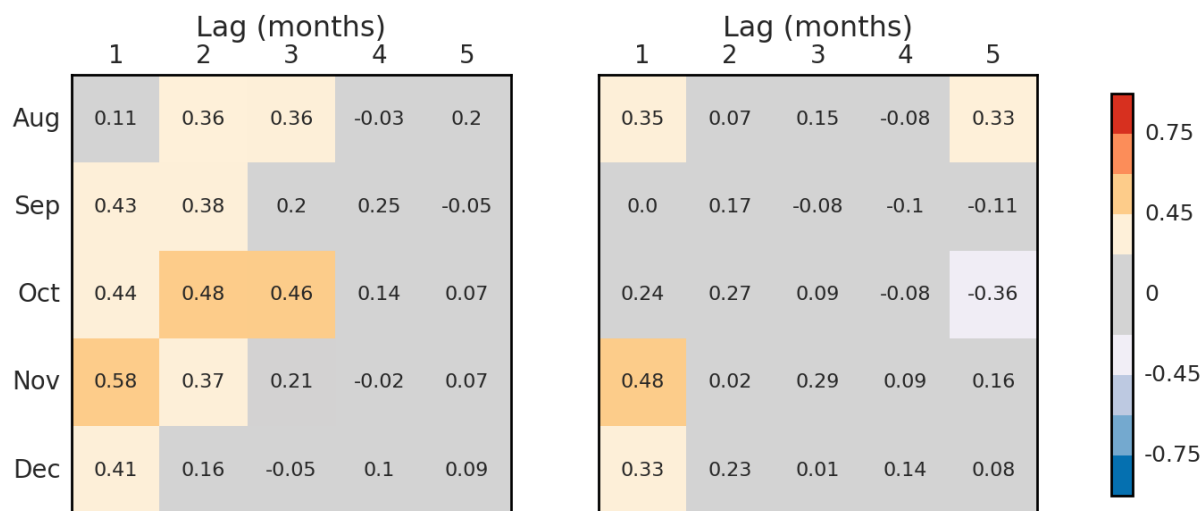


Figure 4-13: (Left) Correlation coefficients between polar cap averaged 30 hPa geopotential height at a given month of the year with ZI in the subsequent months. (Right) Correlation coefficients between ZI at a given month of the year with ZI in the subsequent months. Data has been linearly de-trended for each month prior to calculation in both figures. Shaded cells represent values that are statistically significant at the 5 % level based on a one-tailed test of Student’s t statistic. 2002 is not included in the correlation analysis (see text).

as a predictor of itself (Figure 4-13) the correlations are seen to largely vanish. This is consistent with previous work by Gerber et al. (2010) who used an Annular Mode index to highlight that at this time of the year the stratosphere is a better predictor of the troposphere than the troposphere itself. A visual exploration of the correlation between October stratosphere conditions and subsequent months in the troposphere is shown in Figure 4-14.

As an alternative measure of the potential for skilful seasonal forecasting in the SH troposphere we provide an update of the Annular Mode ‘dripping paint’ plots (Thompson et al., 2005, Figure 4-15). The Annular Modes represent an alternative diagnostic for measuring stratosphere-troposphere coupling and are regularly used in assessments of the potential for seasonal forecasting (e.g., National Research Council, 2010). Although the Annular Modes are usually defined via an EOF analysis, the leading principal component time series is closely related to polar cap averaged geopotential height (Baldwin and Thompson, 2009). As such, much of the behaviour in Figure 4-15 can be interpreted using the analysis from earlier sections. Inspection of this figure reveals a coherent descent of circulation anomalies in the stratosphere,

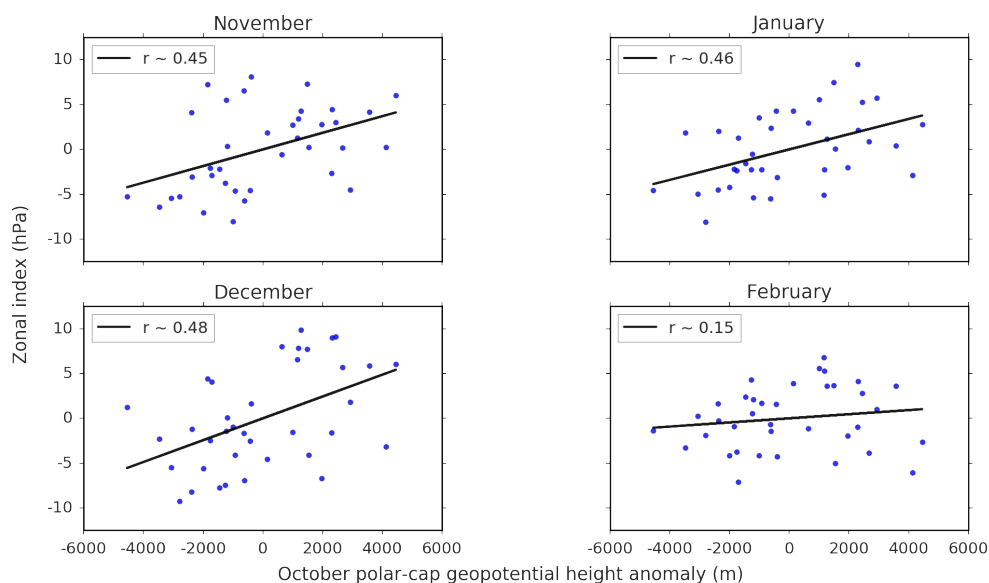


Figure 4-14: Regression of ZI against October polar cap averaged geopotential height anomaly at 30hPa for October - February. Correlation coefficients for each month are indicated by the label in the top left corner of each plot. 2002 is not included in the correlation analysis (see text).

with weak vortex years associated with persistent positive anomalies and with the opposite behaviour for strong vortex years. This behaviour is consistent with a phase delay in the shift-down of the SSPV between W and S years (see Section 3). Furthermore, both weak and strong vortex years are seen to exhibit substantial intraseasonal coherence in the troposphere, consistent with coupled variability between the stratosphere and troposphere (see previous subsection), and supporting the claim of a concomitant potential for skilful seasonal forecasting in the troposphere.

The intraseasonal coherence of anomalies in the troposphere and stratosphere suggests that (Annular Mode) anomalies have a strong synchronisation with the seasonal cycle during this time of year. As a check of this statement, we have computed a plot of weak and strong vortex years as a function of calendar day of the year (Figure 4-15). The anomalies in this calendar year plot are seen to be of a similar magnitude and pattern as those in the previous ‘lag’ plot. This suggests that the timescale separation implicit in a description of circulation variability as (stationary stochastic) anomalies about a slowly-varying seasonal cycle is not well satisfied during this time of year. In particular, the long intraseasonal persistence of the anomalies suggests that variations are more naturally viewed as shifts in the seasonal cycle rather than as

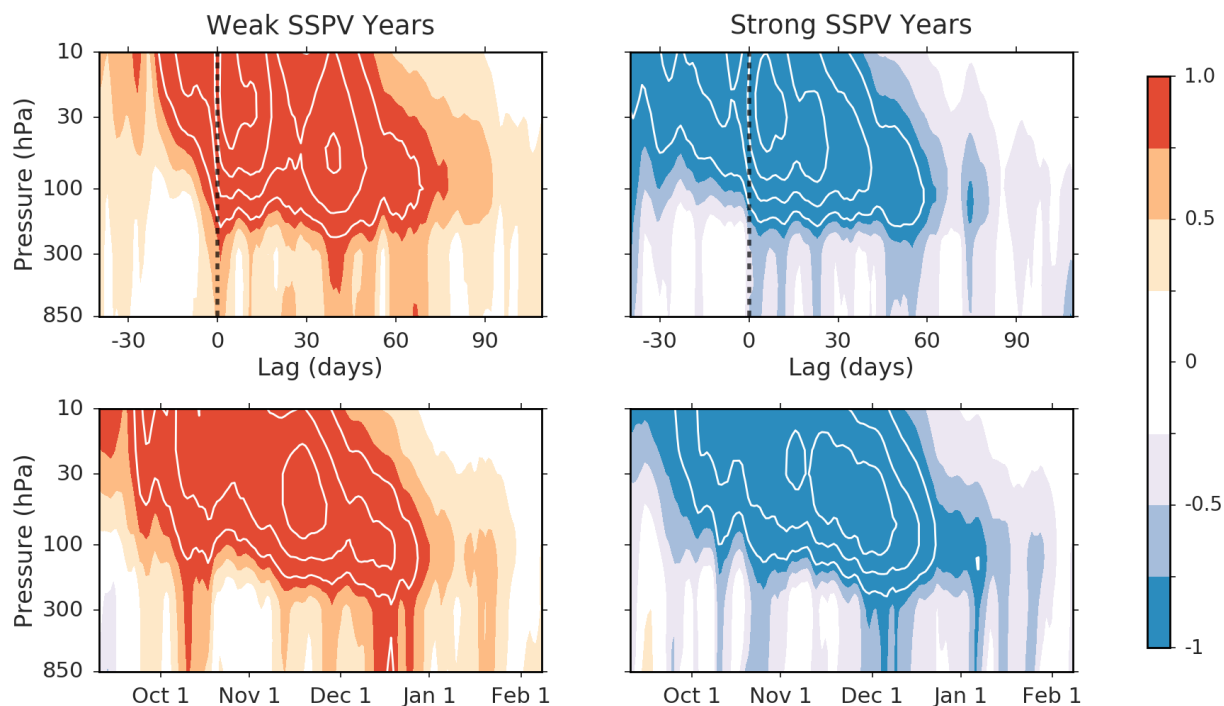


Figure 4-15: (Top) Composite plots of Annular Mode indices for 13 weakest and 13 strongest SSPV years. Weak and strong years are defined using Annular Modex index at 30 hPa. Dashed vertical line represents onset date (see text). Shading interval is 0.25 standard deviations and contour interval is 0.5 standard deviations. Shading is drawn for values greater than ± 0.25 standard deviations. (Bottom) Similar calculation but for calendar day of the year.

anomalies about a seasonal cycle. Thus, combining the results from this and previous sections of the chapter, we are led to propose an alternative perspective for circulation variability between September and February. We argue that during this time of year, variability of the large-scale extra-tropical tropospheric and stratospheric circulations is most naturally viewed as a shift in the seasonal cycle of a single, coupled entity and that the statistics of this variability can be determined by conditioning on the stratospheric circulation from the previous winter. We note the close similarity between this perspective and those proposed by Kuroda and Kodera (1998) and Hio and Yoden (2005) using earlier versions of re-analysis products.

4.5 Summary and discussion

We have considered the predictability of the SH stratospheric polar vortex breakdown event in a re-analysis product. We have focused on the time period from August until February, which is associated with the shift-down of the SSPV from its midwinter position. We have also considered coupled variations between the troposphere and stratosphere during this time. Our results can be broken into three different components.

Firstly, we have presented evidence for significant predictability of the stratospheric polar vortex breakdown event arising from persistent variations of the SSPV in the previous winter and spring. Evidence of predictability is found from August, with peak values emerging around October. This persistence of (stratospheric) initial conditions over the course of several months is notable as being significantly longer than timescales that have previously been associated with atmospheric initial condition skill (Kirtman and Pirani, 2007). A relationship between perturbations to the winter SSPV and the phase of the midwinter QBO has also been documented, consistent with previous results (Anstey and Shepherd, 2014, and references therein). This relationship, along with a similar relationship between ENSO and the SSPV (Chapter 3), may represent an important source of interannual variability for the SSPV.

A separate potential source of interannual variability for the SSPV has been suggested by the distribution of extreme years of our PC1 index (Figure 4-3). Extreme weak years of the SSPV are found to have a tendency to directly follow extreme strong years ($p \sim 0.06$; see 4.A), suggesting that memory of the SSPV can occasionally persist from one year to the next. This is reminiscent of an earlier model result of Scott and Haynes (1998). In addition, extreme years of our PC1 index are found to be clustered in the second half of our dataset ($p \sim 0.02$; see 4.A). Ozone depletion is a well documented property of later years of the satellite record and it may be the case that a feedback between ozone and SSPV dynamics increases the likelihood of extreme SSPV events during this period. A similar remark has previously been made in Black and McDaniel (2007), where the authors noted an apparent increase in interannual variability of the SSPV during later years of the satellite era.

The second component to our results builds on previous work by Kuroda and Kodera (1998) and Hio and Yoden (2005), which documented coupled variability between the stratosphere and troposphere during austral spring and early summer. We have presented evidence for the predictability of variations in the troposphere

during this time, based on knowledge of the stratospheric initial state; moreover, this predictability is seen to largely vanish when the troposphere is used as a predictor of itself (see also Gerber et al., 2010). The physical explanation for this tropospheric skill can be traced to seasonal shifts in latitude of the EDJ: strong SSPV years are associated with an enhanced poleward transition in September/October and a delayed equatorward transition between November and January, with opposite behaviour in weak SSPV years.

Related to this, recent research has provided evidence of model skill in forecasting the poleward transition of the EDJ, based on a model initialisation in early August (Seviour et al., 2014). The present work suggests that such skill should also be realisable in forecasting the equatorward transition of the EDJ, particularly for a model initialisation in early November. The use of a similar diagnostic to that proposed by Newman (1986) may represent a helpful tool for assessing model fidelity around the time of this equatorward transition². While the threshold definition for the date of the stratospheric vortex breakdown date considered in this and previous studies (Black and McDaniel, 2007, Chapter 3) works well for the re-analysis product, it may be the case that it is less suitable for a model with a different climatology.

There is evidence that the benefit of skilful forecasting of the equatorward transition of the EDJ can be quite substantial (see Chapter 3 and Figure 4-1). As a very recent example, we highlight the unprecedented retreat of Antarctic sea-ice during 2016 (Turner et al., 2017). Sea-ice decrease during this season was closely linked to high-latitude circulation anomalies; in particular, the November SAM was notable for assuming its most negative value during the satellite era. Such a large negative value appears to have been closely associated with the equatorward transition of the EDJ, which was one of the earliest during the satellite era (see Table 4.1). Thus, the weak SSPV of 2016 and the exceptionally early transition of the EDJ may offer a partial explanation to the puzzling behaviour of sea-ice during this year (Turner and Comiso, 2017). Furthermore, it implicates the stratosphere as a potentially important source of low-frequency variability in variations of Antarctic sea-ice extent.

The poleward and equatorward transition of the EDJ is part of a broader semi-annual oscillation of the EDJ (van Loon, 1967). The SAO has previously been interpreted as a largely baroclinic phenomenon, emerging as a result of contrasting sea-

²The original diagnostic of Newman (1986) considered the difference between 30hPa zonal-mean temperature at 80 and 50 S. We find that the use of this diagnostic at the 125hPa level results in an almost identical time series for the stratospheric vortex breakdown date as that considered in the present paper.

sonal evolutions of surface temperature over the Southern Ocean and the Antarctic regions. Our work emphasises the additional role of the stratosphere in a complete theory for the SAO, at least between September and February. This role for the stratosphere has previously been considered by Bracegirdle (2011). We further note that the impact of stratospheric ozone depletion offers a natural explanation for the documented modulation of the SAO during the second half of the year since the 1970's (Hurrell and van Loon, 1994). In light of recent research that has implicated stratospheric circulation changes to long-term EDJ changes in May (Ivy et al., 2017), it may also be of interest to explore the potential role of the stratosphere in EDJ behaviour during the first half of the year.

The third and final component to our results again builds on previous work by Kuroda and Kodera (1998) and Hio and Yoden (2005). Based on our earlier results, we have proposed an alternative perspective for large-scale extra-tropical circulation variability between September and February. We argue that during this time of year, variability is most naturally viewed as a shift in the seasonal cycle of a single, coupled entity and that the statistics of this variability can be determined by conditioning on the stratospheric circulation from the previous winter. There are several examples where this perspective may shed new light.

Firstly, this perspective suggests that long Annular Mode timescales during austral spring and summer should not be interpreted as an increased persistence of perturbations to some slowly-varying seasonal cycle. Rather, it suggests that they instead reflect a phase shift of the seasonal cycle. An instructive example of the differences between these two statements can be found by considering the increased persistence of Annular Mode timescales in the troposphere during austral summer (Gerber et al., 2010). From the perspective of perturbations to some slowly-varying seasonal cycle, this increased persistence has been argued to arise from eddy feedbacks in the troposphere (e.g., Kidston et al., 2015). In our proposed perspective, this increased persistence reflects year-to-year variability in the phase of the seasonal cycle (i.e., in the equatorward transition of the jet); eddy feedbacks in the troposphere are not necessarily required.

A second example of the insight offered by this perspective relates to a dynamical explanation for the increased persistence of stratospheric anomalies during austral spring. The present perspective suggests that this persistence can be interpreted in terms of the existence of multiple seasonal evolutions of the SSPV during austral spring. This interpretation has an analogue in the modelling work of Scott and

Haynes (2000, 2002) which highlighted the possibility of multiple-flow equilibria in the stratosphere, and which argued that these equilibria were a function of the strength of the winter SSPV. Scott and Haynes (2000, 2002) interpreted the existence of multiple-flow equilibria in terms of classical wave-mean flow arguments - if a strong SSPV is established in winter, it will be less disturbed by wave-forcing than if a weak SSPV is established. It is left to future work to establish the validity of this hypothesis for the re-analysis product.

A final example is provided in Chapter 3. In this chapter it was noted that SAM anomalies (along with the associated eddy anomalies) persisted for longer during austral spring and early summer than in any other season. The present perspective offers a natural explanation for this increased persistence of circulation anomalies. Furthermore, it also suggests an hypothesis for the quasi-two year peak of the SAM that was documented in Chapter 2: perturbations to the SSPV lifecycle during winter emerge as persistent anomalies in the tropospheric circulation every year between September and February, resulting in a pronounced harmonic of the annual cycle in the SAM index. Low-frequency perturbations to the SSPV (such as the QBO or ENSO) can then imprint a distinct phase (e.g., quasi-two year) to this harmonic. It is left to future work to establish the validity of this hypothesis.

We conclude by noting that the perspective of circulation variability originally proposed by Kuroda and Kodera (1998) and Hio and Yoden (2005) also considered the early and midwinter months of the year. These months have not been considered in the present work. Thus it may be the case that the perspective on circulation variability proposed in this paper can also be extended to other months of the year. In this respect, the month of July looks most promising (see also Kuroda and Kodera (1998) for a more detailed discussion). In the stratosphere, July is notable as the time of year where the SSPV undergoes its annual poleward shift from subtropical to polar latitudes (e.g., Shiotani et al., 1993). In the troposphere, July is notable for large interannual variability in the location of the EDJ (e.g., Trenberth, 1984). It would be of interest to determine the extent of the relationship between these two quantities; however, it should be noted that as a result of the low-latitude position of the SSPV during much of July, Annular Mode (i.e., polar cap) diagnostics may not be the optimum measure of circulation variability for this time of year. We also draw attention again to the theoretical work of (Scott and Haynes, 2000, 2002) which suggests that the late winter configuration of the SSPV (i.e., the emergence of W or S years) can often be traced to the early winter wave forcing (see also Shiotani et al.

(1993) for some observational support of this statement). The year of 2002 would appear to be a particular example of such a scenario (Harnik et al., 2005).

4.A

To quantify whether extreme values of our PC1 index are clustered in the second half of our dataset we proceed as follows. First we generate a synthetic time series of eighteen ‘0s’ and twenty ‘1s’. These ‘0s’ and ‘1s’ are randomly distributed within the time series and are intended to mimic extreme events in our original PC1 index (which contains 20 extreme events). Next we calculate the difference between the sum of the first 19 elements and the remaining 19 elements of this synthetic time series to arrive at a value d . Finally we repeat this calculation 10^6 times to form a distribution for d . The difference for our PC1 time series is $d = 8$. According to our synthetic distribution, the probability of $|d| \geq 8$ is $p \sim 0.02$.

To quantify whether extreme positive values of our PC1 index have a tendency to follow extreme negative years we proceed as follows. First we generate a synthetic time series of ten ‘-1s’ and ten ‘+1s’. These ‘-1s’ and ‘+1s’ are randomly distributed within the time series and are intended to mimic extreme negative and extreme positive events in our original PC1 index. Next we derive a new time series by forming the difference between adjacent entries in our original synthetic time series. For example, if the first and second entries of our synthetic time series are -1 and +1 respectively, the first entry of our derived time series will be +2. Once we have constructed our derived time series, we count the number of occurrences of ‘+2’ in this time series - ‘+2’ is a unique identifier of an extreme positive event directly following an extreme negative event. Finally we repeat this calculation 10^6 times to form a distribution. The number of ‘+2s’ in our PC1 time series is 5. According to our synthetic distribution, this has an approximate p-value of $p \sim 0.06$.

To quantify whether perturbations to the SSPV lifecycle can lead to a shift in the statistics of the vortex breakdown event we begin by dividing our data into the 19 earliest (E) and 19 latest (L) vortex breakdown years (see Table 4.1). We next consider monthly-mean polar-cap averaged geopotential height at 30hPa and sort this data into the 19 largest (L_{30}) and 19 smallest (S_{30}) years. Finally, we calculate how many E and L years are associated with L_{30} years and we do this for each of the months of August, September and October (by symmetry this calculation will be the same for S_{30} years). We denote this calculation as (E, L) . For example, for

the month of August, 12 L_{30} years are also E years and the remaining 7 L_{30} years are L years. We denote this configuration (12, 7). For the months of September and October we have configurations of (13, 6) and (15, 4) respectively. We then test the statistical significance of these results using a hypergeometric sampling distribution. The various configurations are found to have approximate p-values of 0.1, 0.03 and 0.001 respectively.

To quantify whether perturbations to the SSPV lifecycle can lead to a shift in the statistics of extreme vortex breakdown events, we begin by dividing our data into extreme breakdown years, which are defined as the 10 earliest (EX) and 10 latest (LX) vortex breakdown years. For each month we select the 10 largest (LX_{30}) and the 10 smallest (SX_{30}) years for monthly-mean polar-cap averaged geopotential height at 30hPa. Finally, we calculate how many EX years are associated with LX_{30} years (the results are similar if we instead consider SX_{30} years). We denote this calculation as ($EX, N/EX$). For example, for the month of August, 3 LX_{30} years are also EX years and the remaining 7 LX_{30} years are not EX years. We denote this configuration (3, 7). For the months of September and October we have configurations of (5, 5) and (6, 4) respectively. We then test the statistical significance of these results using a hypergeometric sampling distribution. The various configurations are found to have approximate p-values of 0.53, 0.06 and 0.01 respectively.

To determine whether there is a statistical relationship between the phase of the QBO and our PC1 index, we first note that 15 easterly QBO years have been associated with positive PC1 years and 6 easterly QBO years have been associated with negative PC1 years (by symmetry this calculation will be the same for westerly QBO years). We then test the statistical significance of this configuration using a hypergeometric sampling distribution, with the result being an approximate p-value of 0.06.

Chapter 5

Conclusion

5.1 Summary

This thesis has considered the hypothesis that multiple evolutions of the seasonal cycle of the Southern Hemisphere mid-latitude circulation are possible. The main body of work has concerned itself with presenting evidence for (Chapters 2, 3 and 4) and developing deterministic models of (Chapters 3 and 4) different seasonal evolutions of the mid-latitude SH circulation using a re-analysis product. Some applications of these deterministic models (Chapters 3 and 4) have also been discussed. The main results are summarized in the next subsection, followed by a discussion of their theoretical and practical implications. The thesis concludes with some suggestions for potential future directions.

5.1.1 Evidence for non-stationarity in the mid-latitudes

Chapter 2 presented evidence supporting the use of a deterministic (non-stationary) description of SH mid-latitude circulation variability. This evidence consisted of a low-frequency peak in the SAM and EMFC indices that was viewed as a harmonic of the annual cycle (quasi-two year). Whilst the peak in the SAM does not always stand out clearly from the background variability, the peak in the EMFC is strong and robust. Statistically stationary models of circulation anomalies, which permitted the possibility of a potential feedback between the SAM and the mid-latitude eddies, were shown to be unable to account for the presence of this harmonic in the EMFC spectrum. It was argued that the simplest and most robust explanation for this peak was non-stationary interannual variability. Diagnosing the origins of this non-

stationary influence represented a leading motivation for the subsequent chapters of the thesis.

5.1.2 The vortex breakdown event

Chapter 3 built on the notion of a deterministic (non-stationary) influence on the mid-latitude circulation by considering the role of the stratosphere. Specifically, it was proposed that during SH late spring and early summer, high-latitude circulation variability was most usefully viewed as variability in the seasonal transition of the EDJ, which was organised around the date of the stratospheric vortex breakdown. This deterministic model of circulation variability was shown to be consistent with previous results in the literature once a non-stationary description of circulation anomalies was permitted.

Several applications of this proposed perspective were considered. First, it was shown how anomaly composites must be interpreted with care when statistical models of circulation variability exhibit non-stationary behaviour. Second, it was argued that the SH high-latitude zonal-mean ENSO teleconnection could be interpreted as a correlation between the phase of ENSO and the strength of the stratospheric vortex, rather than as a direct effect from the tropics. Third, it was argued that the increased SAM timescales encompassing late spring and summer could be viewed as reflecting variability in the timing of the seasonal transition of the EDJ, rather than as weakened damping of SAM anomalies by eddy feedbacks. Finally, it was argued that SH high-latitude climate change could be separated into at least two distinct time periods, and that for the earliest of these time periods (December), changes were more physically interpreted as a delayed equatorward transition of the jet, rather than the traditional description of a poleward shift.

5.1.3 The shift-down of the stratospheric vortex

Chapter 4 extended the results of the previous chapters by incorporating the downward shift of the stratospheric vortex into the deterministic model from Chapter 3. Building on previous work by Kuroda and Kodera (1998) and Hio and Yoden (2005), it was proposed that between September and February, variability was most naturally viewed as a shift in the seasonal cycle of a single, coupled entity and that the statistics of this variability could be determined by conditioning on the stratospheric circulation from the preceding winter. Evidence for this proposed perspective consisted of

three separate components.

First, it was shown that perturbations to the stratospheric polar vortex during austral winter had a tendency to persist until the final vortex breakdown event the following summer. A simple corollary was that the final vortex breakdown event had a significant degree of predictability each year. Additionally it was shown that there was an association between the QBO and interannual variations in the strength of the stratospheric vortex, suggesting a source for perturbations to the winter stratospheric vortex.

Second, the extent to which the EDJ in the troposphere was coupled with the vortex in the stratosphere during austral spring and summer was considered. This work built on previous work by Kuroda and Kodera (1998) and Hio and Yoden (2005). Evidence was presented for the predictability of variations in the troposphere during this time, based on knowledge of the stratospheric initial state. Moreover, this predictability was seen to largely vanish when the troposphere was used as a predictor of itself (Gerber et al., 2010). The physical explanation for this tropospheric skill was traced to seasonal shifts in latitude of the EDJ: strong stratospheric vortex years were associated with an enhanced poleward transition of the EDJ in September/October and a delayed equatorward transition between November and January, with opposite behaviour in weak stratospheric vortex years.

Finally, composite plots of Annular Mode anomalies were considered. These composite plots were computed as a function of lag relative to an onset date in the stratosphere, and also as a function of calendar day of the year. The close correspondence between the two versions of the composites suggested that anomalies were more naturally viewed as a phase shift in the seasonal cycle, rather than as perturbations about some slowly-varying seasonal cycle. The combination of these various pieces of evidence was argued to provide a justification for the proposed deterministic model of circulation variability, and to support the hypothesis of the thesis of multiple seasonal evolutions of the SH mid-latitude circulation.

5.2 Discussion

The understanding of circulation variability that emerges from this work is of relevance to a number of broader scientific questions. The possible implications to three areas of current interest are discussed below. Firstly, understanding this variability is essential for an accurate assessment of low-frequency variations of SH climate. Sec-

ondly, understanding the dynamics of this variability around the time of the stratospheric vortex breakdown event is crucial to understanding long-term changes during austral summer in particular. Finally, distinguishing between, and improving understanding of, the various spatial and temporal patterns of this variability is necessary for a more informed understanding of systematic model biases.

Low-frequency variations of the circulation

Understanding the low-frequency variations of the circulation is essential for an accurate assessment of long-term changes to the climate. The present work has identified an important component of low-frequency variability in the mid-latitude SH circulation, which has a pronounced quasi-two-year peak in eddy variability (Chapter 2). Several lines of evidence have been presented linking this quasi-two-year peak to variations in the stratosphere. There are at least two direct implications from these results.

Firstly, for climate model simulations, they suggest that an accurate representation of the SH stratosphere is essential for producing realistic representations of the SH mid-latitude circulation. Models that have known deficiencies in the stratosphere should at the very least be regarded with a healthy degree of skepticism, particularly during the period from September until February.

Secondly, it is of interest to determine whether the quasi-two-year phasing is truly representative of a preferred periodicity to low-frequency variations. The length of the time period considered in this thesis (satellite era, approximately 40 years) may not be sufficient for unambiguously distinguishing between low-frequency peaks on interannual timescales. In this respect, a greater understanding of low-frequency variability in the stratosphere may prove fruitful. This thesis has highlighted links between the QBO and the stratospheric vortex (see also Anstey and Shepherd, 2014, and references therein), ENSO and the stratospheric vortex, and it has also speculated on the potential existence of a ‘flywheel’ type mechanism (see Chapter 4). An improved theoretical understanding of how all of these components may/may not be linked would likely lead to greater confidence in the robustness of the quasi-two-year phasing in the troposphere.

SH climate change

Long-term changes to the SH circulation have been extensively documented for the austral summer season (Fogt et al., 2009). The present work (Chapter 3) identifies the stratospheric vortex breakdown event as an important actor in these changes. The results of Chapter 3 suggest that SH high-latitude climate change can be separated into at least two distinct time periods, and that these periods may loosely be categorised as pre- and post-vortex breakdown periods.

In the pre-vortex breakdown period, circulation variability appears well described as variability in the timing of the equatorward transition of the jet. Developing a theoretical basis for understanding how and why the jet transitions in association with the breakdown of the vortex would thus appear to be of some importance for advancing understanding of SH climate change. Furthermore, there is a suggestion that the scale of the jet transition in the troposphere might be a function of the type of vortex breakdown event in the stratosphere - very late breakdown events would appear to be associated with a much reduced transition of the jet in the troposphere with the opposite behaviour expected for very early events.

This potential sensitivity to the type of vortex breakdown event leads naturally into a discussion of changes in the post-vortex breakdown period. Although there was only a limited discussion of these changes in this thesis, there was a suggestion that very late breakdown years played a leading role in their emergence. The latest breakdown years appeared to be associated with a reduced equatorward transition in early summer and an earlier poleward transition in midsummer. Thus, an improved theoretical understanding of circulation dynamics around the time of the vortex breakdown event would also appear to be of importance for understanding January changes. They are also likely to be of benefit for separating the potentially competing influences of ozone recovery and greenhouse gas increase in future changes to SH climate.

Stratosphere-troposphere coupling

Coupling between the stratosphere and troposphere has been the focus of much attention in recent decades (see references in Chapter 4 Introduction). This thesis builds on this body of work and presents evidence for significant coupling in the SH mid-latitudes between September and February. This is a time of year where systematic biases among models would appear to be particularly problematic, at least

in the recent past [see also] (Gerber et al., 2010). The present work suggests two complementary approaches that may be helpful in diagnosing the sources of these model biases.

Firstly, the timing of the shift-down of the stratospheric vortex appears to be influential in the coupling between the stratosphere and troposphere during austral spring and summer. This suggests that models that are unable to realistically simulate this stratospheric behaviour will also be unable to realistically simulate the behaviour of the EDJ in the troposphere (or at least simulate it for the correct reasons). In the troposphere, the leading role played by the EDJ during September through February suggests that analysing daily variability of vertically and zonally averaged wind ($\langle [u] \rangle$) may be most fruitful for diagnosing model biases. The separation of data into variations about a long-term average may be misleading for characterising variability in both the stratosphere and troposphere, and it may be the case that data is best analysed by examining individual years, at least in the initial categorisation of the data.

Secondly, a greater theoretical understanding of how the seasonal cycle in the stratosphere interacts with the seasonal cycle in the troposphere would be of substantial benefit. The present work has provided evidence that as part of the seasonal shift-down and breakup of the stratospheric vortex, the tropospheric EDJ undergoes a seasonal poleward and equatorward transition (i.e., the spring phase of the SAO; this link with the stratosphere provides a different perspective on the SAO than the usual thermodynamic paradigm). The dynamics of the equatorward transition have been discussed in the previous subsection, but it would also be of interest to explore the dynamics associated with the poleward transition. An improved theoretical understanding of these features would lead to greater confidence in diagnosing model biases, as well as likely suggesting more accurate metrics for diagnosing model behaviour.

5.3 Future work

Seasonal forecast skill and model fidelity

The results presented in Chapter 4 suggest that long-range forecast skill may be possible between August and February in the SH mid-latitudes. Recent modelling work supports this statement, for the period between August and October/November

at least (Seviour et al., 2014). It would be of interest to determine whether similar results also exist for the period between November and February. Furthermore, some of the metrics proposed in this thesis (e.g., $\langle [u] \rangle$) may offer a more refined means of evaluating the fidelity of seasonal forecast systems during this time of the year than traditional skill scores.

What is the relationship between ENSO and the stratospheric vortex?

A statistically significant correlation between the phase of ENSO and the strength of the stratospheric vortex was documented in Chapter 3 (see also Hurwitz et al., 2011). It would be of interest to follow up this correlation in more detail and to determine its precise nature. In particular, it would be of interest to determine how robust this relationship is (given the short observational record and limited number of ENSO events), and what is the behaviour underlying this relationship if so?

A deterministic model for the May jet transition?

The results of Chapter 4 extended previous work by Bracegirdle (2011) by presenting evidence for a connection between the SAO in the troposphere and the state of the polar vortex in the stratosphere between September and February. In addition, a deterministic model was introduced for the equatorward transition of the EDJ between November and January in Chapter 3. Recent work has highlighted long-term changes to the tropospheric circulation during May that exhibit qualitative similarities to the well-documented circulation changes between December and February (Ivy et al., 2017). May is also the time of the year where the EDJ undergoes its winter equatorward transition as part of the SAO (see Chapter 4). In this respect it would be of interest (i) to determine whether there is a stratospheric influence on the SAO during the first half of the calendar year, and (ii) to investigate whether a deterministic model of circulation variability might also be appropriate for this time of year.

A deterministic model for the NH vortex breakdown event?

The results of Chapter 3 extended previous work by Black and McDaniel (2007) by proposing a deterministic model of circulation variability around the time of the

vortex breakdown event in the SH. Similar previous work also exists for the NH vortex breakdown event (Black et al., 2006). In light of the results of this thesis, it would be of interest to revisit this work for the NH to see if the development of a deterministic model of circulation variability can offer any further insights.

Bibliography

- J. A. Anstey and T. G. Shepherd. High-latitude influence of the quasi-biennial oscillation. *Q. J. R. Meteorol. Soc.*, 140(678):1–21, 2014.
- M. P. Baldwin and T. J. Dunkerton. Quasi-biennial modulation of the Southern Hemisphere stratospheric polar vortex. *Geophys. Res. Lett.*, 25(17):3343–3346, 1998.
- M. P. Baldwin and T. J. Dunkerton. Stratospheric harbingers of anomalous weather regimes. *Science*, 294(5542):581–584, 2001.
- M. P. Baldwin and D. W. J. Thompson. A critical comparison of stratosphere-troposphere coupling indices. *Q. J. R. Meteorol. Soc.*, 135(644):1661–1672, 2009.
- M. P. Baldwin, D. B. Stephenson, D. W. J. Thompson, T. J. Dunkerton, A. J. Charlton, and A. O’Neill. Stratospheric memory and skill of extended-range weather forecasts. *Science*, 301:636–640, 2003.
- R. X. Black and B. A. McDaniel. Interannual variability in the Southern Hemisphere circulation organized by stratospheric final warming events. *J. Atmos. Sci.*, 64(8):2968–2974, 2007.
- R. X. Black, B. A. McDaniel, and W. A. Robinson. Stratosphere-troposphere coupling during spring onset. *J. Clim.*, 19(19):4891–4901, 2006.
- P. Bloomfield. *Fourier Analysis of Time Series: An Introduction*. Wiley, New York., 2000.
- T. J. Bracegirdle. The seasonal cycle of stratosphere-troposphere coupling at southern high latitudes associated with the semi-annual oscillation in sea-level pressure. *Clim. Dynam.*, 37(11):2323–2333, 2011.

- N. J. Byrne, T. G. Shepherd, T. Woollings, and R. A. Plumb. Annular modes and apparent eddy feedbacks in the Southern Hemisphere. *Geophys. Res. Lett.*, 43(8): 3897–3902, 2016.
- N. J. Byrne, T. G. Shepherd, T. Woollings, and R. A. Plumb. Non-stationarity in Southern Hemisphere climate variability associated with the seasonal breakdown of the stratospheric polar vortex. *J. Clim.*, In press.
- G. Chen and I. M. Held. Phase speed spectra and the recent poleward shift of Southern Hemisphere surface westerlies. *Geophys. Res. Lett.*, 34(21), 2007. L21805.
- D. P. Dee, S. M. Uppala, A. J. Simmons, P. Berrisford, P. Poli, S. Kobayashi, U. Andrae, M. A. Balmaseda, G. Balsamo, P. Bauer, P. Bechtold, A. C M Beljaars, L. van de Berg, J. Bidlot, N. Bormann, C. Delsol, R. Dragani, M. Fuentes, A. J. Geer, L. Haimberger, S. B. Healy, H. Hersbach, E. V. Hólm, L. Isaksen, P. Kållberg, M. Köhler, M. Matricardi, A. P. McNally, B. M. Monge-Sanz, J. J. Morcrette, B. K. Park, C. Peubey, P. de Rosnay, C. Tavolato, J. N. Thépaut, and F. Vitart. The ERA-Interim reanalysis: Configuration and performance of the data assimilation system. *Q. J. R. Meteorol. Soc.*, 137(656):553–597, 2011.
- S. B. Feldstein. An observational study of the intraseasonal poleward propagation of zonal mean flow anomalies. *J. Atmos. Sci.*, 55(15):2516–2529, 1998.
- V. E. Fioletov and T. G. Shepherd. Seasonal persistence of midlatitude total ozone anomalies. *Geophys. Res. Lett.*, 30(7):1417, 2003.
- R. L. Fogt, J. Perlwitz, A. J. Monaghan, D. H. Bromwich, J. M. Jones, and G. J. Marshall. Historical SAM variability. Part II: Twentieth-century variability and trends from reconstructions, observations, and the IPCC AR4 models. *J. Clim.*, 22(20):5346–5365, 2009.
- C. Frankignoul and K. Hasselmann. Stochastic climate models. Part II. Application to sea-surface temperature anomalies and thermocline variability. *Tellus*, 29(4): 289–305, 1977.
- E. P. Gerber, M. P. Baldwin, H. Akiyoshi, J. Austin, S. Bekki, P. Braesicke, N. Butchart, M. Chipperfield, M. Dameris, S. Dhomse, S. M. Frith, R. R. Garcia, H. Garny, A. Gettelman, S. C. Hardiman, A. Karpechko, M. Marchand, O. Morgenstern, J. E. Nielsen, S. Pawson, T. Peter, D. A. Plummer, J. A. Pyle, E. Rozanov,

- J. F. Scinocca, T. G. Shepherd, and D. Smale. Stratosphere-troposphere coupling and annular mode variability in chemistry-climate models. *J. Geophys. Res.*, 115: 1–15, 2010.
- T. M. Hamill and J. Juras. Measuring forecast skill: Is it real skill or is it the varying climatology? *Q. J. R. Meteorol. Soc.*, 132(621C):2905–2923, 2006.
- S. C. Hardiman, N. Butchart, A. J. Charlton-Perez, T. A. Shaw, H. Akiyoshi, A. Baumgaertner, S. Bekki, P. Braesicke, M. Chipperfield, M. Dameris, R. R. Garcia, M. Michou, S. Pawson, E. Rozanov, and K. Shibata. Improved predictability of the troposphere using stratospheric final warmings. *J. Geophys. Res. Atmos.*, 116(D18), 2011. D18113.
- N. Harnik, R. K. Scott, and J. Perlwitz. Wave reflection and focusing prior to the major stratospheric warming of September 2002. *J. Atmos. Sci.*, 62(3):640–650, 2005.
- D. L. Hartmann and F. Lo. Wave-driven zonal flow vacillation in the Southern Hemisphere. *J. Atmos. Sci.*, 55(8):1303–1315, 1998.
- D. L. Hartmann, C. R. Mechoso, and K. Yamazaki. Observations of wave-mean flow interaction in the Southern Hemisphere. *J. Atmos. Sci.*, 41(3):351–362, 1984.
- K. Hasselmann. Stochastic climate models. Part I. Theory. *Tellus*, 28(6):473–485, 1976.
- P. H. Haynes, M. E. McIntyre, T. G. Shepherd, C. J. Marks, and K. P. Shine. On the "Downward Control" of extratropical diabatic circulations by eddy-induced mean zonal forces. *J. Atmos. Sci.*, 48(4):651–678, 1991.
- I. M. Held and B. J. Hoskins. Large-scale eddies and the general circulation of the troposphere. *Advances in Geophysics*, 28:3 – 31, 1985. Issues in Atmospheric and Oceanic Modeling.
- Y. Hio and S. Yoden. Quasi-periodic variations of the polar vortex in the Southern Hemisphere stratosphere due to wave-wave interaction. *J. Atmos. Sci.*, 61(21): 2510–2527, 2004.

- Y. Hio and S. Yoden. Interannual variations of the seasonal march in the Southern Hemisphere stratosphere for 1979 - 2002 and characterization of the unprecedented year 2002. *J. Atmos. Sci.*, 62(3):567–580, 2005.
- S. Hirano, M. Kohma, and K. Sato. A three-dimensional analysis on the role of atmospheric waves in the climatology and interannual variability of stratospheric final warming in the Southern Hemisphere. *J. Geophys. Res. Atmos.*, 121(14):8429–8443, 2016.
- I. Hirota, K. Kuroi, and M. Shiotani. Midwinter warmings in the Southern Hemisphere stratosphere in 1988. *Q. J. R. Meteorol. Soc.*, 116(494):929–941, 1990.
- P. Hitchcock. *The Arctic polar-night jet oscillation. Ph.D. thesis.* University of Toronto, 2012.
- J. W. Hurrell and H. van Loon. A modulation of the atmospheric annual cycle in the Southern Hemisphere. *Tellus A*, 46(3):325–338, 1994.
- M. M. Hurwitz, P. A. Newman, L. D. Oman, and A. M. Molod. Response of the Antarctic stratosphere to two types of El Niño events. *J. Atmos. Sci.*, 68(4):812–822, 2011.
- IPCC. *Climate Change 2013: The Physical Science Basis. Contribution of Working Group I to the Fifth Assessment Report of the Intergovernmental Panel on Climate Change.* Cambridge University Press, 2013.
- D. J. Ivy, C. Hilgenbrink, D. Kinnison, R. A. Plumb, A. Sheshadri, S. Solomon, and D. W. J. Thompson. Observed changes in the Southern Hemispheric circulation in May. *J. Clim.*, 30(2):527–536, 2017.
- P. Kallberg, P. Berrisford, B. J. Hoskins, A. Simmons, S. Lamy-Thepaut, and R. Hine. *ERA-40 Atlas.* 2005.
- D. J. Karoly and D. G. Vincent. *Meteorology of the Southern Hemisphere.* Amer. Meteor. Soc., 1998.
- J. W. Kidson. Indices of the Southern Hemisphere zonal wind. *J. Clim.*, 1(2):183–194, 1988.

- J. Kidston, A. A. Scaife, S. C. Hardiman, D. M. Mitchell, N. Butchart, M. P. Baldwin, and L. J. Gray. Stratospheric influence on tropospheric jet streams, storm tracks and surface weather. *Nat. Geosci.*, 8:433–440, 2015.
- J. Kim and T. Reichler. Quantifying the uncertainty of the annular mode time scale and the role of the stratosphere. *Clim. Dynam.*, 47(1-2):637–649, 2016.
- B. Kirtman and A. Pirani. *WCRP position paper on seasonal prediction. Report from the first WCRP seasonal prediction workshop, 4-7 June 2007, Barcelona, Spain.* 2007.
- K. Kodera, K. Yamazaki, M. Chiba, and K. Shibata. Downward propagation of upper stratospheric mean zonal wind perturbation to the troposphere. *Geophys. Res. Lett.*, 17(9):1263–1266, 1990.
- D. Koutsoyiannis. Hurst-Kolmogorov dynamics and uncertainty. *J. Am. Water Resour. Assoc.*, 47(3):481–495, 2011.
- Y. Kuroda and K. Kodera. Interannual variability in the troposphere and stratosphere of the Southern Hemisphere winter. *J. Geophys. Res.*, 103(D12):13787, 1998.
- Y. Kuroda and K. Kodera. Variability of the polar night jet in the northern and southern hemispheres. *J. Geophys. Res. Atmos.*, 106(D18):20703–20713, 2001.
- P. J. Kushner. *Annular Modes of the Troposphere and Stratosphere.* American Geophysical Union, 2010.
- P. J. Kushner and L. M. Polvani. Stratosphere-troposphere coupling in a relatively simple AGCM: The role of eddies. *J. Clim.*, 17(3):629–639, 2004.
- S. Lee and S. B. Feldstein. Detecting ozone- and greenhouse gas-driven wind trends with observational data. *Science*, 339:563–567, 2013.
- M. L. L’Heureux and D. W. J. Thompson. Observed relationships between the El Niño-Southern Oscillation and the extratropical zonal-mean circulation. *J. Clim.*, 19:276–287, 2006.
- M. L. L’Heureux, K. Takahashi, A. B. Watkins, A. G. Barnston, E. J. Becker, T. E. Di Liberto, F. Gamble, J. Gottschalck, M. S. Halpert, B. Huang, K. Mosquera-Vásquez, and A. T. Wittenberg. Observing and predicting the 2015-16 El Niño. *Bull. Amer. Meteor. Soc.*, pages BAMS-D-16-0009.1, 2016.

- D. J. Lorenz and D. L. Hartmann. Eddy-zonal flow feedback in the Southern Hemisphere. *J. Atmos. Sci.*, 58(21):3312–3327, 2001.
- D. J. Lorenz and D. L. Hartmann. Eddy-zonal flow feedback in the Northern Hemisphere winter. *J. Clim.*, 16(8):1212–1227, 2003.
- J. Lu, G. Chen, and D. M. W. Frierson. Response of the zonal mean atmospheric circulation to El Niño versus global warming. *J. Clim.*, 21(22):5835–5851, 2008.
- M. E. McIntyre. *Balanced Flow*. Academic Press, Second edition, 2015.
- L. R. Mudryk and P. J. Kushner. A method to diagnose sources of annular mode time scales. *J. Geophys. Res.*, 116(14):D14114, 2011.
- National Research Council. *Assessment of intraseasonal to interannual climate prediction and predictability*. The National Academies Press, 2010.
- W. D. Neff. Decadal time scale trends and variability in the tropospheric circulation over the South Pole. *J. Geophys. Res.*, 104:27217–27251, 1999.
- P. A. Newman. The final warming and polar vortex disappearance during the Southern Hemisphere spring. *Geophys. Res. Lett.*, 13(12):1228–1231, 1986.
- P. A. Newman, E. R. Nash, S. R. Kawa, S. A. Montzka, and S. M. Schauffler. When will the Antarctic ozone hole recover? *Geophys. Res. Lett.*, 33(12):L12814, 2006.
- G. R. North, T. L. Bell, R. F. Cahalan, and F. J. Moeng. Sampling errors in the estimation of empirical orthogonal functions. *Mon. Wea. Rev.*, 110(7):699–706, 1982.
- T. N. Palmer. A nonlinear dynamical perspective on climate prediction. *J. Clim.*, 12:575–591, 1999.
- T. N. Palmer and D. L. T. Anderson. The prospects for seasonal forecasting - a review paper. *Q. J. R. Meteorol. Soc.*, 120(518):755–793, 1994.
- L. M. Polvani, L. Sun, A. H. Butler, J. H. Richter, and C. Deser. Distinguishing stratospheric sudden warmings from enso as key drivers of wintertime climate variability over the north atlantic and eurasia. *J. Clim.*, 30(6):1959–1969, 2017.
- M. J. Ring and R. A. Plumb. Forced annular mode patterns in a simple atmospheric general circulation model. *J. Atmos. Sci.*, 64(10):3611–3626, 2007.

- M. J. Ring and R. A. Plumb. The response of a simplified GCM to axisymmetric forcings: Applicability of the fluctuation-dissipation theorem. *J. Atmos. Sci.*, 65(12):3880–3898, 2008.
- W. A. Robinson. Does eddy feedback sustain variability in the zonal index? *J. Atmos. Sci.*, 53(23):3556–3569, 1996.
- C. G. Rossby. Relations between variations in the intensity of the zonal circulation of the atmosphere and the displacements of the semi-permanent centers of action. *J. Mar. Res.*, 2:38–55, 1939.
- R. K. Scott and P. H. Haynes. Internal vacillations in stratosphere-only models. *J. Atmos. Sci.*, 57(19):3233–3250, 2000.
- R. K. Scott and P. H. Haynes. The seasonal cycle of planetary waves in the winter stratosphere. *J. Atmos. Sci.*, 59(4):803–822, 2002.
- R. K. Scott and P.H. Haynes. Internal interannual variability of the extratropical stratospheric circulation: The low-latitude flywheel. *Q. J. R. Meteorol. Soc.*, 124(550):2149–2173, 1998.
- R. Seager, N. Harnik, Y. Kushnir, W. A. Robinson, and J. Miller. Mechanisms of hemispherically symmetric climate variability. *J. Clim.*, 16:2960–2978, 2003.
- W. J. M. Seviour, S. C. Hardiman, L. J. Gray, N. Butchart, C. Maclachlan, and A. A. Scaife. Skillful seasonal prediction of the Southern Annular Mode and Antarctic ozone. *J. Clim.*, 27(19):7462–7474, 2014.
- A. Sheshadri, R. A. Plumb, and E. P. Gerber. Seasonal variability of the polar stratospheric vortex in an idealized AGCM with varying tropospheric wave forcing. *J. Atmos. Sci.*, 72:2248–2266, 2015.
- M. Shiotani, N. Shimoda, and I. Hirota. Interannual variability of the stratospheric circulation in the Southern Hemisphere. *Q. J. R. Meteorol. Soc.*, 119(511):531–546, 1993.
- I. R. Simpson, M. Blackburn, and J. D. Haigh. The role of eddies in driving the tropospheric response to stratospheric heating perturbations. *J. Atmos. Sci.*, 66(5):1347–1365, 2009.

- I. R. Simpson, P. Hitchcock, T. G. Shepherd, and J. F. Scinocca. Stratospheric variability and tropospheric annular-mode timescales. *Geophys. Res. Lett.*, 38(20):L20806, 2011.
- S. Solomon, D. J. Ivy, D. Kinnison, M. J. Mills, R. R. Neely, and A. Schmidt. Emergence of healing in the Antarctic ozone layer. *Science*, 310:307–310, 2016.
- S. W. Son, A. Purich, H. H. Hendon, B. M. Kim, and L. M. Polvani. Improved seasonal forecast using ozone hole variability? *Geophys. Res. Lett.*, 40(23):6231–6235, 2013.
- T. N. Stockdale, F. Molteni, and L. Ferranti. Atmospheric initial conditions and the predictability of the Arctic Oscillation. *Geophys. Res. Lett.*, 42(4):1173–1179, 2015.
- L. Sun and W. A. Robinson. Downward influence of stratospheric final warming events in an idealized model. *Geophys. Res. Lett.*, 36(3):1–5, 2009.
- L. Sun, G. Chen, and W. A. Robinson. The role of stratospheric polar vortex breakdown in Southern Hemisphere climate trends. *J. Atmos. Sci.*, 71:2335–2353, 2014.
- D. W. J. Thompson and J. M. Wallace. The Arctic Oscillation signature in the wintertime geopotential height and temperature fields. *Geophys. Res. Lett.*, 25(9):1297–1300, 1998.
- D. W. J. Thompson and J. M. Wallace. Annular modes in the extratropical circulation. Part I: Month-to-month variability. *J. Clim.*, 13(5):1000–1016, 2000.
- D. W. J. Thompson, J. M. Wallace, and G. C. Hegerl. Annular modes in the extratropical circulation. Part II: Trends. *J. Clim.*, 13(5):1018–1036, 2000.
- D. W. J. Thompson, M. P. Baldwin, and S. Solomon. Stratosphere-troposphere coupling in the Southern Hemisphere. *J. Atmos. Sci.*, 62:708–715, 2005.
- D. W. J. Thompson, J. C. Furtado, and T. G. Shepherd. On the tropospheric response to anomalous stratospheric wave drag and radiative heating. *J. Atmos. Sci.*, 63(10):2616–2629, 2006.
- D. W. J. Thompson, S. Solomon, P. J. Kushner, M. H. England, K. M. Grise, and D. J. Karoly. Signatures of the Antarctic ozone hole in Southern Hemisphere surface climate change. *Nat. Geosci.*, 42:741–749, 2011.

- K. E. Trenberth. Some effects of finite sample size and persistence on meteorological statistics. Part II: Potential predictability. *Mon. Weather Rev.*, 112(12):22369–2379, 1984.
- J. Turner and J. Comiso. Solve Antarctica’s sea-ice puzzle. *Nature*, 547:275277, 2017.
- J. Turner, T. Phillips, G. J. Marshall, J. S. Hosking, J. O. Pope, T. J. Bracegirdle, and P. Deb. Unprecedented springtime retreat of Antarctic sea ice in 2016. *Geophys. Res. Lett.*, TBD, 2017.
- H. van Loon. The half-yearly oscillations in middle and high southern latitudes and the coreless winter. *J. Atmos. Sci.*, 24:472–486, 1967.
- H. Von Storch and F. W. Zwiers. *Statistical Analysis in Climate Research*. Cambridge Univ. Press, Cambridge, U. K., 2002.
- L. J. Wilcox and A. J. Charlton-Perez. Final warming of the Southern Hemisphere polar vortex in high- and low-top CMIP5 models. *J. Geophys. Res.*, 118(6):2535–2546, 2013.
- D. S. Wilks. *Statistical Methods in the Atmospheric Sciences*. Academic Press, Third edition, 2011.
- M. A. H. Wittman, A. J. Charlton, and L. M. Polvani. The effect of lower stratospheric shear on baroclinic instability. *J. Atmos. Sci.*, 64(2):479–496, 2007.